MSAT STRUCTURAL DYNAMICS
MODEL
FOR CONTROL SYSTEM DESIGN

[DOC-CR-SP-82-057]

DYNACON

DYNACON Enterprises Ltd.
DYNAMICS AND CONTROL ANALYSIS
18 Cherry Blossom Lane Thornhill, Ontario L3T 3B9 (416) 889-9260

MSAT STRUCTURAL DYNAMICS MODEL FOR CONTROL SYSTEM DESIGN

[DOC-CR-SP-82-057]

(This document was previously referred to as DOC-CR-SP-82-054)

G.B. Sincarsin
P.C. Hughes

August 1982 Dynacon Report MSAT-7

Checked 10/83

Government of Canada Gouvernement du Canada

Department of Communications

DOC CONTRACTOR REPORT DOC-CR-SP -82-057

DEPARTMENT OF COMMUNICATIONS - OTTAWA - CANADA

SPACE PROGRAM

TITLE: MSAT Structural Dynamics Model for Control System Design

AUTHOR(S): G.B. Sincarsin and P.C. Hughes

ISSUED BY CONTRACTOR AS REPORT NO: Dynacon Report MSAT-7

PREPARED BY: Dynacon Enterprises Ltd.
18 Cherry Blossom Lane
Thornhill, Ontario
L3T 3B9

DEPARTMENT OF SUPPLY AND SERVICES CONTRACT NO: 15ST.36001-1-0953

DOC SCIENTIFIC AUTHORITY: A.H. Reynaud (Communications Research Centre)

CLASSIFICATION: Unclassified

DATE: August 1982

SUMMARY

This report completes the present phase of structural dynamics modeling for the 'lazy-Z' MSAT configuration. Substructural models, described in earlier reports in this series, are reduced in size with very little loss in accuracy. These models are then combined to form a structural model for the overall spacecraft. This model is, in turn, reduced in size (i.e., in number of coordinates) with only a small penalty in accuracy. 'Modal cost analysis' is shown to be an effective technique for this purpose.

Two specific models are recommended in this report, and all system data is given in the appendices for each of these models. The model appropriate to control system *design* includes four elastic modes; the final data for this model are tabulated in Appendix C. For control system *evaluation*, a model that incorporates an additional seven modes is recommended; the data for this model are tabulated in Appendix D.

TABLE OF CONTENTS

PREFACE

Acknowledgments

The authors are pleased to acknowledge the assistance of the following persons. Thanks are due

- to A. H. Reynaud and S. P. Altman (CRC), G. Rodriguez and A. F. Tolivar (JPL), and A. Woods (Lockheed), for assisting in providing the JPL model of the wrap-rib reflector.
- to M. El-Raheb and A. F. Tolivar (JPL) for assisting with the interpretation of the JPL model.
- to H. Barker (Spar) for assisting in providing the Spar model of the solar array.
- to I. A. Stoddard (Dynacon) for assisting with the machine computation.

Proprietary Rights

Units and Spelling

This report uses S.I. units and North American spelling.

LIST OF FIGURES

LIST OF TABLES

Note: Tables of data defining the 'control design model' and the 'control evaluation model' are given as Appendices C and D, respectively.

1. INTRODUCTION

This is the final installment in a series of reports prepared under the present contract (apart from the Executive Summary, Dynacon Report MSAT-9)†. This investigation is based on the satellite configuration shown in Fig. 2.1 (p. 3) and Fig. 2.2 (p. 14). This is intended to be representative of 'third-generation' satellites (for the meaning of 'third generation', see MSAT-9), and is motivated by earlier studies into possible configurations for an 'operational' mobile-communications satellite (MSAT). This 'Operational-MSAT' configuration, which is also of considerable interest in the U.S.A, represents a typical large, flexible communications satellite of the type likely to follow the current Demonstration-MSAT. The problems of attitude control and shape stabilization for the 'third-generation' vehicle shown in Figs. 2.1 and 2.2 are anticipated to be considerably more challenging than for the Demonstration MSAT, and the aim of this and other collateral work is to advance the state of Canadian technology in this area.

In accordance with this aim, the spacecraft has been modeled with the same degree of accuracy as if it were a 'real' spacecraft. To the authors' knowledge, the dynamical modeling in the present series of reports has a degree of accuracy that is as high, or higher, than for any previous Canadian spacecraft, including the shuttle remote manipulator arm.

In this report the substructural models described in MSAT-4 for the solar-cell array, the antenna reflector, and the reflector tower are combined in accordance with the methodology outlined in MSAT-3. The result is a quite large model (i.e., a large number of coordinates) that requires still further pruning before it can be used as an efficient tool for control system design and evaluation. These two ideas--substructural model synthesis and spacecraft model order reduction--are the twin themes underlying the developments described in this report.

---

†For brevity, reports in this series will be designated simply as MSAT-1, MSAT-2, etc.

2. SYSTEM MATRICES

2.1 Summary of MSAT Dynamics Model

The MSAT spacecraft is shown in Fig. 2.1. It consists of a rigid bus structure and three flexible substructures -- the solar array, the tower and the reflector (antenna). The dynamics models for these substructures are provided in MSAT - 4, while the dynamics model for the entire assembled spacecraft is given in MSAT - 5. In brief, the equations governing the MSAT spacecraft take the form

$$\underline{M}\ddot{\underline{q}} + (\underline{\mathcal{D}} + \underline{\mathcal{G}})\dot{\underline{q}} + \underline{K}\underline{q} = \underline{\mathcal{B}}\underline{u} + \underline{u}_d \tag{2.1}$$

where the system mass $\underline{M}$ and stiffness $\underline{K}$ matrices are given explicity in MSAT - 5. It remains to specify the system, damping matrix $\underline{\mathcal{D}}$, gyroscopic matrix $\underline{\mathcal{G}}$ and control matrix $\underline{\mathcal{B}}$. The disturbance inputs $\underline{u}_d$, save for a minor omission (see Appendix A), are as given in MSAT - 5. Also, the assembled spacecraft coordinates are

$$\underline{q} = \mathrm{col}\{\underline{w}_b, \underline{\theta}_b, \underline{\beta}, \underline{\delta}, \underline{\alpha}, \underline{\eta}_a, \underline{q}_i, \underline{\eta}_r\} \tag{2.2}$$

where $\underline{w}_b$ and $\underline{\theta}_b$ are the translational and rotational displacements of the bus, $\underline{\beta}$ contains the reflector gimbal angles (there are two: β_1 about the x_r-axis and β_2 about the y_r-axis), $\underline{\delta}$ and $\underline{\alpha}$ are the translational and rotational displacement of the tip of the tower (O_r) relative to the root of the tower (O_t) caused by the structural flexibility within the tower, $\underline{q}_i$ are the 'internal' elastic tower coordinates and $\underline{\eta}_a$ and $\underline{\eta}_r$ are modal coordinates for the solar array and the reflector, respectively.

In what follows, $\underline{\mathcal{D}}$, $\underline{\mathcal{G}}$, and $\underline{\mathcal{B}}$ for MSAT will be given in analytical form prior to modal selection; however, only the reduced design- and evaluation-model modal system matrices will be given numerically. Also, prior to performing these reductions, it will be necessary to specify the output matrix $\underline{P}$. This matrix relates the spacecraft coordinates to the *important outputs* $\underline{y}$ (rather than the *sensed outputs*, see MSAT - 1.):

$$\underline{y} = \underline{P}\underline{q} \tag{2.3}$$

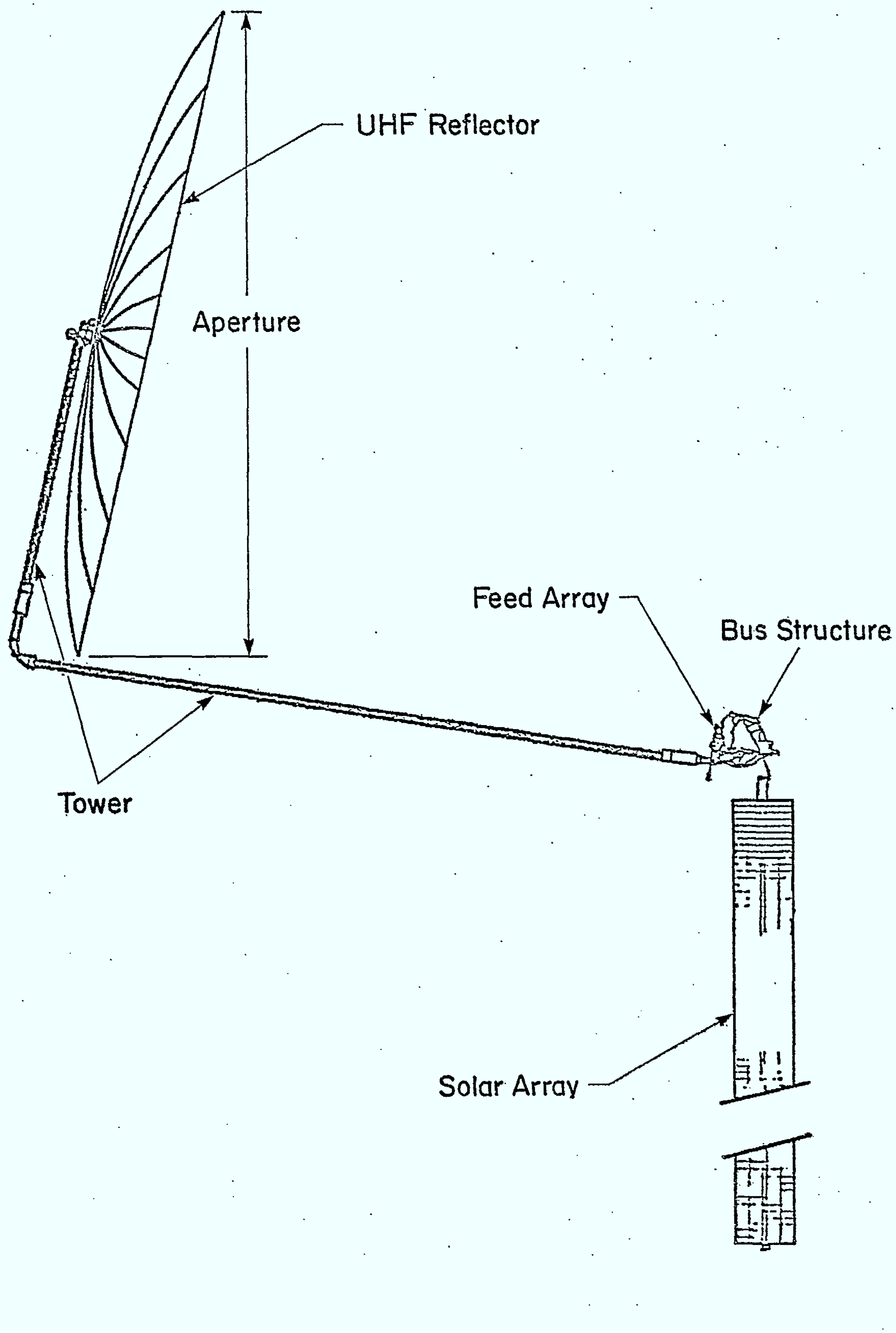

Fig. 2.1 The MSAT Spacecraft

2.2 The Damping Matrix

2.2.1 Damping Matrix for Assembled Spacecraft

Much of what follows is taken from MSAT-6 which describes the modeling of energy dissipation (damping) in flexible space structures. We adopt the view cited in Section 5.4 of the report, that the elastic damping matrix $\underline{\mathcal{D}}_e$, where

$$\underline{\mathcal{D}} = \begin{bmatrix} \underline{0} & \underline{0} \\ \underline{0} & \underline{\mathcal{D}}_e \end{bmatrix} \tag{2.4}$$

and

$$\underline{q} = \text{col}\{\underline{q}_{r(igid)}, \underline{q}_{e(lastic)}\} \tag{2.5}$$

should be partitioned into a block diagonal form, one block for each substructure and with each block being proportional to the corresponding stiffness matrix. To quote MSAT-6, "the rationale for this choice runs as follows: an element of the stiffness matrix, k_{ij} is nonzero if the stiffness of the structure offers a resistance at coordinate q_j to a force in the direction of q_i; if the structure offers zero *static* resistance at q_j to a force at q_i, how can it offer any *dynamic* (i.e. damping) resistance at q_j to a force at q_i? If we agree that the answer is "It can't", then the (block diagonal form for $\underline{\mathcal{D}}_e$) follows immediately." (Note, it is not assumed that $\underline{\mathcal{D}}$ is proportional to $\underline{K}$ for the assembled spacecraft.)

For the MSAT spacecraft $\underline{\mathcal{D}}_e$ takes the form ($\tau = \delta\delta, \delta\alpha, \alpha\alpha, \delta i, \alpha i$, ii, a or r and γ_τ a constant):

$$\underline{\mathcal{D}}_e = \begin{bmatrix} \underline{\mathcal{D}}_{\delta\delta} & \underline{\mathcal{D}}_{\delta\alpha} & \underline{0} & \underline{\mathcal{D}}_{\delta i} & \underline{0} \\ & \underline{\mathcal{D}}_{\alpha\alpha} & \underline{0} & \underline{\mathcal{D}}_{\alpha i} & \underline{0} \\ & & \hat{\underline{\mathcal{D}}}^a & \underline{0} & \underline{0} \\ & \text{(symmetric)} & & \underline{\mathcal{D}}_{ii} & \underline{0} \\ & & & & \hat{\underline{\mathcal{D}}}^r \end{bmatrix} ; \quad \underline{\mathcal{D}}_\tau = \gamma_\tau \underline{K}_\tau \tag{2.6}$$

with

$$\underline{q}_r = \text{column } \{\underline{w}_b, \theta_b, \underline{\beta}\}$$
$$\underline{q}_e = \text{column } \{\underline{\delta}, \underline{\alpha}, \underline{\eta}_a, \underline{q}_i, \underline{\eta}_r\} \tag{2.7}$$

given the stiffness matrix cited in MSAT-5. $\underline{\mathcal{D}}_e$ is not strictly in block diagonal form according to substructure in that to consolidate the tower substructure damping, $\underline{\mathcal{D}}_{\delta i}$, $\underline{\mathcal{D}}_{\alpha i}$ and $\underline{\mathcal{D}}_{ii}$ must be grouped with $\underline{\mathcal{D}}_{\delta\delta}$, $\underline{\mathcal{D}}_{\delta\alpha}$ and $\underline{\mathcal{D}}_{\alpha\alpha}$ to form

$$\underline{\mathcal{D}}_t = \begin{bmatrix} \underline{\mathcal{D}}_{\delta\delta} & \underline{\mathcal{D}}_{\delta\alpha} & \underline{\mathcal{D}}_{\delta i} \\ & \underline{\mathcal{D}}_{\alpha\alpha} & \underline{\mathcal{D}}_{\alpha i} \\ (\text{symmetric}) & & \underline{\mathcal{D}}_{ii} \end{bmatrix} \tag{2.8}$$

Then $\underline{\mathcal{D}}_e$ can be written in the desired form

$$\underline{\mathcal{D}}_e = \begin{bmatrix} \underline{\mathcal{D}}_t & \underline{0} & \underline{0} \\ & \underline{\hat{\mathcal{D}}}^a & \underline{0} \\ (\text{symmetric}) & & \underline{\hat{\mathcal{D}}}^r \end{bmatrix} \tag{2.9}$$

As (2.6) and (2.9) are equivalent representations, except for a minor difference in form, and as $\underline{M}$ and $\underline{K}$ already exist both analytically and in computer code in a form analogous to (2.6), the split-block diagonal form (2.6) is adopted to represent $\underline{\mathcal{D}}_e$

The carets (^) appearing over $\underline{\mathcal{D}}^a$ and $\underline{\mathcal{D}}^r$ emphasize that the solar array and reflector damping matrices appear in modal form ($\tau = r$ or a):

$$\underline{\hat{\mathcal{D}}}^\tau = \underline{E}_\tau^T \underline{\mathcal{D}}_\tau \underline{E}_\tau \tag{2.10}$$

The modal matrix of eigenvectors $\underline{E}_\tau$ is comprised of the 'constrained' modes for the substructure as it appears in the *system* mass and stiffness matrices, not in its pre-assembled form! While this distinction is of no consequence for the solar array and the reflector, it is important for the tower. Defining $\underline{M}_t$ and $\underline{K}_t$ analogous in form to (2.8), where $\underline{M}_t$ and $\underline{K}_t$ are 'extracted' from $\underline{M}$ and $\underline{K}$, and solving the eigenvalue problem yields $\underline{E}_t$. This substructural tower model has the mass and interias of the reflector lumped, as if it were rigid, at the tip of the tower. The pre-assembled tower model given in MSAT-5 by $\underline{M}_{tt}$ (3.15) and $\underline{K}_{tt}$ (3.16) does not contain this lumping and consequently solving its eigenvalue problem produces $\underline{E}_t \neq \underline{E}_t$.

The modal damping matrix for the entire assembled spacecraft is defined in a manner analogous to (2.10). Simply

$$\hat{\underline{\mathcal{D}}} = \underline{E}^T \underline{\mathcal{D}} \underline{E} \tag{2.11}$$

where $\underline{\mathcal{D}}$ is given by (2.4) and $\underline{E}$ is the modal matrix of eigenvectors for the entire spacecraft. Partitioning $\underline{E}$ according to rigid (r) and elastic (e) coordinates,

$$\underline{E} = \begin{bmatrix} \underline{E}_r & \underline{E}_{re} \\ \underline{O} & \underline{E}_e \end{bmatrix} \tag{2.12}$$

and expanding (2.11) one obtains

$$\hat{\underline{\mathcal{D}}} = \begin{bmatrix} \underline{O} & \underline{O} \\ \underline{O} & \hat{\underline{\mathcal{D}}}_e \end{bmatrix} ; \qquad \hat{\underline{\mathcal{D}}}_e = \underline{E}_e^T \underline{\mathcal{D}}_e \underline{E}_e \tag{2.13}$$

Furthermore, following MSAT-6, $\underline{E}_e$ itself can be partitioned according to substructures, so that here

$$\hat{\underline{\mathcal{D}}}_e = \underline{E}_e^{tT} \underline{\mathcal{D}}_t \underline{E}_e^t + \underline{E}_e^{aT} \hat{\underline{\mathcal{D}}}^a \underline{E}_e^a + \underline{E}_e^{rT} \hat{\underline{\mathcal{D}}}^r \underline{E}_e^r \tag{2.14}$$

where

$$\underline{E}_e^t = \begin{bmatrix} \underline{E}_e^\delta \\ \underline{E}_e^\alpha \\ \underline{E}_e^i \end{bmatrix}$$

and $\underline{\mathcal{D}}_t$ is given by (2.8). At this juncture $\hat{\underline{\mathcal{D}}}_e$ no longer retains a split-block-diagonal form but rather is a full matrix. It remains to assign the individual damping matrices for the tower, array and reflector. These, of course, depend on the type of damping assumed.

2.2.2 Damping Matrices for Substructures

In the previous section, it is assumed that the damping in each substructure τ (τ = t,a,r) is *proportional* to its stiffness (γ_τ a constant):

$$\underline{D}_\tau = \gamma_\tau \underline{K}_\tau \tag{2.15}$$

$$\hat{\underline{D}}^\tau = \underline{E}_\tau^T \underline{D}_\tau \underline{E}_\tau \tag{2.16}$$

It is futher assumed that each substructure is *lightly* damped. As a consequence, only the diagonal elements $\hat{d}^\tau_{\alpha\alpha}$ of the modal damping matrix $\hat{\underline{D}}^\tau$ have an important impact on the vibrational motion of substructure τ (see MSAT-6). Furthermore, for vibration mode α of the substructure ($\alpha = 1,\ldots n_\tau$), the linear viscous damping coefficient is

$$\zeta^\tau_\alpha = \tfrac{1}{2}\hat{d}^\tau_{\alpha\alpha}/\omega^\tau_\alpha \tag{2.17}$$

where ω^τ_α is the constrained natural frequency of mode α. The modal damping matrix is, therefore,

$$\hat{\underline{D}}^\tau = 2\underline{Z}^\tau \underline{\Omega}^\tau \tag{2.18}$$

where

$$\underline{Z}^\tau = \text{diag}\{\zeta^\tau_1,\ldots,\zeta^\tau_{n_\tau}\} \tag{2.19}$$

$$\underline{\Omega}^\tau = \text{diag}\{\omega^\tau_1,\ldots,\omega^\tau_{n_\tau}\} \tag{2.20}$$

Now, substituting (2.15) into (2.16) and equating the result to (2.18) yields

$$\zeta^\tau_\alpha = \tfrac{1}{2}\gamma_\tau \omega^\tau \tag{2.21}$$

since $\underline{E}_\tau^T \underline{K}_\tau \underline{E}_\tau = \underline{\Omega}^{\tau 2}$. Hence, for arbitrary γ_τ, the loss factors increase with an increase in frequency, a tendency not supported by experimental evidence. To avoid this discrepancy linear hysteretic damping is considered; however, the option of a linear vicous damping model for the substructures is retained in the computer software for the MSAT dynamics. In this regard, for substructures in physical coordinates, (2.15) is applied directly to obtain $\underline{D}^{\tau}$, while for substructures in modal coordinates, $\hat{\underline{D}}^{\tau} = \gamma_{\tau}\underline{\Omega}^{\tau 2}$ is formed. The factor γ_{τ} is chosen to have a default value of 0.01 for all three substructures.

If one assumes the substructures to be linearly hysteretically damped, then (2.15) must be replaced by

$$\underline{H}^{\tau} = \varepsilon_{\tau}\underline{K}_{\tau} \tag{2.22}$$

where in the frequency domain $j\,\mathrm{sgn}(\omega)\underline{H}$ replaces $j\omega\underline{D}$ (see MSAT-6 Section 6) in (2.1). Again, to quote MSAT-6, "(This) model has two disadvantages:

(i) It is in the frequency domain and does not lend itself to a time-domain interpretation.

(ii) The modal equations are coupled by $\hat{\underline{H}}^{\tau} = \underline{E}_{\tau}^{T}\underline{H}_{\tau}\underline{E}_{\tau}$."

However, because the damping is assumed to be light it can be shown (see MSAT-6) that

$$\hat{d}_{\alpha\alpha}^{\tau} = \hat{h}_{\alpha\alpha}^{\tau}/\omega_{\alpha}^{\tau} \tag{2.23}$$

and therefore; 'effective linear viscous damping coefficients' given by

$$\zeta_{\alpha}^{\tau} = \tfrac{1}{2}\hat{h}_{\alpha\alpha}^{\tau}/\omega_{\alpha}^{\tau 2} \tag{2.24}$$

can be used in the modal equations for the substructure. Substitution of (2.22) into the equation for $\hat{\underline{H}}^{\tau}$ given (2.24) implies that now

$$\zeta_{\alpha}^{\tau} = \tfrac{1}{2}\varepsilon_{\tau} \tag{2.25}$$

The loss factors, are no longer proportional to frequency, but rather are independent of the frequency. While this is not an exact model, it is, from experiment, a reasonable approximation to reality, and is the model adopted for the MSAT spacecraft substructures.

Assuming light-hysteretic proportional-damping, the damping matrices for the array and reflector (which are modeled in modal coordinates) are

$$\underline{\hat{\mathcal{D}}}^a = \varepsilon_a \underline{\Omega}^a \; ; \qquad \underline{\hat{\mathcal{D}}}^r = \varepsilon_r \underline{\Omega}^r \tag{2.26}$$

A default value of 0.01 is chosen for both ε_r and ε_a. Unfortunately, the damping matrix for the tower (which is modeled in physical coordinates) is not as easily obtained. It is necessary to generate $\underline{\mathcal{D}}^t$ using (see MSAT-6)

$$\underline{\mathcal{D}}^t = \underline{M}_t \underline{E}_t \underline{\hat{\mathcal{D}}}^t \underline{E}_t^T \underline{M}_t \tag{2.27}$$

given

$$\underline{\hat{\mathcal{D}}}^t = \varepsilon_t \underline{\Omega}^t \tag{2.28}$$

where, recall from the previous section that, $\underline{M}_t$ and $\underline{E}_t$ are for the tower-plus-lumped-reflector substructure ($\varepsilon_t = 0.01$). The constrained natural frequencies $\omega_\alpha^t(\varepsilon\underline{\Omega}^t)$ for this substructure, assuming either a two- or four-element finite-element tower model (see MSAT-4), are shown in Table 1. The inertia checks (involving a few extra terms) and modal identity checks performed on the original tower model were also conducted on this augmented model. The analytically predicted inertias and their numerical counterparts were the same. The results of the modal identity checks are given in Table 2 and again show good agreement.

2.3 The Gyroscopic Matrix

The system gyroscopic matrix is necessary to represent stored angular momentum in the bus (from, for example, reaction wheels or a biased momentum wheel). If $\underline{h}_s$ is the stored angular momentum, then the additional term $\underline{\dot{\theta}}_b^{\times} \underline{h}_s$ must be added to the bus rotational equation. The gyroscopic matrix, therefore, is

$$\underline{G} = \begin{bmatrix} \underline{G}_r & \underline{O} \\ \underline{O} & \underline{O} \end{bmatrix}; \qquad \underline{G}_r = \begin{bmatrix} \underline{O} & \underline{O} & \underline{O} \\ \underline{O} & \underline{G}_{\theta\theta} & \underline{O} \\ \underline{O} & \underline{O} & \underline{O} \end{bmatrix} \tag{2.29}$$

Table 1

Natural Frequencies for Two- and Four-Element Tower-Plus-Lumped-Reflector Model

(rad/sec)

	Free-Free Vibration*		Constrained Vibration	
Elastic Mode No.	Two-Element Model	Four-Element Model	Two-Element Model	Four-Element Model
1	1.67^{-1} †	1.66^{-1}	4.37^{-3}	4.37^{-3}
2	3.22^{-1}	3.21^{-1}	9.01^{-3}	9.01^{-3}
3	1.10	1.10	2.93^{-2}	2.93^{-2}
4	2.09	2.09	6.42^{-2}	6.42^{-2}
5	1.23^{1}	9.31	1.17^{-1}	1.17^{-1}
6	2.19^{1}	1.30^{1}	1.15	1.15
7	9.65^{1}	8.32^{1}	1.61	1.61
8	1.72^{2}	1.11^{2}	1.74^{1}	9.39
9	1.86^{2}	1.19^{2}	4.04^{1}	1.34^{1}
10	2.59^{2}	1.51^{2}	2.30^{2}	1.20^{2}
11	-	2.40^{2}	-	1.26^{2}
12	-	5.37^{2}	-	1.37^{2}
13	-	8.79^{2}	-	2.57^{2}
14	-	9.78^{2}	-	4.31^{2}
15	-	1.11^{3}	-	6.12^{2}
16	-	1.86^{3}	-	1.02^{3}
17	-	2.08^{3}	-	1.24^{3}
18	-	2.14^{3}	-	1.82^{3}
19	-	4.66^{3}	-	4.46^{3}
20	-	1.01^{4}	-	9.98^{3}

* Note: For the free-free vibration cases there are also 6 zero frequencies.

† $1.67 \times 10^{-1} = 1.67^{-1}$ etc.

Table 2

Modal Identity Check for the Two- and Four-Element Tower-Plus-Lumped-Reflector Model

Inertia Properties

$$\begin{bmatrix} m\underline{1} & -\underline{c}^{x} \\ \underline{c}^{x} & \underline{J} \end{bmatrix} =$$

571	0	0	0	24,003	-8,166
	571	0	-24,003	0	0
		571	8,166	0	0
			1,252,168	0	0
(symmetric)				1,066,284	-347,925
					266,300

Modal Identity

$$\begin{bmatrix} \underline{P}_t \\ \underline{H}_t \end{bmatrix} \underline{M}_{tt}^{-1} \begin{bmatrix} \underline{P}_t \\ \underline{H}_t \end{bmatrix}^{T} =$$

Two-Element Model

555	0	0	0	23,921	-8,166
	554	2.4	-23,914	0	0
		356*	8,140	0	0
			1,251,542	0	0
(symmetric)				1,065,731	-347,925
					226,289

Four-Element Model

562	0	0	0	23,979	-8,166
	562	0.3	-23,979	0	0
		361*	8,164	0	0
			1,252,082	0	0
(symmetric)				1,066,198	-347,925
					226,295

* $(m_t)_{\text{elastic in } \hat{\underset{\rightarrow}{t}}_3 \text{ direction}} = (m_t + m_g + m_r)\cos^2\gamma_2 = 391$ kg $(\gamma_2 = 7.21^{\circ})$

where

$$\underline{\mathcal{G}}_{\theta\theta} = -\underline{h}_s^{\times} \tag{2.30}$$

and the dimensions for the respective zero matrices follow from the partitioning of $\dot{\underline{q}}$ implied by (2.7). The modal gyroscopic matrix is then found by forming

$$\underline{\hat{\mathcal{G}}} = \underline{E}^T\underline{\mathcal{G}}\underline{E} \tag{2.31}$$

Now, row partitioning $\underline{E}$ according to the spacecraft coordinates given in (2.2), (2.31) becomes

$$\underline{\hat{\mathcal{G}}} = \underline{E}_{\theta q}^T\underline{\mathcal{G}}_{\theta\theta}\underline{E}_{\theta q} \tag{2.32}$$

Forms (2.29) and (2.32) for the system gyroscopic matrices, however, are not very useful for design purposes because any change in $\underline{h}_s$ requires $\underline{\hat{\mathcal{G}}}$ to be recomputed from (2.32) -- a laborious and computationally inefficient process. Instead, let

$$\underline{\mathcal{G}} = \sum_{i=1}^{3}\underline{\mathcal{G}}_i h_i \tag{2.33}$$

where

$$\underline{\mathcal{G}}_i = \begin{bmatrix} \underline{\mathcal{G}}_{ri} & \underline{O} \\ \underline{O} & \underline{O} \end{bmatrix}; \qquad \underline{\mathcal{G}}_{ri} = \begin{bmatrix} \underline{O} & \underline{O} & \underline{O} \\ \underline{O} & -\underline{1}_i^{\times} & \underline{O} \\ \underline{O} & \underline{O} & \underline{O} \end{bmatrix} \tag{2.34}$$

$$\underline{1}_1 = [1 \quad 0 \quad 0]^T ; \quad \underline{1}_2 = [0 \quad 1 \quad 0]^T ; \quad \underline{1}_3 = [0 \quad 0 \quad 1]^T$$

and h_i is the ith component of $\underline{h}_s$ (expressed in the bus frame). Then,

$$\underline{\hat{\mathcal{G}}} = \sum_{i=1}^{3}\underline{\hat{\mathcal{G}}}_i h_i \tag{2.35}$$

where

$$\underline{\hat{\mathcal{G}}}_i = \underline{E}_{\theta q}^T\underline{\mathcal{G}}_{ri}\underline{E}_{\theta q} \tag{2.36}$$

Now $\hat{\underline{G}}_i$ need only be computed once for each i, thus greatly reducing the effect required to recompute $\hat{\underline{G}}$ whenever $\underline{h}_s$ is changed.

2.4 The Input Matrix

For this report, it is assumed that the control actuators for the MSAT spacecraft are localized on the bus and at the reflector gimbal. Pure torquers (for example, reaction wheels) and a cluster of four thrusters are located on the bus. It is assumed that a pure torque can be applied directly about each of the bus axes. At the reflector gimbal, pure torques about the reflector axes x_r and y_r are required to control the gimbal angles β_1 and β_2. A cluster of four thrusters also exists at the reflector gimbal (these thrusters, however, are attached to the tower and do not move with the reflector). These actuator locations are shown in Fig. 2.2 (taken from SPAR R.1113).

The thruster clusters on the bus and at the reflector gimbal can be resolved into a net force $\vec{f}_{tc}$ acting at O_r and a net force $\vec{f}_{bc}$ acting on the bus at a location defined by $\vec{r}_{bc}$ relative to O_b (see Fig. 2.3). Also, denote the control torques acting on the bus by $\vec{g}_c$ and those at the reflector gimbal by $\vec{g}_\beta$ ($\vec{g}_\beta$ is in the $x_r - y_r$ plane of the reflector frame). Furthermore, let $\underline{f}_{tc}$, $\underline{f}_{bc}$, $\underline{g}_c$ and $\underline{r}_{bc}$ be the components of $\vec{f}_{tc}$, $\vec{f}_{bc}$, $\vec{g}_c$ and $\vec{r}_{bc}$ expressed in the bus frame, while $\underline{g}_\beta$ are the components of $\vec{g}_\beta$ expressed in the reflector frame. Then, adding $\underline{f}_{bc}$ and $\underline{g}_c + \underline{r}_{bc}^{\times}\underline{f}_{bc}$ to the bus equations, $\underline{C}_{tb}\underline{f}_{tc}$ and $\underline{r}_{tr}^{\times}\underline{C}_{tb}\underline{f}_{tc}$ to the tower equations, and $\underline{g}_\beta$ to the reflector equations, as given in MSAT-5, and performing the operations cited in Section 4.3 of that reference, the system input matrix becomes

$$\underline{B} = \begin{bmatrix} \underline{O} & \underline{O} & \underline{1} & \underline{1} \\ \underline{1} & \underline{O} & \underline{r}_{bc}^{\times} & \underline{r}_{br}^{\times} \\ \underline{O} & \underline{1} & \underline{O} & \underline{O} \\ \underline{O} & \underline{O} & \underline{O} & \underline{C}_{tb} \\ \underline{O} & \underline{O} & \underline{O} & \underline{r}_{tr}^{\times}\underline{C}_{tb} \\ \underline{O} & \underline{O} & \underline{O} & \underline{O} \\ \underline{O} & \underline{O} & \underline{O} & \underline{O} \\ \underline{O} & \underline{O} & \underline{O} & \underline{O} \end{bmatrix} \tag{2.37}$$

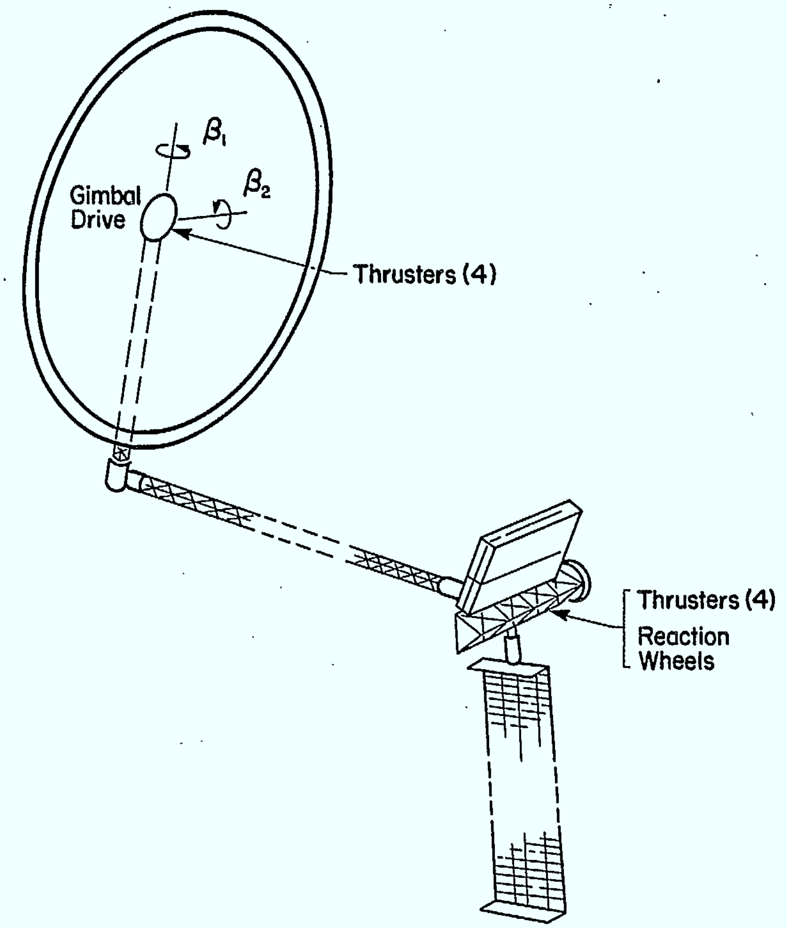

(a) Actuator Locations (specified by Spar R.1113)

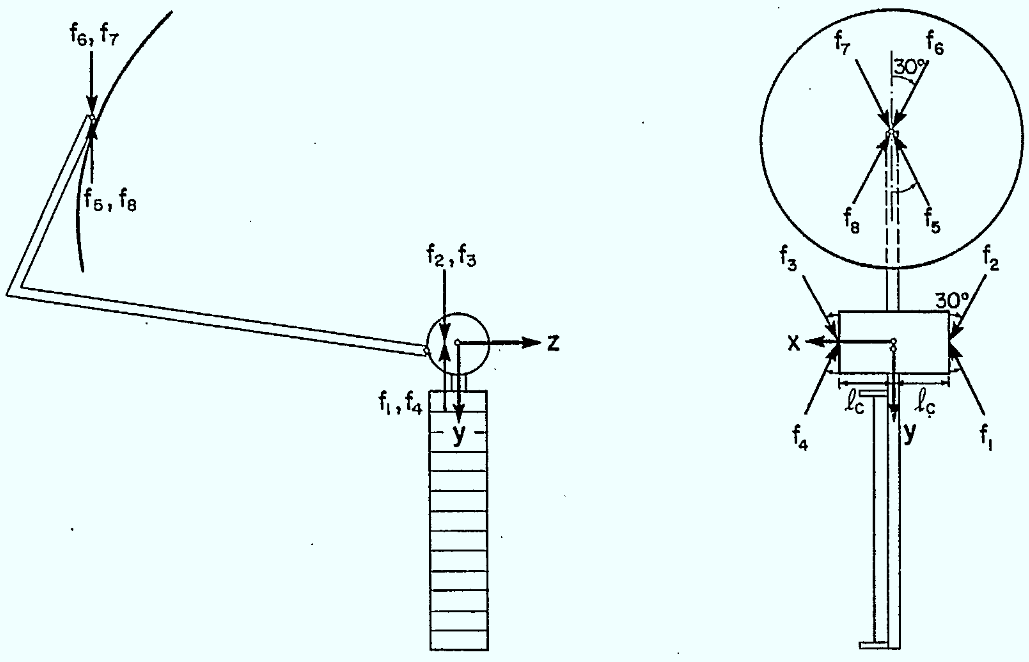

(b) Thrust Directions (specified by Spar R.1113)

Fig. 2.2 Assumed Control Inputs for MSAT Spacecraft

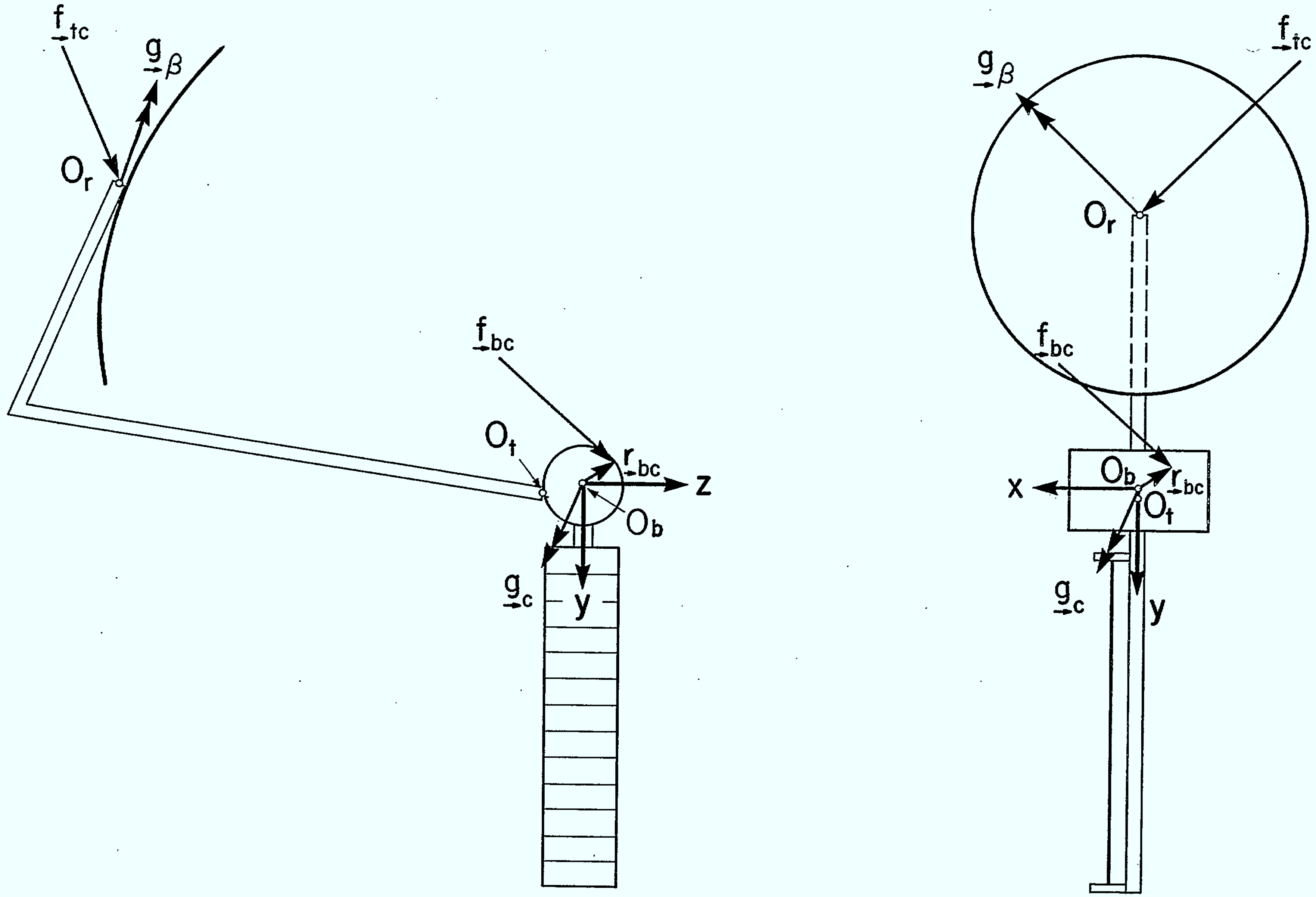

Fig. 2.3 Model of Control Inputs for MSAT Spacecraft

where

$$\underline{u} = \text{col}\{\underline{g}_c, \underline{g}_\beta, \underline{f}_{bc}, \underline{f}_{tc}\} \tag{2.38}$$

and $\underline{B}$ is row-partitioned as implied by (2.2). It remains to establish $\underline{f}_{bc}$, $\underline{f}_{tc}$ and $\underline{r}_{bc}$ from the clustered-thruster formations shown in Fig. 2.2.

Summing the forces and torques, resulting from control inputs on the bus, it follows that

$$\underline{f}_{bc} = \sum_{i=1}^{4} \underline{f}_i \tag{2.39}$$

$$\underline{r}_{bc}^{x}\underline{f}_{bc} = \sum_{i=1}^{4} \underline{r}_i^{x}\underline{f}_i \tag{2.40}$$

where $\underline{f}_i$ is the force from thruster i and $\underline{r}_i$ locates thruster i relative to O_b. Similarly for the tower,

$$\underline{f}_{tc} = \sum_{i=5}^{8} \underline{f}_i \tag{2.41}$$

Now, defining f_i to be the magnitude of the thrust from thruster i, so that $\underline{f}_i = \hat{\underline{f}}_i f_i$, and given the geometry of Fig. 2.2, one obtains

$$\begin{aligned} \hat{\underline{f}}_1 &= -\hat{\underline{f}}_3 = \hat{\underline{f}}_5 = -\hat{\underline{f}}_7 \\ \hat{\underline{f}}_2 &= -\hat{\underline{f}}_4 = \hat{\underline{f}}_6 = -\hat{\underline{f}}_8 \end{aligned} \tag{2.42}$$

where

$$\hat{\underline{f}}_1 = [\tfrac{1}{2} \quad -\tfrac{\sqrt{3}}{2} \quad 0]^T \qquad \hat{\underline{f}}_2 = [\tfrac{1}{2} \quad \tfrac{\sqrt{3}}{2} \quad 0]^T \tag{2.43}$$

Similarly, letting r_i be the magnitude of $\underline{r}_i$ ($\underline{r}_i = \hat{\underline{r}}_i r_i$)

$$\hat{\underline{r}}_1 = \hat{\underline{r}}_2 = -\hat{r}_3 = -\hat{\underline{r}}_4 = -\underline{1}_1\ell_c \quad ; \ \ell_c = 5\text{m} \tag{2.44}$$

Also, let the components of $\underline{r}_{br}$ in the bus frame be

$$\underline{r}_{br} = [0, -\ell_y, -\ell_z]^T \tag{2.45}$$

where ℓ is the distance from the bus to the reflector gimbal. Substitution of (2.42) - (2.45) into (2.39) - (2.41) yields the desired result.

A more useful form for $\underline{B}$, whereby the inputs from the individual actuators are highlighted, can now be obtained. This is accomplished by defining $\underline{u}$ to be

$$\underline{u} = \text{col}\{g_{c1}, g_{c2}, g_{c3}, g_{\beta 1}, g_{\beta 2}, f_1, f_2, f_3, f_4, f_5, f_6, f_7, f_8\} \tag{2.46}$$

and factoring $\underline{Bu}$ as given by (2.37), (2.38), (2.39) and (2.40). The resulting input matrix can be partitioned as follows

$$\underline{B} = [\underline{b}_{c1}, \underline{b}_{c2}, b_{c3}, \underline{b}_{\beta 1}, \underline{b}_{\beta 2}, \underline{b}_{f1}, \underline{b}_{f2}, \underline{b}_{f3}, \underline{b}_{f4}, \underline{b}_{f5}, \underline{b}_{f6}, \underline{b}_{f7}, \underline{b}_{f8}] \tag{2.47}$$

where

$$\underline{b}_k = \text{col}\{\underline{b}_{wk}, \underline{b}_{\theta k}, \underline{b}_{\beta k}, \underline{b}_{\delta k}, \underline{b}_{\alpha k}, \underline{b}_{ak}, \underline{b}_{ik}, \underline{b}_{rk}\} \tag{2.48}$$

$$k \in (c1, c2, c3, \beta 1, \beta 2, f1, f2, f3, f4, f5, f6, f7, f8)$$

that is, $\underline{b}_k$ is a column, row-partitioned according to (2.2).

Now, the only non-zero elements in $\underline{B}$ are

$$\underline{b}_{wf1} = -b_{wf3} = \underline{b}_{wf5} = -\underline{b}_{wf7} = \underline{\hat{f}}_1$$

$$\underline{b}_{wf2} = -\underline{b}_{wf4} = \underline{b}_{wf6} = -\underline{b}_{wf8} = \underline{\hat{f}}_2$$

$$\underline{b}_{\theta c1} = \underline{1}_1; \qquad \underline{b}_{\theta c2} = \underline{1}_2; \qquad \underline{b}_{\theta c3} = \underline{1}_3$$

$$\underline{b}_{\theta f1} = -\underline{b}_{\theta f2} = \underline{b}_{\theta f3} = -\underline{b}_{\theta f4} = [0, 0, \tfrac{\sqrt{3}}{2}\ell_c]^T$$

$$\underline{b}_{\theta f5} = -\underline{b}_{\theta f7} = [-\tfrac{\sqrt{3}}{2}\ell_z, -\tfrac{1}{2}\ell_z, \tfrac{1}{2}\ell_y]^T \tag{2.49}$$

$$\underline{b}_{\theta f6} = -b_{\theta f8} = [\tfrac{\sqrt{3}}{2}\ell_z, -\tfrac{1}{2}\ell_z, \tfrac{1}{2}\ell_y]^T$$

$$\underline{b}_{\beta\beta 1} = [1, 0]^T; \qquad \underline{b}_{\beta\beta 2} = [0, 1]^T$$

$$\underline{b}_{\delta f5} = -\underline{b}_{\delta f7} = \underline{C}_{tb}\hat{\underline{f}}_1 \; ; \qquad \underline{b}_{\delta f6} = -\underline{b}_{\delta f8} = \underline{C}_{tb}\hat{\underline{f}}_2$$

$$\underline{b}_{\alpha f5} = -\underline{b}_{\alpha f7} = \underline{r}_{tr}^{x}\underline{C}_{tb}\hat{\underline{f}}_1 \; ; \quad \underline{b}_{\alpha f6} = -\underline{b}_{\alpha f8} = \underline{r}_{tr}^{x}\underline{C}_{tb}\hat{\underline{f}}_2 \qquad \text{(2.49) con't}$$

Here, $\underline{C}_{tb}$ is the rotation matrix from the bus to the tower frame (see MSAT-5) and $\underline{r}_{tr}$ is the 'vector' locating the tower end O_r relative to the tower root O_t (again, see MSAT-5).

The modal input matrix corresponding to (2.47) is

$$\hat{\underline{\mathcal{B}}} = \underline{E}^T\underline{\mathcal{B}} = \begin{bmatrix} \underline{E}_r^T\underline{\mathcal{B}}_r \\ \underline{E}_{ee}^T\underline{\mathcal{B}} \end{bmatrix} \qquad (2.50)$$

where (2.12) has been applied and

$$\underline{\mathcal{B}} = \begin{bmatrix} \underline{\mathcal{B}}_r \\ \underline{\mathcal{B}}_e \end{bmatrix} \; ; \qquad \underline{E}_{ee} = \begin{bmatrix} \underline{E}_{re} \\ \underline{E}_e \end{bmatrix} \qquad (2.51)$$

The individual rows of $\underline{E}_{ee}^T\underline{\mathcal{B}}_e$, denoted $\hat{\underline{b}}_\alpha^T$, where

$$\hat{\underline{b}}_\alpha^T = \underline{e}_\alpha^T\underline{\mathcal{B}} \qquad (2.52)$$

will later prove useful in the modal cost evaluation of the flexible spacecraft modes. Here, $\underline{e}_\alpha$ (a column of $\underline{E}_{ee}$) is the eigenvector associated with the flexible mode α of the assembled spacecraft.

2.5 The Output Matrix

2.5.1 The Important Outputs

As stated in section 2.1 the output matrix $\underline{P}$ relates the important outputs $\underline{y}$ to the spacecraft coordinates $\underline{q}$ via

$$\underline{y} = \underline{Pq} \qquad (2.53)$$

Here, *important* outputs refers to the configurational variables that must be maintained within suitable limits. For MSAT these are assumed to be:

(i) the three attitude angles of the bus, $\underline{\theta}_b$.

(ii) the relative displacement of the reflector to the bus (normalized by the reflector focal length, f) caused by structural deformations in the tower, $\underline{\delta}/f$.

(iii) the relative rotation of the reflector to the bus, caused by structural deformations in the tower, $\underline{\alpha}$.

(iv) the reflector gimbal angles, $\underline{\beta}$.

All of these variables are especially 'important' in the case of MSAT as they affect the pointing accurracy for either the bus [(i)] or the reflector [(i) - (iv)]. Now, recalling (2.2), the output and modal output matrices are

$$\underline{P} = [\underline{P} \quad \underline{O}]; \qquad \hat{\underline{P}} = \underline{PE} \tag{2.54}$$

where

$$\underline{P} = \begin{bmatrix} \underline{0} & \underline{1} & \underline{0} & \underline{0} & \underline{0} \\ \underline{0} & \underline{0} & \underline{0} & f^{-1}\underline{1} & \underline{0} \\ \underline{0} & \underline{0} & \underline{0} & \underline{0} & \underline{1} \\ \underline{0} & \underline{0} & \underline{1} & \underline{0} & \underline{0} \end{bmatrix} \tag{2.55}$$

and

$$\underline{y} = \mathrm{col}\{\underline{\theta}_b, f^{-1}\underline{\delta}, \underline{\alpha}, \underline{\beta}\} \tag{2.56}$$

2.5.2 The Weighted Output

Rather than assess the relative importance of each of the eleven important outputs, a weighted sum of squares of the y_i is used as a single measure of system deviation from the desired (null) state:

$$y_Q^2(t) = \underline{y}^T \underline{Q} \underline{y} \tag{2.57}$$

Here,

$$y_Q^2(t) = w_1(\theta_{b1}^2 + \theta_{b2}^2) + w_2\theta_{b3}^2$$
$$+ w_3[(\theta_{b1} + \theta_{rx} + \beta_{rx})^2 + (\theta_{b2} + \theta_{ry} + \beta_{ry})^2]$$
$$+ w_4(\theta_{b3} + \theta_{rz} + \beta_{rz})^2 \qquad (2.58)$$

is assumed. Roll and pitch (θ_{b1} and θ_{b2}) are weighted equally; however, yaw (θ_{b3}) is weighted differently. The small rotations of the groundward reflector beam about the bus axes, as a consequence of structural deformations of the tower and the gimbal angles at the reflector, are represented by $\underline{\theta}_r$ and $\underline{\beta}_r$, respectively. To obtain the total deflection of the beam from the ideal vertical direction, $\underline{\theta}_r$, $\underline{\beta}_r$ and $\underline{\theta}_b$ must be summed. Again, the roll and pitch (x and y) components of the beam deflection are weighted equally, while the yaw (z) component is given a different weight. (To be consistent with MSAT-1, the chosen weights are $w_1 = w_3 = 1.0$, $w_2 = w_4 = 0.6$.)

Now, since from MSAT-1, $\theta_{rz} = 0$ and, from Appendix B, $\beta_{rz} = 0$, the matrix equivalent to (2.58) becomes

$$y_Q^2 = \underline{y}^T\underline{W}\,\underline{y} \qquad (2.59)$$

where

$$\underline{y} = \text{col}\{\underline{\theta}_b, \theta_{rx}, \theta_{ry}, \beta_{rx}, \beta_{ry}\} \qquad (2.60)$$

$$\underline{W} = \begin{bmatrix} \underline{W}_{11} & \underline{W}_{12} & \underline{W}_{12} \\ & w_3\underline{1} & w_3\underline{1} \\ \text{(symmetric)} & & w_3\underline{1} \end{bmatrix} \qquad (2.61)$$

and

$$\underline{W}_{11} = \text{diag}\{(w_1 + w_3), (w_1 + w_3), (w_2 + w_4)\} \qquad (2.62)$$

$$\underline{W}_{12}^T = w_3 \begin{bmatrix} 1 & 0 & 0 \\ 0 & 1 & 0 \end{bmatrix} \tag{2.63}$$

Furthermore, the important outputs are related to $\underline{\mathcal{y}}$ by the expression

$$\underline{\mathcal{y}} = \begin{bmatrix} \underline{1} & \underline{0} & \underline{0} & \underline{0} \\ \underline{0} & \underline{P}_{r\delta} & \underline{P}_{r\alpha} & \underline{0} \\ \underline{0} & \underline{0} & \underline{0} & \underline{P}_{r\beta} \end{bmatrix} \underline{y} \tag{2.64}$$

where, $\underline{P}_{r\delta}$, $\underline{P}_{r\alpha}$, and $\underline{P}_{r\beta}$ depend only on f* (= f/D_p), the ratio of the focal length to the (aperture) diameter of the 'parent' paraboloid of revolution, a portion of which forms the MSAT reflector (see Appendix B). Consequently, the weighting matrix in (2.57) becomes

$$\underline{Q} = \begin{bmatrix} \underline{W}_{11} & \underline{W}_{12}\underline{P}_{r\delta} & \underline{W}_{12}\underline{P}_{r\alpha} & \underline{W}_{12}\underline{P}_{r\beta} \\ & w_3\underline{P}_{r\delta}^T\underline{P}_{r\delta} & w_3\underline{P}_{r\delta}^T\underline{P}_{r\alpha} & w_3\underline{P}_{r\delta}^T\underline{P}_{r\beta} \\ & & w_3\underline{P}_{r\alpha}^T\underline{P}_{r\alpha} & w_3\underline{P}_{r\alpha}^T\underline{P}_{r\beta} \\ (\text{symmetric}) & & & w_3\underline{P}_{r\beta}^T\underline{P}_{r\beta} \end{bmatrix} \tag{2.65}$$

Finally, (2.57) can be written in terms of the spacecraft coordinates $\underline{q}$ using (2.56):

$$y_Q^2 = \underline{q}^T\underline{\mathcal{Q}}\underline{q} = \underline{n}^T\underline{\hat{\mathcal{Q}}}\underline{n} \tag{2.66}$$

where, given (2.54),

$$\underline{\mathcal{Q}} = \underline{P}^T\underline{QP} = \begin{bmatrix} \underline{\mathcal{P}}^T\underline{Q}\underline{\mathcal{P}} & \underline{0} \\ \underline{0} & \underline{0} \end{bmatrix} \quad ; \quad \underline{\hat{\mathcal{Q}}} = \underline{E}^T\underline{\mathcal{Q}}\underline{E} \tag{2.67}$$

The advantages of this form will become apparent during the modal cost evaluation of the flexible spacecraft modes.

3. SUBSTRUCTURE MODEL REDUCTION

3.1 Pre-Reduction Spacecraft Coordinates

As eluded to in Chapter 2, the assembled spacecraft coordinates are the translation and rotation of the bus, the reflector gimbal angles, the relative displacement and rotation of the tower tip to the tower root, the modal array coordinates, the internal tower coordinates, and the modal reflector coordinates. Recall (2.2),

$$\underline{q} = \text{col}\{\underline{w}_b, \underline{\theta}_b, \underline{\beta}, \underline{\delta}, \underline{\alpha}, \underline{n}_a, \underline{q}_i, \underline{n}_r\} \tag{3.1}$$

The number of spacecraft coordinates (and hence modes) prior to substructure model reduction is, therefore, $n_{TOT} = 3+3+2+3+3+n_a+n_i+n_r = 14+n_a+n_i+n_r$. Now, from MSAT-4, the pre-reduced reflector and solar array substructures have 42 and 38 modes, respectively. Also, the number of internal tower modes is either 4 or 14, depending on whether a two- or four-element finite-element model is chosen. Consequently, n_{TOT} = 98 or 108. The natural frequencies for each case are shown in Table 3. The large values for n_{TOT} suggest that it is desirable to perform some model reduction at the substructural level prior to applying modal cost analysis to the spacecraft modes.

3.2 A Modal Momentum Selection Criterion

It was argued in MSAT-4, that the *modal identities*

$$\sum_{\alpha=1}^{\infty} \underline{P}_\alpha \underline{P}_\alpha^T = m\underline{1} \tag{3.2}$$

$$\sum_{\alpha=1}^{\infty} \underline{H}_\alpha \underline{P}_\alpha^T = \underline{c}^\times \tag{3.3}$$

$$\sum_{\alpha=1}^{\infty} \underline{H}_\alpha \underline{H}_\alpha^T = \underline{J} \tag{3.4}$$

Table 3

Spacecraft Natural Frequencies Prior to Substructure Reduction

Four-Element Tower Model

MODE	(rad/sec)	(Hz)
1	0.000	0.000
2	0.000	0.000
3	0.000	0.000
4	0.000	0.000
5	0.000	0.000
6	0.000	0.000
7	0.000	0.000
8	0.000	0.000
9	0.124	0.020
10	0.151	0.024
11	0.240	0.038
12	0.341	0.054
13	0.556	0.089
14	0.690	0.110
15	0.744	0.118
16	0.780	0.124
17	1.023	0.163
18	1.087	0.173
19	1.156	0.184
20	1.460	0.232
21	1.553	0.247
22	1.623	0.258
23	1.661	0.264
24	1.747	0.278
25	1.831	0.291
26	1.937	0.308
27	2.262	0.360
28	2.298	0.366
29	2.306	0.367
30	2.429	0.387
31	2.429	0.387
32	2.472	0.393
33	2.790	0.444
34	2.790	0.444
35	3.137	0.499
36	3.957	0.630
37	5.971	0.950
38	6.025	0.959
39	6.651	1.058
40	7.547	1.201
41	8.633	1.374
42	8.804	1.401
43	9.949	1.583
44	10.107	1.609
45	10.107	1.609
46	10.161	1.617
47	10.241	1.630
48	10.242	1.630
49	10.242	1.630
50	10.679	1.700
51	10.679	1.700
52	10.700	1.703
53	10.700	1.703
54	11.236	1.708
55	11.652	1.854
56	12.821	2.041
57	13.159	2.094
58	13.180	2.098
59	13.478	2.145
60	13.857	2.205
61	13.857	2.205
62	13.865	2.207
63	13.865	2.207
64	14.008	2.229
65	14.125	2.248
66	14.275	2.272
67	15.514	2.469
68	15.519	2.470
69	15.736	2.504
70	15.736	2.504
71	15.742	2.505
72	15.742	2.505
73	15.881	2.528
74	17.183	2.735
75	17.184	2.735
76	17.238	2.743
77	17.238	2.743
78	17.241	2.744
79	17.241	2.744
80	17.264	2.748
81	20.469	3.258
82	21.617	3.440
83	21.915	3.488
84	24.027	3.824
85	24.739	3.937
86	28.935	4.605
87	30.942	4.925
88	33.726	5.368
89	37.040	5.895
90	39.003	6.208
91	40.031	6.371
92	40.388	6.428
93	41.594	6.620
94	42.133	6.706
95	46.740	7.439
96	47.930	7.628
97	51.107	8.134
98	55.801	8.881
99	57.803	9.200
100	64.908	10.330
101	77.784	12.380
102	87.024	13.850
103	90.101	14.340
104	100.423	15.983
105	117.201	18.653
106	119.198	18.971
107	138.402	22.027
108	143.140	22.781

Two-Element Tower Model

MODE	(rad/sec)	(Hz)
1	0.000	0.000
2	0.000	0.000
3	0.000	0.000
4	0.000	0.000
5	0.000	0.000
6	0.000	0.000
7	0.000	0.000
8	0.000	0.000
9	0.124	0.020
10	0.151	0.024
11	0.240	0.038
12	0.341	0.054
13	0.556	0.089
14	0.690	0.110
15	0.744	0.118
16	0.781	0.124
17	1.023	0.163
18	1.087	0.173
19	1.156	0.184
20	1.460	0.232
21	1.571	0.250
22	1.626	0.259
23	1.663	0.265
24	1.747	0.278
25	1.831	0.291
26	1.937	0.308
27	2.263	0.360
28	2.300	0.366
29	2.306	0.367
30	2.429	0.387
31	2.429	0.387
32	2.472	0.393
33	2.790	0.444
34	2.790	0.444
35	4.071	0.648
36	5.781	0.920
37	6.009	0.956
38	6.045	0.962
39	6.651	1.059
40	7.548	1.201
41	8.804	1.401
42	10.107	1.609
43	10.107	1.609
44	10.162	1.617
45	10.233	1.629
46	10.242	1.630
47	10.242	1.630
48	10.679	1.700
49	10.679	1.700
50	10.700	1.703
51	10.700	1.703
52	11.632	1.851
53	12.646	2.013
54	12.826	2.041
55	13.159	2.094
56	13.180	2.098
57	13.402	2.146
58	13.857	2.205
59	13.857	2.205
60	13.865	2.207
61	13.865	2.207
62	14.193	2.259
63	15.514	2.469
64	15.519	2.470
65	15.736	2.504
66	15.736	2.504
67	15.742	2.505
68	15.742	2.505
69	15.840	2.521
70	15.861	2.524
71	16.888	2.688
72	17.183	2.735
73	17.184	2.735
74	17.238	2.743
75	17.238	2.743
76	17.241	2.744
77	17.241	2.744
78	17.272	2.749
79	21.777	3.466
80	21.922	3.489
81	24.027	3.824
82	24.722	3.935
83	33.701	5.364
84	37.037	5.895
85	39.009	6.208
86	40.026	6.370
87	40.414	6.432
88	41.593	6.620
89	47.874	7.619
90	55.801	8.881
91	57.798	9.199
92	64.865	10.324
93	77.779	12.379
94	86.970	13.842
95	90.101	14.340
96	119.189	18.970
97	138.399	22.027
98	143.140	22.781

can be used in conjunction with the norms of $\underline{P}_\alpha$ and $\underline{H}_\alpha$ to select the important reflector and array modes. Simply, the modes with the most linear and angular momentum should be retained. The number of modes retained is determined by how well the selected modes satisfy (3.2) - (3.4) compared to the original identities with ∞ = 42 for the reflector and 38 for the array. That is, combining (3.2) - (3.4) according to

$$\underline{M}_\alpha = \begin{bmatrix} \underline{P}_\alpha \underline{P}_\alpha^T & \underline{P}_\alpha \underline{H}_\alpha^T \\ \underline{H}_\alpha \underline{P}_\alpha^T & \underline{H}_\alpha \underline{H}_\alpha^T \end{bmatrix} \tag{3.5}$$

where

$$\underline{M}_\infty = \begin{bmatrix} m\underline{1} & -\underline{c}^X \\ \underline{c}^X & \underline{J} \end{bmatrix} \quad ; \quad \sum_{\alpha=1}^{\infty} \underline{M}_\alpha = \underline{M}_\infty \tag{3.6}$$

and defining

$$\varepsilon_M(N) = \rho[\underline{1} - \underline{M}_\infty^{-\frac{1}{2}}(\sum_{\alpha=1}^{N} \underline{M}_\alpha)\underline{M}_\infty^{-\frac{1}{2}}] \tag{3.7}$$

where $\rho[\cdot]$ is the spectral norm of $[\cdot]$, the original modal identity error is found by setting N = 42 (38) for the reflector (array) in (3.7). The modal identity error for the modes selected on the basis of the norms of $\underline{P}_\alpha$ and $\underline{H}_\alpha$ is then

$$\varepsilon_M(\alpha_N) = \rho[\underline{1} - \underline{M}_\infty^{-\frac{1}{2}}\left(\sum_{\alpha=\alpha_1}^{\alpha_N} \underline{M}_\alpha\right)\underline{M}_\infty^{-\frac{1}{2}}] \tag{3.8}$$

where

$$\begin{aligned} &\| \underline{P}_{\alpha_1} \| \geq \| \underline{P}_{\alpha_2} \| \geq \| \underline{P}_{\alpha_3} \| \geq \cdots \\ &\| \underline{H}_{\alpha_1} \| \geq \| \underline{H}_{\alpha_2} \| \geq \| \underline{H}_{\alpha_3} \| \geq \cdots \end{aligned} \tag{3.9}$$

Unfortunately, as Tables 4 and 5 show, (3.9) is not, in general, true. Not surprisingly, the fact that the magnitude of the linear momentum in one mode

Table 4

Modal Momentum Norms for the MSAT Reflector

MODAL MOMENTUM COEFFICIENT NORMS

MODE	FREQ (rad/sec)	P-NORMS ($kg^{1/2}$)	H-NORMS ($kg^{1/2}m$)
1	2.0892	7.667D-05	1.910D+02
2	2.1793	5.984D+00	1.249D+01
3	2.1793	5.984D+00	1.249D+01
4	2.4285	6.640D-08	3.557D-07
5	2.4285	1.165D-07	8.959D-07
6	2.7902	8.500D-08	3.289D-07
7	2.7902	1.403D-07	2.964D-07
8	9.9974	5.764D-04	5.119D+01
9	10.0251	3.589D+00	1.558D+00
10	10.0251	3.589D+00	1.558D+00
11	10.1075	3.414D-08	7.083D-07
12	10.1075	3.568D-09	8.781D-08
13	10.2421	3.906D-08	1.611D-07
14	10.2421	6.258D-08	2.324D-07
15	10.6624	7.727D+00	1.836D-04
16	10.6665	5.587D-01	1.254D+02
17	10.6665	5.587D-01	1.254D+02
18	10.6792	1.315D-08	2.052D-06
19	10.6792	1.181D-08	1.250D-06
20	10.7000	1.514D-08	2.875D-06
21	10.7000	3.025D-08	1.550D-06
22	13.8573	4.525D-09	9.548D-07
23	13.8573	4.925D-09	4.512D-07
24	13.8652	1.443D-08	4.405D-07
25	13.8652	2.463D-09	4.357D-07
26	13.8700	1.907D-01	5.041D+01
27	13.8700	1.907D-01	5.057D+01
28	13.8716	3.203D+00	2.027D-03
29	15.7355	3.285D-09	3.117D-07
30	15.7355	2.686D-09	1.773D-07
31	15.7423	2.384D-09	1.078D-07
32	15.7423	6.382D-09	9.833D-08
33	15.7464	9.251D-02	2.520D+01
34	15.7464	9.252D-02	2.520D+01
35	15.7478	1.776D+00	3.227D-03
36	17.2378	6.953D-10	2.593D-07
37	17.2378	3.763D-10	1.328D-07
38	17.2408	2.031D-10	1.846D-07
39	17.2408	3.293D-09	1.423D-07
40	17.2424	3.800D-02	1.048D+01
41	17.2424	3.785D-02	1.048D+01
42	17.2430	6.919D-01	2.138D-03

ORDERED MODAL MOMENTUM COEFFICIENT NORMS

P-NORMS ($kg^{1/2}$)	MODE	H-NORMS ($kg^{1/2}m$)	MODE
7.727D+00	15	1.910D+02	1
5.984D+00	2	1.254D+02	16
5.984D+00	3	1.254D+02	17
3.589D+00	9	5.119D+01	8
3.589D+00	10	5.057D+01	27
3.203D+00	28	5.041D+01	26
1.776D+00	35	2.520D+01	34
6.919D-01	42	2.520D+01	33
5.587D-01	17	1.249D+01	2
5.587D-01	16	1.249D+01	3
1.907D-01	27	1.048D+01	41
1.907D-01	26	1.048D+01	40
9.252D-02	34	1.558D+00	9
9.251D-02	33	1.558D+00	10
3.800D-02	40	3.227D-03	35
3.785D-02	41	2.138D-03	42
5.764D-04	8	2.027D-03	28
7.667D-05	1	1.836D-04	15
1.403D-07	7	2.875D-06	20
1.165D-07	5	2.052D-06	18
8.500D-08	6	1.550D-06	21
6.640D-08	4	1.250D-06	19
6.258D-08	14	9.548D-07	22
3.906D-08	13	8.959D-07	5
3.414D-08	11	7.083D-07	11
3.025D-08	21	4.512D-07	23
1.514D-08	20	4.405D-07	24
1.443D-08	24	4.357D-07	25
1.315D-08	18	3.557D-07	4
1.181D-08	19	3.289D-07	6
6.382D-09	32	3.117D-07	29
4.925D-09	23	2.964D-07	7
4.525D-09	22	2.593D-07	36
3.568D-09	12	2.324D-07	14
3.293D-09	39	1.846D-07	38
3.285D-09	29	1.773D-07	30
2.686D-09	30	1.611D-07	13
2.463D-09	25	1.423D-07	39
2.384D-09	31	1.328D-07	37
6.953D-10	36	1.078D-07	31
3.763D-10	37	9.833D-08	32
2.031D-10	38	8.781D-08	12

Table 5

Modal Momentum Norms for the MSAT Solar Array

MODAL MOMENTUM COEFFICIENT NORMS

MODE	FREQ (rad/sec)	P-NORMS ($kg^{1/2}$)	H-NORMS ($kg^{1/2}m$)
1	0.1563	1.285D+01	3.548D+02
2	0.1945	1.288D+01	3.533D+02
3	0.3409	1.160D-01	1.367D+01
4	0.6648	2.754D+00	2.262D+01
5	0.7446	7.969D-02	1.502D+00
6	1.0769	3.104D+00	1.197D+01
7	1.1555	1.842D-01	2.909D+00
8	1.4590	4.353D-01	3.504D+00
9	1.6148	1.155D+00	5.099D+00
10	1.6562	1.008D+00	4.342D+00
11	1.7442	1.660D+00	4.282D+00
12	1.8309	1.359D-01	2.768D-01
13	1.9365	7.867D-02	1.187D+00
14	2.2745	5.772D+00	7.706D+00
15	2.4272	6.136D+00	1.474D+01
16	5.8823	8.322D+00	6.286D+00
17	6.6413	2.394D+00	8.367D+00
18	7.4079	6.604D+00	6.658D+00
19	8.7902	2.751D+00	1.975D+00
20	12.7046	5.356D+00	4.459D+00
21	13.3141	5.504D+00	4.475D+00
22	18.5668	1.547D+01	1.815D+00
23	24.0269	1.216D-01	1.086D-01
24	24.5044	3.080D+00	2.035D+00
25	33.4454	3.222D+00	1.828D+00
26	36.9200	3.245D+00	1.948D+00
27	39.9359	2.093D+00	1.191D+00
28	41.5821	7.740D-01	4.002D-01
29	46.9982	5.129D+00	1.058D+00
30	55.8010	1.195D-01	5.809D-02
31	57.7048	1.666D+00	4.185D-01
32	64.0257	4.764D+00	9.969D-01
33	77.6602	1.641D+00	6.595D-01
34	86.0796	3.810D+00	5.983D-01
35	90.1009	2.548D-02	2.200D-02
36	119.0664	1.121D+00	5.593D-02
37	138.3557	5.969D-01	3.128D-01
38	143.1310	4.080D-01	3.706D-01

ORDERED MODAL MOMENTUM COEFFICIENT NORMS

P-NORMS ($kg^{1/2}$)	MODE	H-NORMS ($kg^{1/2}m$)	MODE
1.547D+01	22	3.548D+02	1
1.288D+01	2	3.533D+02	2
1.285D+01	1	2.262D+01	4
8.322D+00	16	1.474D+01	15
6.604D+00	18	1.367D+01	3
6.136D+00	15	1.197D+01	6
5.772D+00	14	8.367D+00	17
5.504D+00	21	7.706D+00	14
5.356D+00	20	6.658D+00	18
5.129D+00	29	6.286D+00	16
4.764D+00	32	5.099D+00	9
3.810D+00	34	4.475D+00	21
3.245D+00	26	4.459D+00	20
3.222D+00	25	4.342D+00	10
3.104D+00	6	4.282D+00	11
3.080D+00	24	3.504D+00	8
2.754D+00	4	2.909D+00	7
2.751D+00	19	2.035D+00	24
2.394D+00	17	1.975D+00	19
2.093D+00	27	1.948D+00	26
1.666D+00	31	1.828D+00	25
1.660D+00	11	1.815D+00	22
1.641D+00	33	1.502D+00	5
1.155D+00	9	1.191D+00	27
1.121D+00	36	1.187D+00	13
1.008D+00	10	1.058D+00	29
7.740D-01	28	9.969D-01	32
5.969D-01	37	6.595D-01	33
4.353D-01	8	5.983D-01	34
4.080D-01	38	4.185D-01	31
1.842D-01	7	4.002D-01	28
1.359D-01	12	3.706D-01	38
1.216D-01	23	3.128D-01	37
1.195D-01	30	2.768D-01	12
1.160D-01	3	1.086D-01	23
7.969D-02	5	5.809D-02	30
7.867D-02	13	5.593D-02	36
2.548D-02	35	2.200D-02	35

is greater than that in another does not ensure that the same relationship holds for the angular momentum. However, (3.8) can still be used, where now $\alpha_i \varepsilon [(\delta_1, \delta_2, \ldots \delta_m) \cup (\varepsilon_1, \varepsilon_2, \ldots \varepsilon_n)]$, with δ_i and ε_i determined from the criteria

$$\begin{aligned} \| \underline{P}_{\delta_1} \| \geq \| \underline{P}_{\delta_2} \| \geq \cdots \| \underline{P}_{\delta_m} \| \geq \| \underline{P}_0 \| ; m \leq N \\ \| \underline{H}_{\varepsilon_1} \| \geq \| \underline{H}_{\varepsilon_2} \| \geq \cdots \| \underline{P}_{\varepsilon_n} \| \geq \| \underline{H}_0 \| ; n < N \end{aligned} \qquad (3.10)$$

for some chosen $\| \underline{P}_0 \|$ and $\| \underline{H}_0 \|$. This selection criteria was applied to both the reflector and the array for several $\| \underline{P}_0 \|$ and $\| \underline{H}_0 \|$. In particular, the chosen values were

$$\| \underline{P}_0 \| = \kappa \| P_{max} \| ; \qquad \| \underline{H}_0 \| = \kappa \| \underline{H}_{max} \| \qquad (3.11)$$

$$\kappa = (0.1, 0.05, 0.02, 0.01, 0.001) \qquad (3.12)$$

The modes retained in each case are documented in Table 6 along with the resulting sums from (3.7) and (3.8) [the α_i were ordered according to ascending frequency in calculating (3.8)].

It is disturbing that, for the array, selecting 23 of 38 possible modes according to (3.10) produces an $\varepsilon_M(23) = 0.736$ in comparison to $\varepsilon_M(38) = 0.0145$. Furthermore, it can also be shown that simple modal truncation outperforms criteria (3.10) in this case (see Fig. 3.4). Hence, an alternate modal selection criterion was sought. One possible criterion is suggested by the form of (3.7), namely, rank the modes according to

$$\rho_{\alpha 1} > \rho_{\alpha 2} > \rho_{\alpha 3} \quad \cdots \qquad (3.13)$$

where ρ_α is defined by

$$\rho_\alpha = \rho [\underline{M}_\infty^{-\frac{1}{2}} \underline{M}_\alpha \underline{M}_\infty^{-\frac{1}{2}}] \qquad (3.14)$$

The ρ_α for the MSAT reflector and array are given in Figs. 3.1 and 3.2. Figures 3.3 and 3.4 show the consequence of applying (3.8) based on modes re-ordered according to (3.13), rather than applying the modes in natural

Table 6

Modes Selected According to Modal Momentum

Reflector: $\varepsilon_M(42) = 0.659$

κ	Modes Retained (α_i)	Number of modes (N)	$\varepsilon_M(N)$
0.1	1,2,3,8,9, 10,15,16,17,26, 27,28,33,34,35	15	0.659
0.05 0.02 0.01 0.001	as for $\kappa = 0.1$ plus: 40,41,42	18	0.659

Array: $\varepsilon_M(38) = 0.0142$

κ	Modes Retained (α_i)	Number of modes (N)	$\varepsilon_M(N)$
0.1	1,2,4,6,11, 14,15,16,17,18, 19,20,21,22,24, 25,26,27,29,31, 32,33,34	23	0.736
0.05	as for $\kappa = 0.1$ plus: 9,10,28,36	27	0.638
0.02	as for $\kappa = 0.05$ plus: 3,8,37,38	31	0.0347
0.01	as for $\kappa = 0.02$ plus: 7	32	0.0146
0.001	as for $\kappa = 0.01$ plus: 5,13	34	0.0145

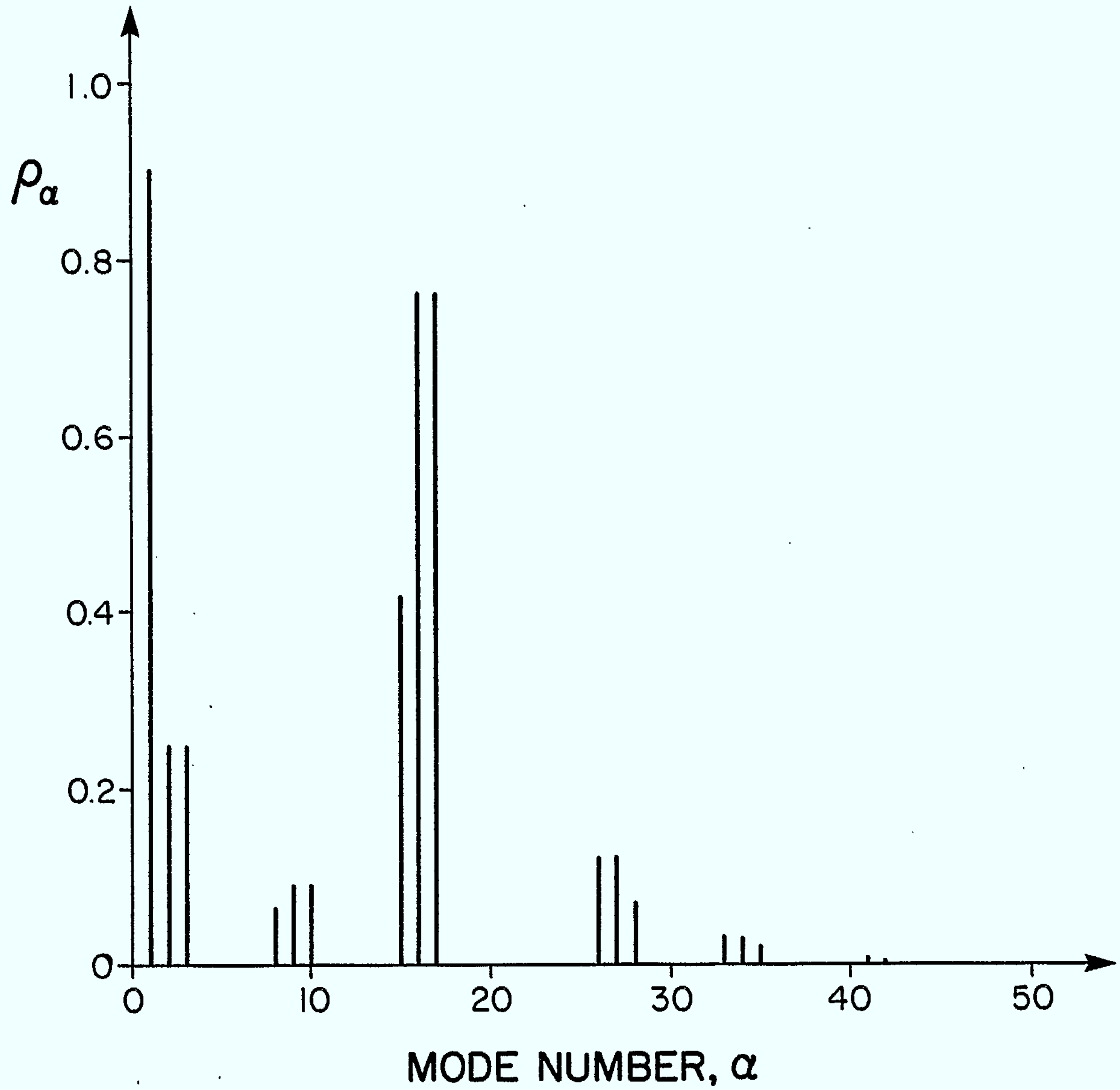

Fig. 3.1 Dynamical Significance of Reflector Modes Measured by ρ_α (3.14)

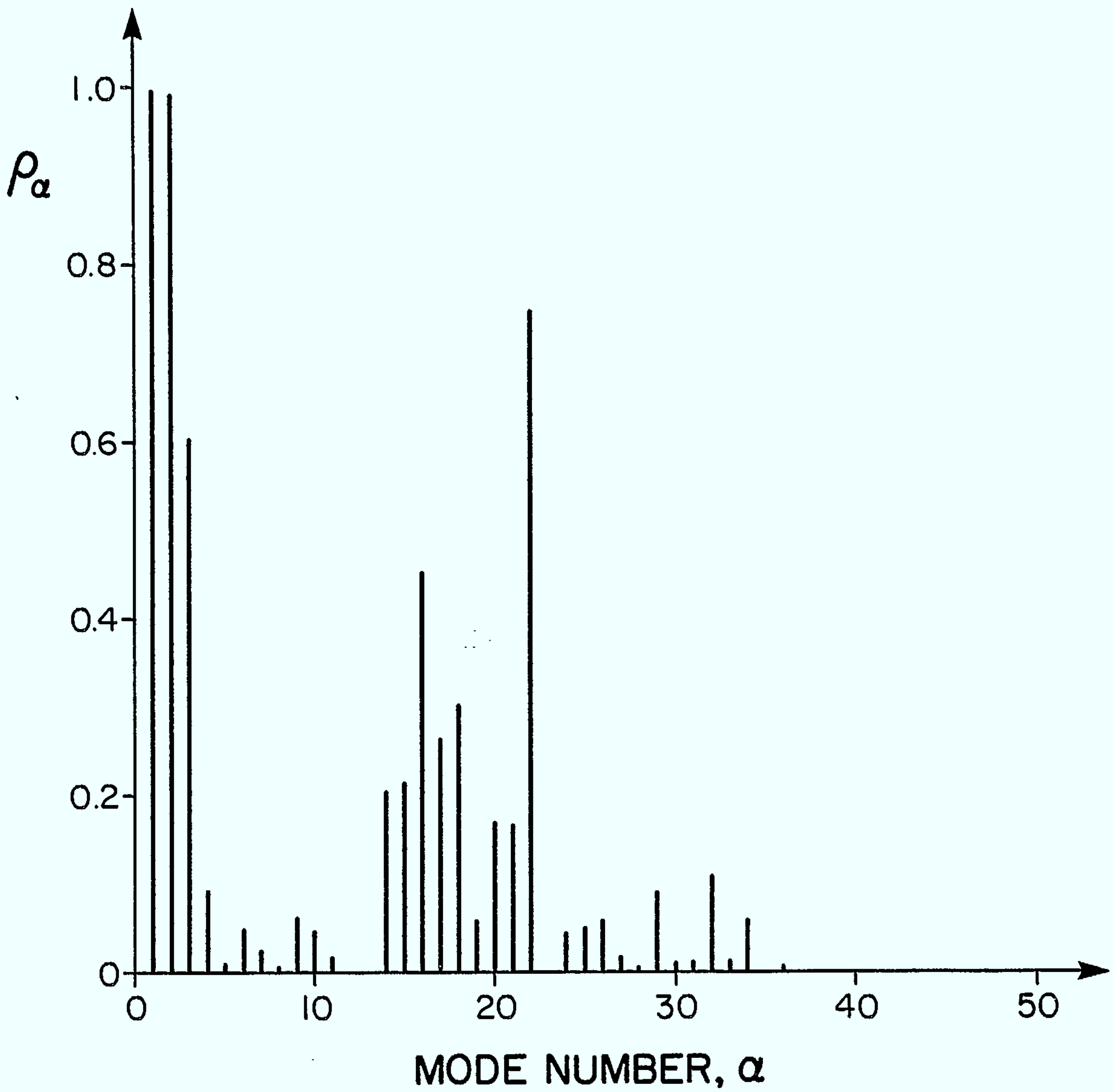

Fig. 3.2 Dynamical Significance of Array Modes Measured by ρ_α (3.14)

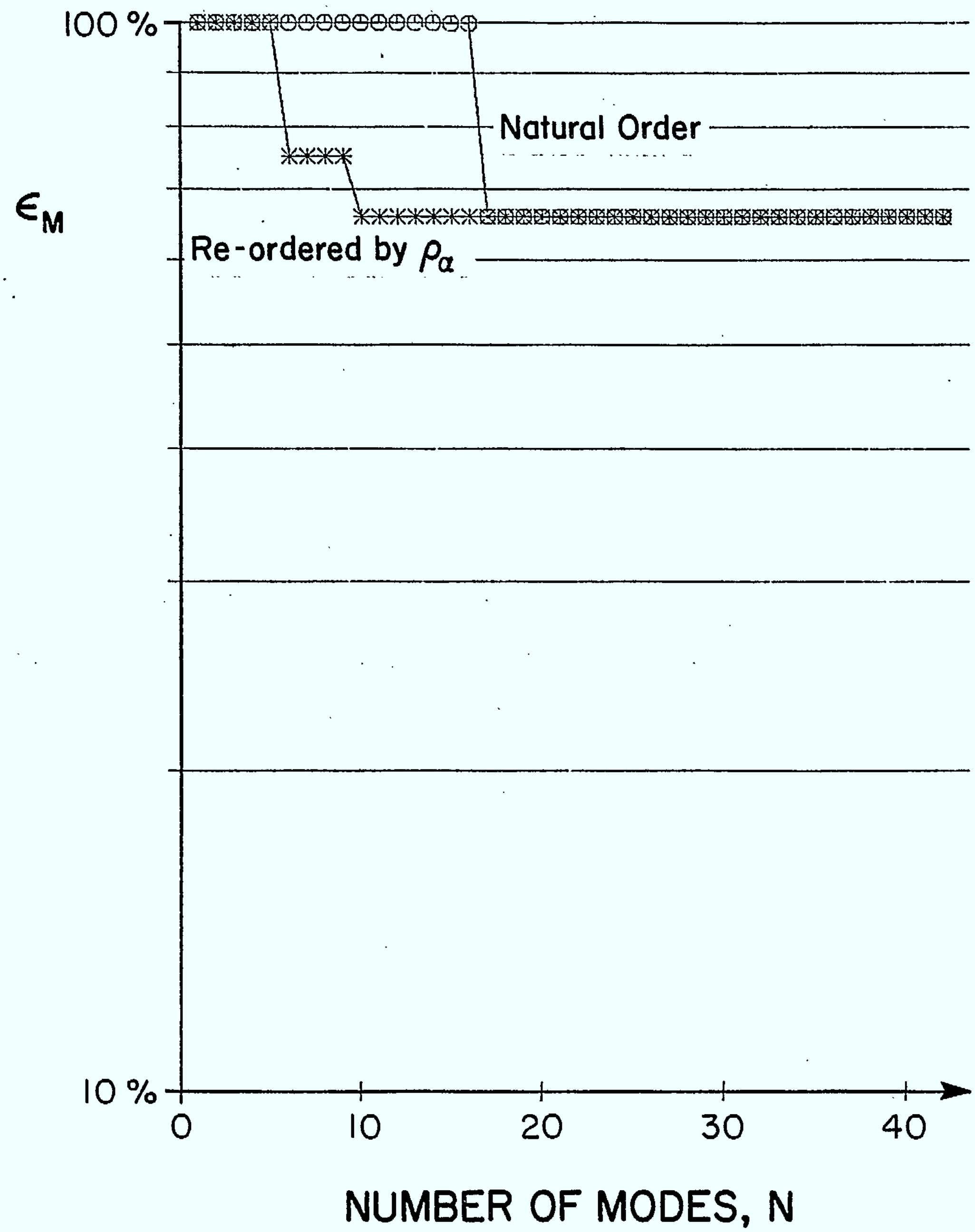

Fig. 3.3 Reduction of Model Error for Reflector Using (3.7) and (3.8)

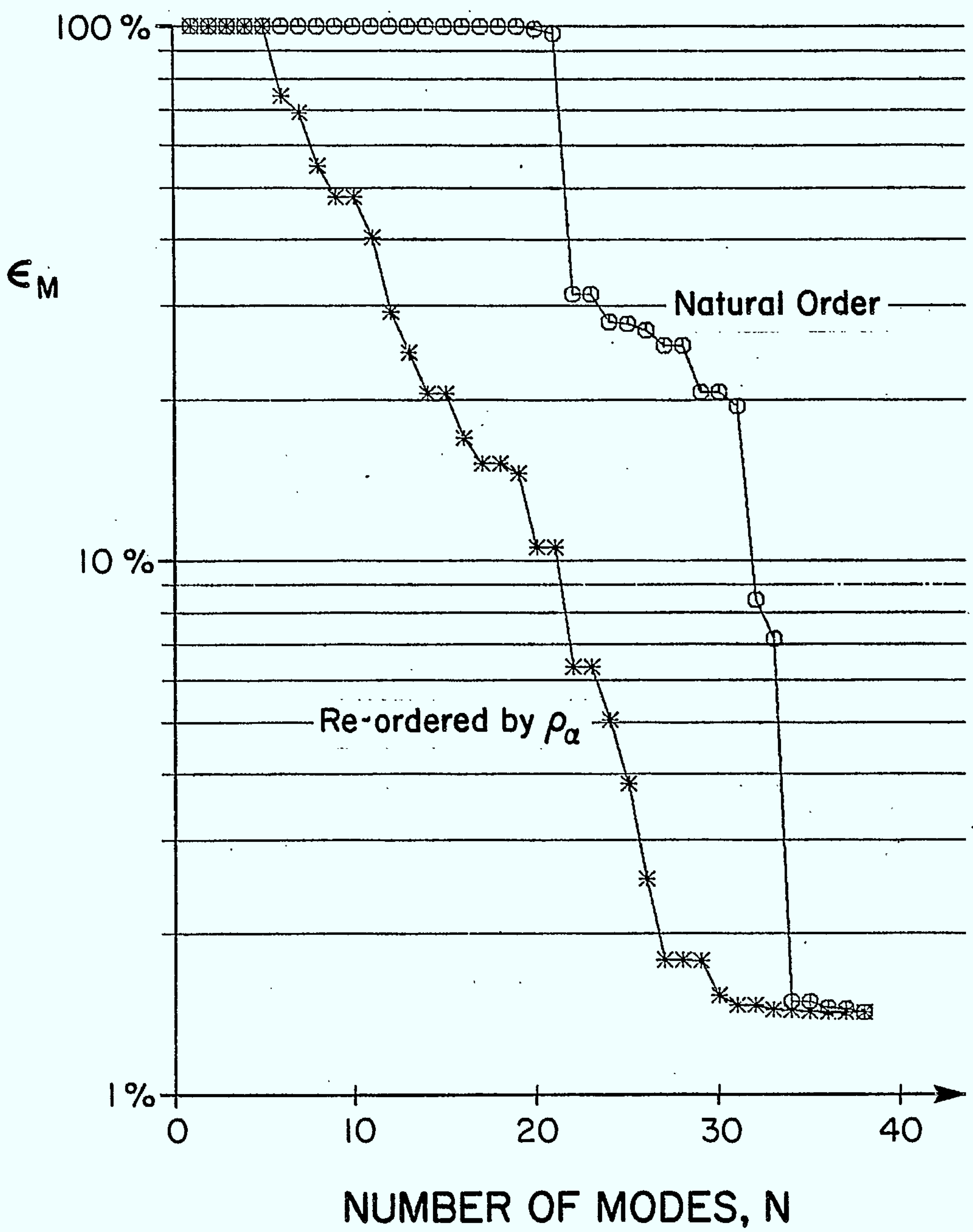

Fig. 3.4 Reduction of Model Error for Array Using (3.7) and (3.8)

order (i.e. according to ascending frequency) as is done in (3.7). The improvement is dramatic for both the reflector and array. Very few modes are required to obtain acceptable agreement between $\varepsilon_M(\alpha_N)$ and $\varepsilon_M(N)$. Note however, that for the reflector the best that can be achieved is $\varepsilon_M(42) = 0.659$, where theoretically for an infinite number of modes $\varepsilon_M(\infty) = 0$. This suggests that the 42-mode reflector model is 66% in error. Obviously equation (3.7) is too stringent a criterion upon which to base modal selection. Essentially, the application of criteria based on (3.7), which neglect frequency information, is just as gross an over-simplification as truncating modes based solely on ascending frequency and neglecting modal momentum. Happily, a modal selection criteria incorporating both frequency and modal momentum information exists [Hughes, 1980]. This is the topic of the next section. However, prior to considering this combined criterion it is interesting to highlight certain aspects of Fig. 3.3 and Fig. 3.4.

As stated in [Hughes, 1982], "just because a portion of $\varepsilon_M(N)$, or $\varepsilon_M(\alpha_N)$, versus N is 'flat' does not mean that intermediate modes are not making a positive contribution. This behavior just means that they are not contributing to reducing the maximum eigenvalue of (3.7)," that is, the spectral radius of (3.7). The slow convergence in Fig. 3.3 was traced to the slow convergence of the $\sum_{\alpha=1}^{\infty} \underline{P}_{\alpha}\underline{P}_{\alpha}^T = m\underline{1}$ identity implicit in (3.7). Note, however, that re-ordering the modes according to (3.13) improves the rate of convergence, but does not alter the final value for $\varepsilon_M(N)$. The improvement in the rate of convergence is most apparent for the array model (see Fig. 3.4).

Finally, while (3.7) is not the best relation upon which to base modal selection criterion it is useful in assessing the initial completeness of the reflector and array models. As stated previously, ideally $\varepsilon_M(N) = 0$, for $N = \infty$. This condition is enforced by the structure of (3.7), where the fact that $\sum_{\alpha=1}^{\infty} \underline{M}_{\alpha} = \underline{M}_{\infty}$ has been used to normalize the cummulative sum $\sum_{\alpha=1}^{N} \underline{M}_{\alpha}$ and $\underline{M}_{\infty}$, through pre- and post-multiplication by $\underline{M}_{\infty}^{-\frac{1}{2}}$. This retains symmetry while transforming the ideal sum to $\underline{1}$ (6×6). Now, the cummulative sum in (3.7) is non-decreasing since $\underline{M}_{\alpha}$ is positive definite. Hence the matrix difference in (3.7) is also positive definite for finite N. The six eigenvalues of this resultant matrix are, therefore, real numbers between 0 and 1. For $N = \infty$ all six eigenvalues are zero. For $N < \infty$, $\varepsilon_M(N)$ is the largest of the six eigenvalues and hence represents the largest error. Consequently, $\varepsilon_M(N)$ may be large while the majority of the eigenvalues are small. This is exactly what occurs in Fig. 3.3 where the $\sum_{\alpha=1}^{N} \underline{P}_\alpha \underline{P}_\alpha^T$ portion of $\sum_{\alpha=1}^{N} \underline{M}_\alpha$ is slow to converge while the other portions of $\sum_{\alpha=1}^{N} \underline{M}_\alpha$ are much more rapidly convergent. This suggests that, from the point of view of completeness, only a portion of the MSAT reflector model is truly 66% incomplete, namely, the linear momentum associated with the reflector 'breathing' modes. The remainder of the model is much more complete. The MSAT solar array model, however, does not suffer from this difficiency and is over 98% complete, based on (3.7).

3.3 A Modal Momentum and Frequency Selection Criterion

It is a well established result [Hughes, 1980] that the modal momentum and natural frequencies of a flexible structure satisfy the following identities,

$$\sum_{\alpha=1}^{\infty} \frac{\underline{P}_\alpha \underline{P}_\alpha^T}{\omega_\alpha^2} = \int_E \int_E \underline{F}(\underline{r},\underline{\xi})\sigma(\underline{r})\sigma(\underline{\xi})d\underline{r}\, d\underline{\xi} \tag{3.15}$$

$$\sum_{\alpha=1}^{\infty} \frac{\underline{H}_\alpha \underline{P}_\alpha^T}{\omega_\alpha^2} = \int_E \int_E \underline{r}^\times \underline{F}(\underline{r},\underline{\xi})\sigma(\underline{r})\sigma(\underline{\xi})d\underline{r}\, d\underline{\xi} \tag{3.16}$$

$$\sum_{\alpha=1}^{\infty} \frac{\underline{H}_\alpha \underline{H}_\alpha^T}{\omega_\alpha^2} = \int_E \int_E \underline{r}^\times \underline{F}(\underline{r},\underline{\xi})\underline{\xi}^\times\sigma(\underline{r})\sigma(\underline{\xi})d\underline{r}\, d\underline{\xi} \tag{3.17}$$

Here, $\underline{F}(\underline{r},\underline{\xi})$ is the flexibility kernel of the structure, $\sigma(\underline{r})$ is the volumne mass density at $\underline{r}$, where $\underline{r}$ is a position vector to a point on the structure relative to some arbitrary reference point, and the integration is performed over the volume of the elastic portion of the structure E. In a manner analogous to that employed in the previous section (3.15) - (3.17) can be written in the matrix form

$$\sum_{\alpha=1}^{\infty} \underline{\Xi}_\alpha = \underline{\Xi}_\infty \tag{3.18}$$

where

$$\underline{\Xi}_\alpha = \omega_\alpha^{-2} \underline{M}_\alpha \tag{3.19}$$

$$\underline{\Xi}_\infty = \int_E \int_E \left[\frac{1}{\underline{r}^X}\right] \underline{F}(\underline{r},\underline{\xi}) \left[\frac{1}{\underline{\xi}^X}\right] \sigma(\underline{r})\sigma(\underline{\xi}) d\underline{r}\, d\underline{\xi} \tag{3.20}$$

The error indicator corresponding to (3.7) is then

$$\varepsilon_\Xi(N) = \rho\left[\underline{1} - \underline{\Xi}_\infty^{-\frac{1}{2}} \left(\sum_{\alpha=1}^{N} \underline{\Xi}_\alpha\right) \underline{\Xi}_\infty^{-\frac{1}{2}}\right] \tag{3.21}$$

with the 'best' value for $\underline{\Xi}_\infty$ given by the sum $\sum_{\alpha=1}^{N} \underline{\Xi}_\alpha$ evaluated over all the available structural modes [N = 42 (38) for the reflector (array)]. Again, (3.21) is written in a normalized form, with $\varepsilon_\Xi(N)$ representing the largest eigenvalue of the matrix difference. It is also possible to define an error indicator analogous to (3.8),

$$\varepsilon_\Xi(\alpha_N) = \rho\left[\underline{1} - \underline{\Xi}_\infty^{-\frac{1}{2}} \left(\sum_{\alpha=\alpha_1}^{\alpha_N} \underline{\Xi}_\alpha\right) \underline{\Xi}_\infty^{-\frac{1}{2}}\right] \tag{3.22}$$

where

$$\rho_{\alpha 1} > \rho_{\alpha 2} > \rho_{\alpha 3} > \cdots \tag{3.23}$$

and the new definition for ρ_α is patterned after (3.14):

$$\rho_\alpha = \rho\left[\underline{\Xi}_\infty^{-\frac{1}{2}} \underline{\Xi}_\alpha \underline{\Xi}_\infty^{-\frac{1}{2}}\right] \tag{3.24}$$

Plots of $\varepsilon_\Xi(N)$ and $\varepsilon_\Xi(\alpha_N)$, labeled 'natural order' and 're-ordered by ρ_α', respectively, are given in Fig. 3.5 for the MSAT reflector. The corresponding plots for the array are shown in Fig. 3.6. The relative magnitudes for the various ρ_α in each case are presented in Figs. 3.7 and 3.8. As before, a substantial improvement in the percentage error results when the modes

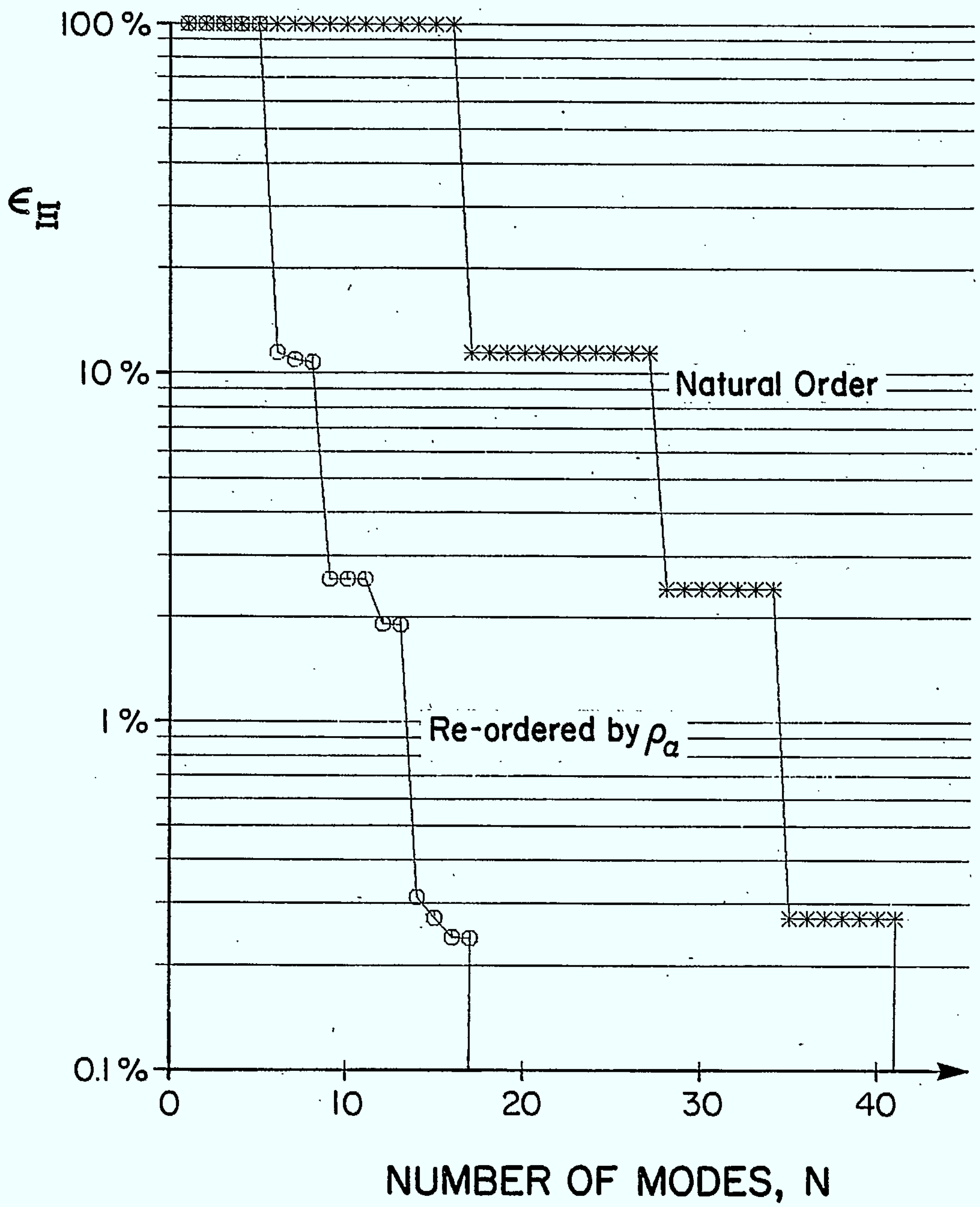

Fig. 3.5 Reduction of Model Error for Reflector Using (3.21) and (3.22)

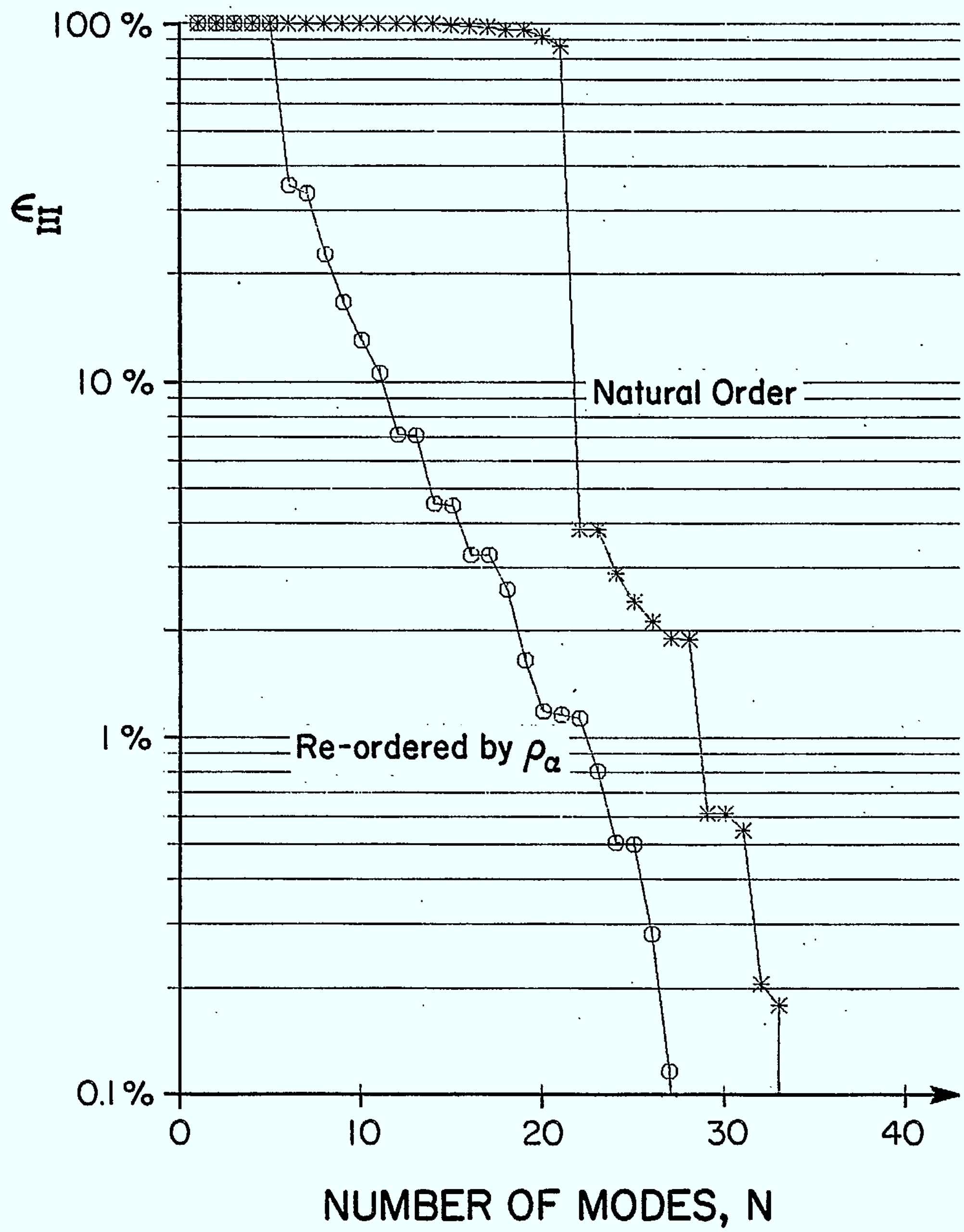

Fig. 3.6 Reduction of Model Error for Array Using (3.21) and (3.22)

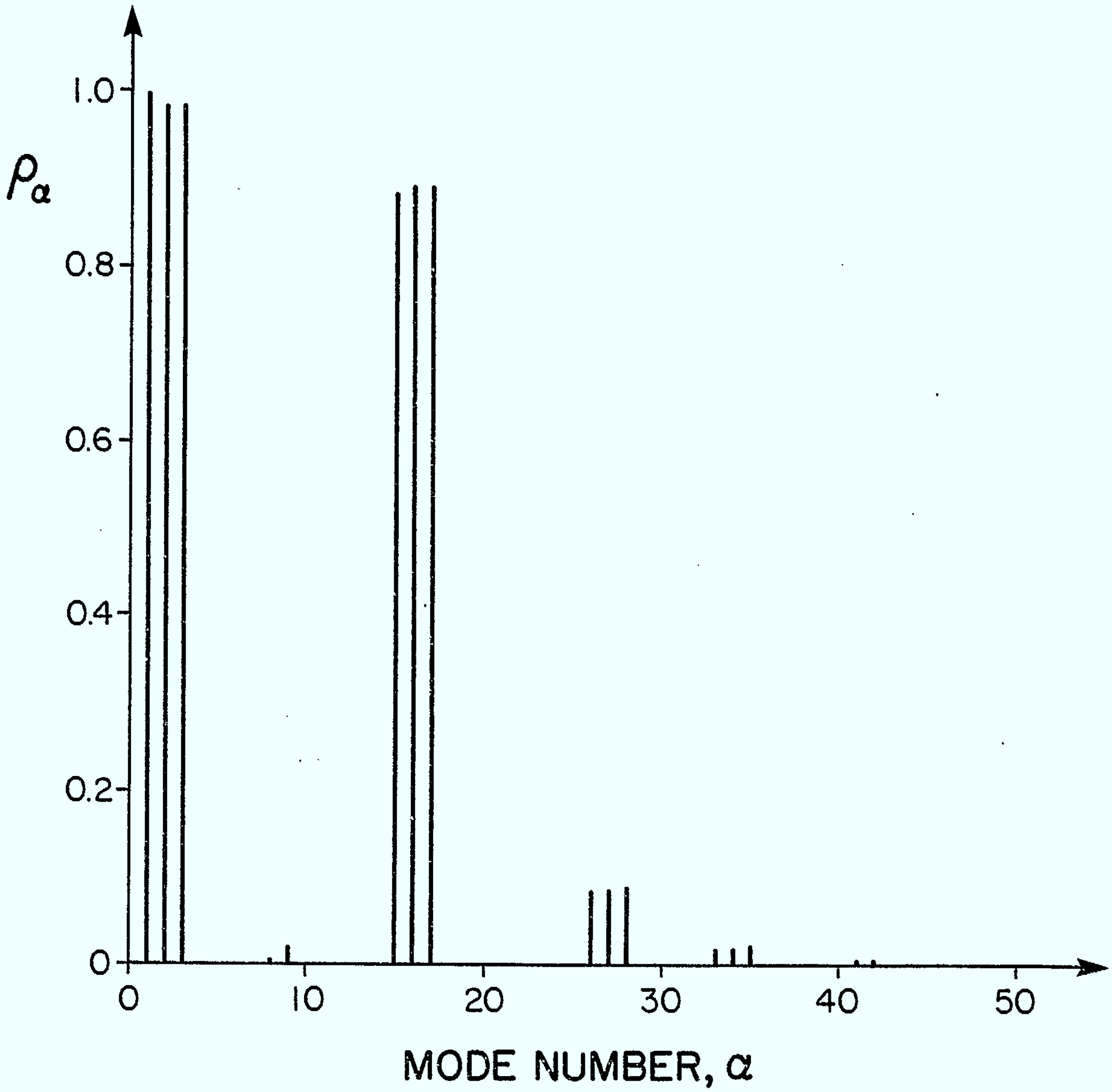

Fig. 3.7 Dynamical Significance of Reflector Modes Measured by ρ_α (3.24)

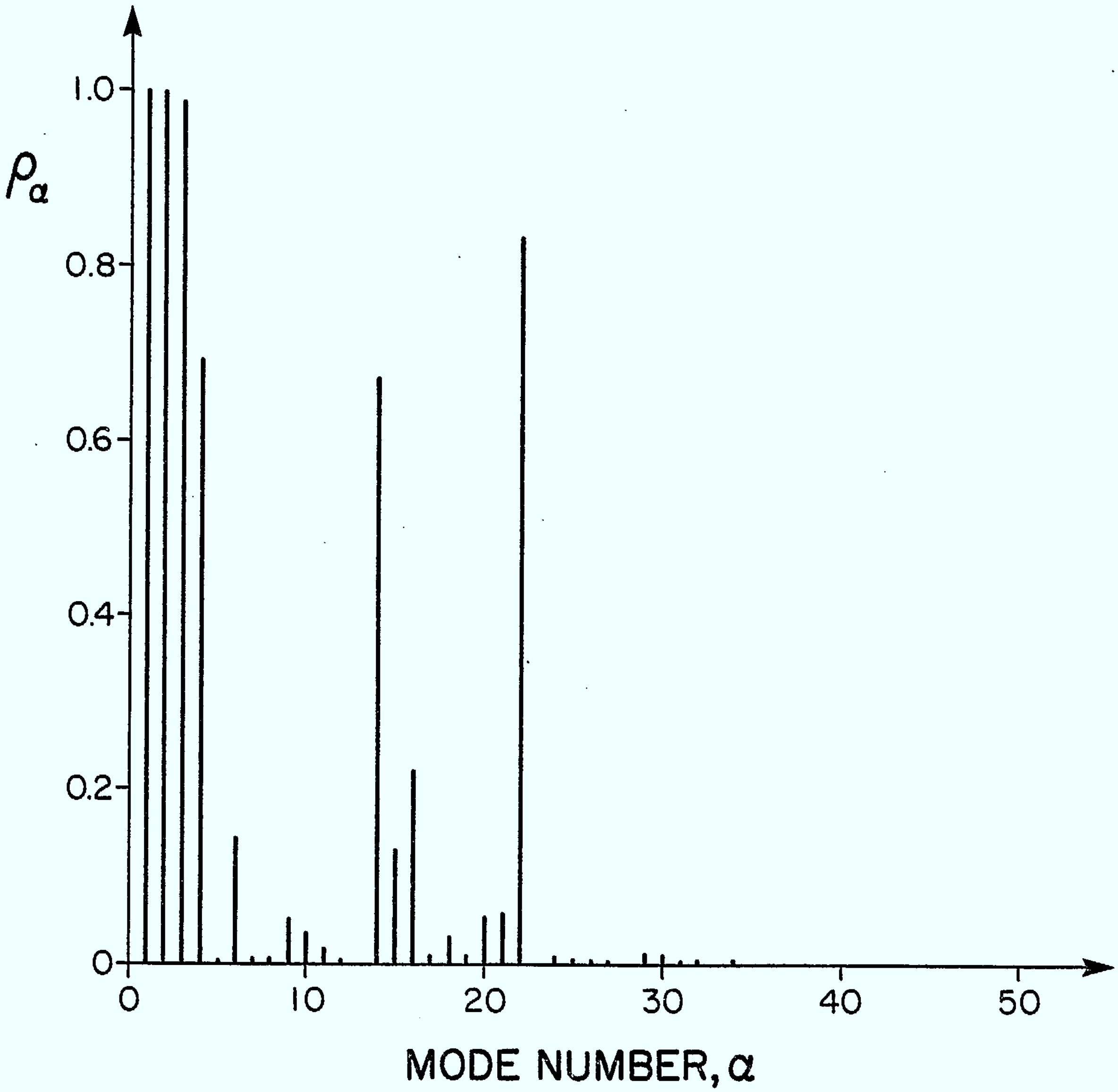

Fig. 3.8 Dynamical Significance of Array Modes Measured by ρ_α (3.24)

are re-ordered. For the reflector, prior to re-ordering, 35 modes are necessary to guarantee an error of less than 0.1%, while after re-ordering only 18 modes are required. Similarly, only 27 array modes are required to guarantee an error of less than 0.1% after re-ordering compared with 34 before re-ordering.

It should be emphasized that once the modes required to guarantee a given error are determined, the final percentage error is independent of the order of the chosen modes because the cummulative sum in (3.22) commutes. For example, say that based on (3.23) and (3.24), $\alpha_1 = 10$, $\alpha_2 = 5$ and $\alpha_3 = 6$ ($N = 3$), then $\sum_{\alpha=\alpha_1}^{\alpha_N} \Xi_\alpha$ remains unchanged for $(\alpha_1,\alpha_2,\alpha_3) = (10,5,6)$ or $(5,6,10)$. The 18 reflector modes and 27 array modes selected according to (3.22) - (3.24) are given in Table 7, ranked according to (3.23); however, they are returned to 'natural' order in the actual software dynamics model for the MSAT spacecraft.

3.4 Post-Reduction Spacecraft Coordinates

Based on the decisions made in the previous section ($n_a = 27$ and $n_r = 18$), the total number of spacecraft modes becomes $n_{TOT} = 14 + n_a + n_i + n_r = 63$ or 73, depending on whether a two- or four-element tower model is adopted. To retain the highest degree of accuracy prior to applying modal cost analysis, we choose to adopt the four-element model. Consequently, substructure model reduction has decreased the size of the total system by 35 modes, a substantial saving. Furthermore, based on Figs. 3.5 and 3.6 this reduction has introduced very little error into the overall model. The natural frequencies for both the 63-mode and the 73-mode spacecraft models are provided in Table 8. By direct comparison with Table 3, one can easily identify which spacecraft modes have been deleted and the degree to which a given frequency changes as a consequence of the overall model reduction. It is noteworthy that the lower frequency modes change little as a result of this preliminary model reduction.

Table 7

Final Modes Selected According to a Combined Modal Momentum and Frequency Criterion

Reflector: $\varepsilon_{\Xi}(42) = 2.6 \times 10^{-16}$

Modes Retained (α_i)	Number of Modes (N)	$\varepsilon_{\Xi}(\alpha_N)$
1,2,3,16,17, 15,28,27,26,35, 10,9,34,33,8, 42,41,40	18	7.6×10^{-16}

Array: $\varepsilon_{\Xi}(38) = 1.6 \times 10^{-15}$

Modes Retained (α_i)	Number of Modes (N)	$\varepsilon_{\Xi}(\alpha_N)$
1,2,3,22,4, 14,16,6,15,21, 20,9,10,18,11, 29,19,17,24,25, 7,8,32,26,5, 27,34	27	5.8×10^{-4}

Table 8

Spacecraft Natural Frequencies After Substructure Reduction

Four-Element Tower Modal

MODE	(rad/sec)	(Hz) *
1	0.000	0.000
2	0.000	0.000
3	0.000	0.000
4	0.000	0.000
5	0.000	0.000
6	0.000	0.000
7	0.000	0.000
8	0.000	0.000
9	0.124	0.020
10	0.151	0.024
11	0.240	0.038
12	0.341	0.054
13	0.556	0.089
14	0.690	0.110
15	0.744	0.118
16	0.780	0.124
17	1.023	0.163
18	1.087	0.173
19	1.156	0.184
20	1.460	0.232
21	1.553	0.247
22	1.623	0.258
23	1.661	0.264
24	1.747	0.278
25	2.262	0.360
26	2.298	0.366
27	2.306	0.367
28	2.472	0.393
29	3.137	0.499
30	3.957	0.630
31	5.971	0.950
32	6.025	0.959
33	6.651	1.058
34	7.547	1.201
35	8.633	1.374
36	8.804	1.401
37	9.949	1.583
38	10.161	1.617
39	10.241	1.630
40	11.236	1.788
41	11.652	1.854
42	12.821	2.041
43	13.159	2.094
44	13.180	2.098
45	13.478	2.145
46	14.008	2.229
47	14.125	2.248
48	14.275	2.272
49	15.514	2.469
50	15.519	2.470
51	15.881	2.528
52	17.183	2.735
53	17.184	2.735
54	17.264	2.748
55	20.469	3.258
56	21.617	3.440
57	21.918	3.488
58	24.740	3.937
59	28.935	4.605
60	30.942	4.925
61	33.727	5.368
62	37.041	5.895
63	39.003	6.208
64	40.032	6.371
65	40.388	6.428
66	42.133	6.706
67	46.740	7.439
68	47.937	7.629
69	51.107	8.134
70	64.899	10.329
71	87.005	13.847
72	100.423	15.983
73	117.201	18.653

Two-Element Tower Model

MODE	(rad/sec)	(Hz)
1	0.000	0.000
2	0.000	0.000
3	0.000	0.000
4	0.000	0.000
5	0.000	0.000
6	0.000	0.000
7	0.000	0.000
8	0.000	0.000
9	0.124	0.020
10	0.151	0.024
11	0.240	0.038
12	0.341	0.054
13	0.556	0.089
14	0.690	0.110
15	0.744	0.118
16	0.781	0.124
17	1.023	0.163
18	1.087	0.173
19	1.156	0.184
20	1.460	0.232
21	1.571	0.250
22	1.626	0.259
23	1.663	0.265
24	1.747	0.278
25	2.263	0.360
26	2.300	0.366
27	2.306	0.367
28	2.472	0.393
29	4.071	0.648
30	5.781	0.920
31	6.009	0.956
32	6.045	0.962
33	6.651	1.059
34	7.548	1.201
35	8.804	1.401
36	10.162	1.617
37	10.233	1.629
38	11.632	1.851
39	12.646	2.013
40	12.826	2.041
41	13.159	2.094
42	13.180	2.098
43	13.482	2.146
44	14.193	2.259
45	15.514	2.469
46	15.519	2.470
47	15.840	2.521
48	15.861	2.524
49	16.888	2.688
50	17.183	2.735
51	17.184	2.735
52	17.272	2.749
53	21.779	3.466
54	21.922	3.489
55	24.723	3.935
56	33.702	5.364
57	37.037	5.895
58	39.009	6.208
59	40.027	6.370
60	40.414	6.432
61	47.879	7.620
62	64.858	10.322
63	86.953	13.839

* adopted model

4. SPACECRAFT MODEL REDUCTION

4.1 Modal Cost Analysis

A detailed explanation of the concept of modal cost is presented in Appendix E of MSAT-1, where a single control input is assumed. This analysis is extended to include multiple inputs in Section 4.4 of MSAT-6. Rather than repeat the details here, only a brief summary will be presented.

Let us assume that the control objective is to minimize some weighted scalar performance measure over time. From Section 2.5.2, for MSAT, this performance measure is $y_Q^2(t)$ and hence, one must minimize

$$V = \int_0^\infty y_Q^2(t)\,dt \tag{4.1}$$

It is shown in MSAT-1 that

$$V = \sum_{\alpha=1}^{n_{TOT}} V_\alpha \tag{4.2}$$

where, for a single impulsive control input

$$u_j(t) = \delta(t - t_j) \qquad (t_j > 0) \tag{4.3}$$

that is, the only non-zero component in $\underline{u}$ given in (2.1) is an impulse in the jth location, the *modal cost* is

$$V_{\alpha j} = \frac{\ell_\alpha^2 \hat{b}_{\alpha j}^2}{4\zeta_\alpha \omega_\alpha^3} \tag{4.4}$$

If all the components in $\underline{u}$ are simultaneously taken to be impulses, then from MSAT-6

$$V_\alpha = \frac{\ell_\alpha^2 \hat{\underline{b}}_\alpha^T \hat{\underline{b}}_\alpha}{4\zeta_\alpha \omega_\alpha^3} = \sum V_{\alpha j} \tag{4.5}$$

Here, ω_α and ζ_α are the natural frequency and the damping factor of the αth flexible mode, while $\hat{b}_{\alpha j}$ is the jth element in the row $\underline{\hat{b}}_\alpha^T$, defined by (2.52). $\hat{b}_{\alpha j}$ is a measure of how much a particular control input excites a given mode. The remaining variable i_α is called the involvement index and measures how 'involved' a particular mode is in the performance measure $y_Q^2(t)$. The reasoning is as follows, assume only the αth mode is present, and that the associated modal coordinate $\eta_\alpha = 1$ at the same instant. Then, since

$$\underline{q} = \underline{E\eta} \tag{4.6}$$

it follows that for the present situation $\underline{q}$ is simply the eigenvector associate with mode α, that is

$$\underline{q} = \underline{e}_\alpha \tag{4.7}$$

Consequently, with only the αth mode present

$$y_Q^2 = \underline{e}_\alpha^T \underline{Q} \underline{e}_\alpha \tag{4.8}$$

by virtue of (2.63). In fact, (4.8) is a measure of how much mode α contributes to, or is 'involved' in, y_Q^2. Hence the name, and the definition

$$i_\alpha^2 = \underline{e}_\alpha^T \underline{Q} \underline{e}_\alpha \tag{4.9}$$

Now, the desire to minimize (4.1) suggests that the flexible modes which produce the largest modal costs are the modes of greatest concern and should be the modes retained. They will require the largest control effort in order to minimize V. The modal costs for the 65 flexible modes of the 73-mode MSAT spacecraft model, ordered according to decreasing magnitude, are given in Table 9. The V_α shown in the table are those obtained from (4.5) because, although the actuators are considered to operate in pairs or alone, the total cost per mode over the range $(0, \infty)$ is the same whether the actuators act independently or simultaneously. Tables 10 and 11 give the damping factors and the involvement indices used in obtaining Table 9. The scalar factor $\underline{\hat{b}}_\alpha^T \underline{\hat{b}}_\alpha$ is not cited explicitly but can be obtained by applying (4.5) to the above tables.

Table 9

Reordered Modal Costs for the MSAT Spacecraft

FLEXIBLE MODE	MODAL COST	FLEXIBLE MODE	MODAL COST
1	3.29773D-04	61	3.76026D-09
8	1.60073D-04	37	1.48300D-09
3	1.34686D-04	23	1.35706D-09
5	5.22642D-05	50	1.28308D-09
13	3.70080D-05	4	1.14529D-09
2	1.83134D-05	11	1.06595D-09
6	1.15876D-05	16	5.21373D-10
22	7.71301D-06	35	4.86201D-10
38	6.90950D-06	36	4.26488D-10
29	6.16837D-06	64	3.14835D-10
21	2.93106D-06	24	1.86129D-10
14	1.69814D-06	26	1.34627D-10
59	1.44563D-06	33	4.14504D-11
58	1.26246D-06	53	3.90907D-11
15	6.00022D-07	34	3.90679D-11
51	3.05652D-07	65	3.37703D-11
10	2.28073D-07	28	2.65581D-11
57	1.56488D-07	62	1.20009D-11
31	1.36919D-07	25	5.95508D-12
32	1.10865D-07	12	5.53081D-12
49	8.01223D-08	47	5.06876D-12
27	5.91569D-08	42	3.26227D-12
7	4.30057D-08	63	3.25926D-12
39	3.85084D-08	41	3.15784D-12
9	3.54245D-08	43	1.26369D-12
20	3.37328D-08	30	1.06320D-12
40	2.76165D-08	60	3.94984D-13
55	2.75963D-08	56	3.22020D-13
18	2.67639D-08	54	2.41419D-13
17	1.78506D-08	44	3.25943D-14
52	1.54919D-08	45	2.35710D-14
19	1.10488D-08	46	8.64353D-15
48	3.90679D-11		

Table 10

Equivalent Viscous Modal Damping Factors for the

MSAT Spacecraft

FLEXIBLE MODE	ZETA	FLEXIBLE MODE	ZETA
1	7.42075D-03	34	5.11287D-03
2	5.64249D-03	35	5.11783D-03
3	7.11611D-03	36	5.11685D-03
4	5.01333D-03	37	5.18934D-03
5	1.53744D-02	38	8.35771D-02
6	8.03304D-03	39	7.40756D-03
7	5.15501D-03	40	7.31003D-03
8	2.70302D-02	41	5.04518D-03
9	7.89320D-03	42	5.04310D-03
10	5.58088D-03	43	5.08605D-03
11	5.04505D-03	44	5.01449D-03
12	5.00810D-03	45	5.01389D-03
13	4.83331D-02	46	5.01114D-03
14	9.22807D-03	47	1.01262D-02
15	7.27801D-03	48	1.86048D-02
16	5.03169D-03	49	7.41976D-03
17	5.32409D-03	50	5.27181D-03
18	5.68591D-03	51	1.53139D-02
19	5.32294D-03	52	1.91591D-02
20	5.27620D-03	53	5.16389D-03
21	8.94154D-03	54	5.03019D-03
22	1.33406D-02	55	1.68409D-02
23	5.23412D-03	56	5.02858D-03
24	1.26738D-02	57	1.73691D-02
25	5.01615D-03	58	2.25148D-02
26	5.18386D-03	59	7.22325D-02
27	1.77175D-02	60	5.25336D-03
28	5.02782D-03	61	3.35685D-02
29	5.30000D-02	62	5.12471D-03
30	5.07944D-03	63	5.09781D-03
31	8.15188D-03	64	5.50885D-03
32	7.75260D-03	65	8.62407D-02
33	5.47163D-03		

Table 11

Involvement Indicies for the MSAT Spacecraft

FLEXIBLE MODE	INDEX	FLEXIBLE MODE	INDEX
1	1.41916D-03	34	9.80672D-04
2	3.67406D-04	35	3.50192D-03
3	1.05611D-03	36	3.50496D-03
4	1.05026D-04	37	1.03251D-03
5	6.51688D-03	38	9.33199D-03
6	3.42988D-03	39	1.35604D-03
7	4.90099D-04	40	1.14655D-03
8	5.92777D-03	41	2.24036D-03
9	2.68372D-03	42	2.16799D-03
10	1.22012D-03	43	7.47846D-05
11	3.07661D-04	44	1.29749D-03
12	2.48061D-04	45	1.25779D-03
13	9.65069D-03	46	2.42500D-05
14	3.07082D-03	47	6.92218D-04
15	2.27739D-03	48	2.05238D-03
16	3.42394D-04	49	6.49602D-03
17	1.19566D-03	50	2.21829D-03
18	1.36707D-03	51	4.83260D-03
19	1.01576D-03	52	1.35736D-03
20	1.12827D-03	53	1.75973D-03
21	2.64229D-03	54	7.19197D-04
22	6.08602D-03	55	4.51211D-02
23	1.08914D-03	56	8.37266D-04
24	3.94046D-04	57	4.53702D-02
25	2.88634D-04	58	1.36197D-02
26	1.09115D-03	59	1.46283D-02
27	6.88617D-04	60	2.59509D-03
28	1.96311D-04	61	1.03089D-03
29	6.26902D-03	62	1.90550D-03
30	9.41901D-05	63	1.85055D-03
31	1.47269D-03	64	1.54467D-03
32	1.56342D-03	65	2.19222D-04
33	1.68215D-04		

It is now possible to select models for control design and evaluation based on modal costs.

4.2 The Design Model

A design model must incorporate two conflicting desires. The first is to choose all the flexible modes necessary to best approximate the true total modal cost. Let us assume that the original modal costs for each mode are reordered as in Table 9,

$$V_{\alpha 1} < V_{\alpha 2} < V_{\alpha 3} < \dots V_{\alpha_{n_{TOT}}} \tag{4.10}$$

Then ideally one retains modes $\alpha_1, \alpha_2, \dots \alpha_m$ ($m < n_{TOT}$) such that

$$V_m = \sum_{\alpha=\alpha_1}^{\alpha_m} V_{\alpha_1} \simeq V \tag{4.11}$$

However, the second desire--a relatively low-order model to limit computational expense at the design stage--implies that the smaller m, the better. This is especially true for MSAT where there are already 8 rigid modes to be included. It was decided, therefore, to choose m such that V_m is at least 85% of V. The modal costs in Table 9 are added in a cummulative sum until this requirement is satisfied. By retaining the four most important flexible modes, namely, modes 1, 8, 3 and 5 (these modes are listed in order of decreasing importance) a 12.5% error in V results. The design model for the MSAT spacecraft, therefore, consists of these four modes, plus the 8 rigid modes--12 modes altogether.

The system matrices for the design model are given in modal form in Appendix C. The corresponding governing equations are

$$\ddot{\underline{\eta}} + (\hat{\underline{\mathcal{D}}} + \hat{\underline{G}})\dot{\underline{\eta}} + \underline{\Omega}^2\underline{\eta} = \hat{\underline{\mathcal{B}}}\,u \tag{4.12}$$

$$\underline{y} = \hat{\underline{P}}\underline{\eta} \qquad y_Q^2 = \underline{\eta}^T\hat{\underline{\mathcal{Q}}}\underline{\eta} \tag{4.13}$$

where the modal damping matrix $\hat{\underline{D}}$ is given by (2.11), the modal gyroscopic matrix is a sum of three submatrices $\hat{\underline{G}}_i h_i$ according to (2.35), $\underline{\Omega}^2$ is zero except for the diagonal which consists of the squares of the natural frequencies of the system $\underline{M}\ddot{q} + \underline{K}q = \underline{0}$ (arranged in ascending order), the modal input (or control distribution) matrix $\hat{\underline{B}}$ is given by (2.50). Equation (2.54) describes the modal output matrix $\hat{\underline{P}}$, and the modal output weighing matrix $\hat{\underline{Q}}$ is represented by (2.63). The original physical coordinates $\underline{q}$ are related to the modal coordinates $\underline{\eta}$ by the transformation

$$\underline{q} = \underline{E}\,\underline{\eta} \tag{4.14}$$

where $\underline{E}$ is the eigenvector matrix for the system $\underline{M}\ddot{\underline{q}} + \underline{K}\underline{q} = \underline{0}$. The matrices given in Appendix C are ordered as follows: $\hat{\underline{B}}$, $\hat{\underline{P}}$, $\hat{\underline{Q}}$, $\hat{\underline{D}}_e$ and $\hat{\underline{G}}_i$ $(i = 1,2,3)$. The natural frequencies for the selected modes (ordered according to increasing frequency) are also included. Finally, the first 14 rows (those which correspond to the 11 output variables in $\underline{y}$, plus $\underline{w}_b$) of the matrix $\underline{E}$ are provided. The procedure used to obtain these matricies from their 73-mode model counterparts is detailed in Appendix C of MSAT-1 and is not repeated here.

4.3 The Evaluation Model

As the name suggests, the evaluation model is used to evaluate the control system design after the design has been completed. Consequently, the order of this model must be larger than that chosen for the control design model. Furthermore, this model is not used to iterate upon a control design and hence a larger order can also be tolerated from the point of view of computational expense. As with the design model, a threshold value for V_m can be chosen and modes retained until the accumlated sum of the V_α from Table 9 reaches this threshold value. For the evaluation model, $V_m < 0.99V$ has been chosen. (Recall that V is the sum of all the V_α in Table 9.) A 0.82% error results if the eleven flexible modes 1, 8, 3, 5, 13, 2, 6, 22, 38, 29, and 21 are retained. It is noteworthy that simple modal truncation would replace modes 13, 22, 38, 29 and 21 with less important lower modes.

The system matrices $\hat{\underline{B}}$, $\hat{\underline{P}}$, $\hat{\underline{Q}}$, $\hat{\underline{D}}_e$ and $\hat{\underline{G}}_i$. $(i = 1, 2, 3)$ for the 19-mode evaluation model are given in Appendix D, along with the corresponding natural frequencies and the top 14 rows of $\underline{E}$.

4.4 Some Comments on Damping

While the damping is assumed 'light' in each flexible substructure, it is interesting to enquire into the damping characteristics for the final assembled spacecraft model. In this regard, the spacecraft will be considered to be 'lightly' damped if

$$\| \underline{\Omega}^{-\frac{1}{2}} \underline{\mathcal{D}}_e \underline{\Omega}^{-\frac{1}{2}} \| \ll 2 \tag{4.1}$$

and the modal damping matrix will be considered 'diagonally dominant' if

$$\| \hat{\underline{\mathcal{D}}}_e^{off} \| \ll \| \hat{\underline{\mathcal{D}}}_e^{diag} \| \tag{4.2}$$

where (from MSAT-1) the norms of the off-diagonal terms ($\hat{\underline{\mathcal{D}}}_e^{off}$) and the diagonal terms ($\hat{\underline{\mathcal{D}}}_e^{diag}$) are given by

$$\| \hat{\underline{\mathcal{D}}}_e^{off} \| = \frac{2}{m(m-1)} \sum_{\substack{\alpha=1 \\ \alpha \neq \beta}}^{m} \sum_{\beta=1}^{m} | \hat{d}_{e\alpha\beta} | \tag{4.3}$$

$$\| \hat{\underline{\mathcal{D}}}_e^{diag} \| = \left[\prod_{\alpha=1}^{m} \hat{d}_{e\alpha\alpha} \right]^{1/m} \tag{4.4}$$

Here m is again the number of retained flexible modes and m = (4,11) for the (design, evaluation) model. A second criterion for diagonal dominance is given in MSAT-6, whereby (4.3) and (4.4) are replaced by

$$\| \hat{\underline{\mathcal{D}}}_e^{off} \|_\alpha = \| 4 \sum_{\substack{\beta=1 \\ \beta \neq \alpha}}^{m} \frac{\omega_\alpha^2}{\omega_\alpha^2 - \omega_\beta^2} \hat{d}_{e\alpha\beta} \underline{e}_{e\beta} \| \tag{4.5}$$

$$\| \hat{\underline{\mathcal{D}}}_e^{diag} \|_\alpha = \| \hat{d}_{e\alpha\alpha} \underline{e}_{e\alpha} \| \tag{4.6}$$

and (4.1) is applied on a mode-by-mode basis. Here, $\underline{e}_{e\gamma}$ ($\gamma = \alpha, \beta$) is a column of the matrix partition $\underline{E}_e$ defined in (2.12).

Application of (4.1) to the modal damping matrices for the design and evaluation spacecraft models reveals the system to be only marginally 'lightly' damped. The norm in (4.1) is always less than 0.4; however, a somewhat higher damping than anticipated occurs in the higher modes, resulting in (4.1) being only weakly satisfied. This tendency of the damping to increase (non-monotonically) with frequency in the assembled spacecraft, when the substructures are assumed to be hysteretically damped, is an unexpected result. It suggests that, while the damping model used for MSAT goes beyond the realm of a 'knowledgeable' guess, further work is still required to completely understand the various aspects of modeling damping.

Criterion (4.2) reveals, using each possible set of norms, that the modal damping matrices for the design and the evaluation models are not always diagonally dominant. While diagonal dominance is not a required assumption in the damping model assumed here, the control design will likely be formulated neglecting the off-diagonal terms in $\hat{\underline{\mathcal{D}}}_e$. If such a strategy is followed, then to assess the true importance of the off-diagonal terms the full $\hat{\underline{\mathcal{D}}}_e$ matrix should be employed in the computer simulations used to evaluate the design. In anticipation of this procedure, the full $\hat{\underline{\mathcal{D}}}_e$ matrix is provided in Appendices C and D.

5. CONCLUDING REMARKS

This brings to successful completion the current effort in modeling the structural dynamics of an MSAT-type spacecraft. This model has also been given to Spar Aerospace Ltd. and Electrical Engineering Consociates Ltd. as a meaningful math model on which to focus their control-system design efforts. It is also being given to the Jet Propulsion Laboratory to reciprocate for the JPL antenna reflector model used in this study. It is expected that other groups will also exercise their control design ideas on this model. The more individuals and groups there are who use *the same dynamical model*, the more concrete conclusions will be arrived at on control-related subjects.

Much technical experience has been gleaned in the process of developing this model. The reports in this series have been written with the objective of conveying to the reader as much of this experience as possible. Through this work a firm foundation has been constructed on which can be built dynamical models for a wide variety of communications satellites of the general class typified by the 'Operational MSAT' or 'Lazy-Z' configuration shown in Fig. 2.1 (p. 3).

Table of Reports in this Series

Dynacon Number	DOC Number	Author(s)	Title
MSAT-1	CR-SP-81-005	Hughes, P.C.	MSAT Structural Flexibility and Control Assessment
MSAT-2	CR-SP-81-006	Hughes, P.C.	A Dynamics Modeling Plan for MSAT
MSAT-3	(see Note 1)	Hughes, P.C.	Structural Dynamics Modeling Plan for Control System Design and Evaluation
MSAT-4†	CR-SP-82-022	Hughes, P.C. Sincarsin, G.B.	MSAT Structural Dynamics Model for Control System Evaluation
MSAT-5†	CR-SP-82-023	Sincarsin, G.B. Stoddard, I.A. Hughes, P.C.	Computer Code for MSAT Structural Dynamics Model (Preliminary)
MSAT-6†	CR-SP-82-024	Hughes, P.C.	Modeling of Energy Dissipation (Damping) in Flexible Space Structures
MSAT-7†	CR-SP-82-054	Sincarsin, G.B. Hughes, P.C.	MSAT Structural Dynamics Model for Control System Design
MSAT-8†	CR-SP-82-055	Sincarsin, G.B. Stoddard, I.A. Hughes, P.C.	Computer Code for MSAT Structural Dynamics Model
MSAT-9†	CR-SP-82-056	Hughes, P.C.	Development of Dynamics Models and Control System Design for Third Generation Spacecraft (Executive Summary)

†Prepared under the current contract
Note 1: Report MSAT-3 was prepared for Spar Aerospace Ltd. RMS Division

Appendix A

The disturbance inputs $\underline{u}_d$ given by (4.16) of reference 2 contain a minor omission. Specifically, the disturbances governing $\underline{\alpha}$ (the relative rotation of the reflector frame F_r with respect to the tower frame F_t, as a consequence of the tower's flexibility) should read

$$\underline{\delta}_\alpha + \underline{C}_{tr}\underline{g}_r + \underline{r}_{tr}^{\times}\underline{f}_{rt} \tag{A.1}$$

rather than

$$\underline{\delta}_\alpha + \underline{C}_{tr}\underline{g}_r \tag{A.2}$$

Appendix B

Effect of Reflector Gimbal Angles on Beam Pointing Accuracy

This appendix follows very closely Appendix D of MSAT-1. As such, much of the detail presented there is omitted here. Furthermore, a thorough knowledge of Appendix D is assumed. To aid comparison the section headings of Appendix D are duplicated here.

Ray Reflection

This section remains unchanged from that given in Appendix D of MSAT-1 except that, here, Fig. 1 is replaced by Fig. B1.

The Ideal Case: Parabolic Reflector and No Structural Deformations (and Zero Gimbal Angles)

Again, this section remains intact; however, the ideal case also includes the assumption of zero gimbal angles at the reflector hub ($\underline{\beta} \equiv 0$).

Perturbation in the Reflected Ray

No change is required here either; however, one should note that the change ($\delta\underline{n}$) in the beam pointing direction is now not just a function of structural deformations but also depends on the small gimbal angles β_1 and β_2 ($\beta_3 \equiv 0$).

Reflector Deformations

This section should be re-titled, "Variation in Beam Pointing Direction Caused by Structural Deformations and Gimbal Angles." As in Appendix D, the elastic deformations in the reflector support tower are considered, while those of the reflector surface itself are neglected. To be consistent with MSAT-5, the displacement of O_r, the origin of the reflector reference

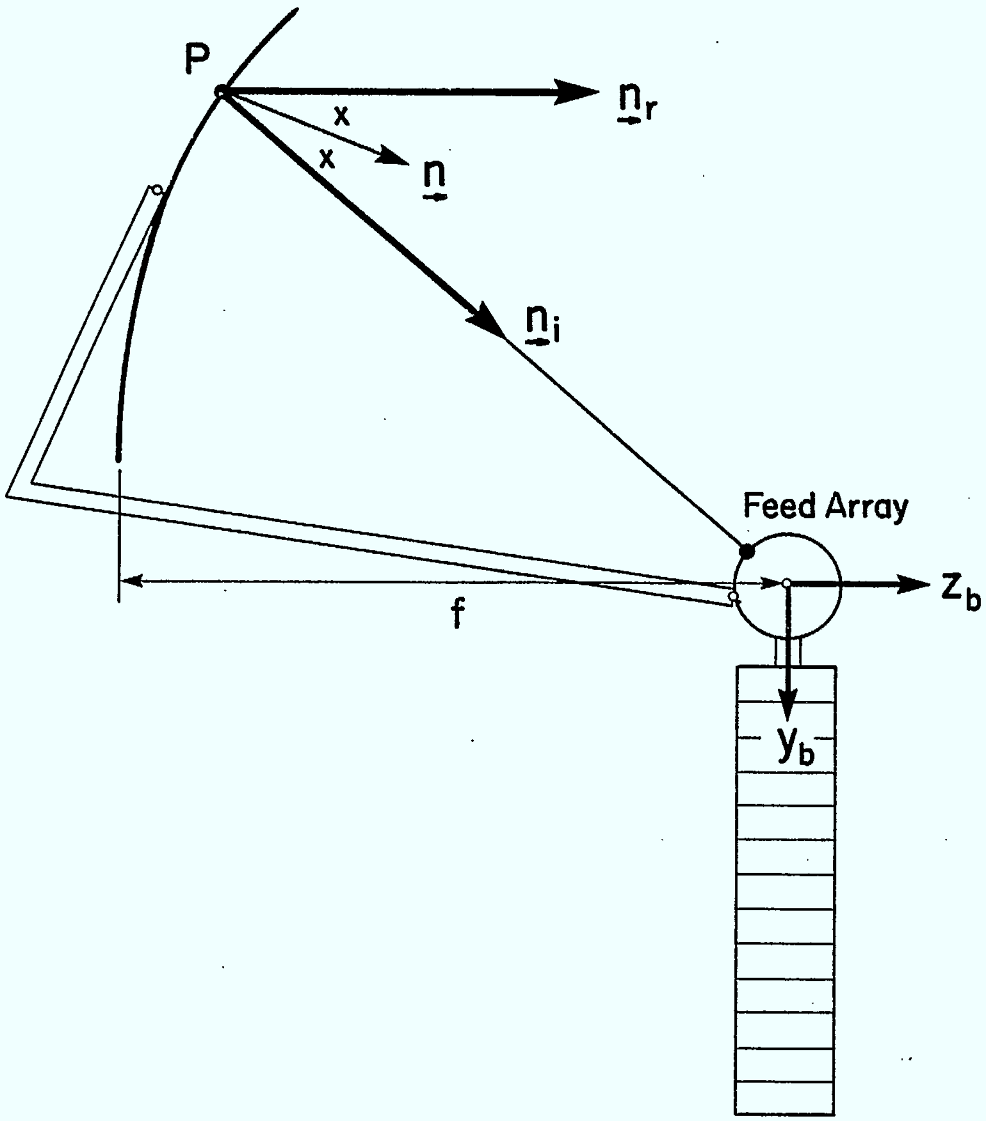

Fig. B1 Basic Ray Geometry

frame F_r, with respect to O_t, the origin of the tower reference frame F_t (as a consequence of structural deformations in the tower) is denoted $\underline{\delta}$ and expressed in F_t. Similarly, the angular displacement of F_r relative to F_t (arising from structural deformations) retains the notation $\underline{\alpha}$, with $\underline{\alpha}$ also expressed in F_t.

Now, as shown in Fig. B2, the constant vector $\vec{r}_{bt}$ locates O_t relative to O_b, the mass center of the rigid bus. Consequently, the displacement of O_r relative to O_b, as the result of structural deformations in the tower, is also given by $\underline{\delta}$. Furthermore, since F_t and F_b are related by a constant rotation matrix, the angular displacement of F_r relative F_b, as a consequence of tower deformations (and assuming zero gimbal angles), is $\underline{\alpha}$. If the gimbal angles $\underline{\beta}$ at O_r are non-zero, then the total angular displacement of F_r from its nominal orientation with respect to F_b is $\underline{\alpha} + \underline{\beta}$. As a consequence, the vector $\vec{r}_b$ from O_b to a point P on the reflector (after the tower has deformed and gimbal angles have been applied at O_r) can be written in the form (see Fig. B2)

$$\vec{r}_b = \vec{r}_{bo} + \vec{\delta}_r \tag{B.1}$$

where $\vec{r}_{bo}$ is the reference vector that moves over the surface of the undeflected, unrotated reflector. The matrix equivalent of (B.1), expressed in F_b, is

$$\underline{r}_b = \underline{r}_{bo} + \underline{\delta}_r \tag{B.2}$$

where

$$\begin{aligned}\underline{\delta}_r = \underline{C}_{bt}\underline{\delta} &+ (\underline{C}_{bt}\underline{\alpha})^{\times}(\underline{r}_{bo} - \underline{r}_{br}) \\ &+ (\underline{C}_{br}\underline{\beta})^{\times}(\underline{r}_{bo} - \underline{r}_{br})\end{aligned} \tag{B.3}$$

and $\underline{r}_{br}$ locates O_r relative to O_b when the reflector is undeflected and unrotated. Again, to be consistent with MSAT-5 the gimbal angles are expressed in F_r.

Equation (B.2) replaces equation (19) of Appendix D. Also, equation (20) of that appendix is replaced here by

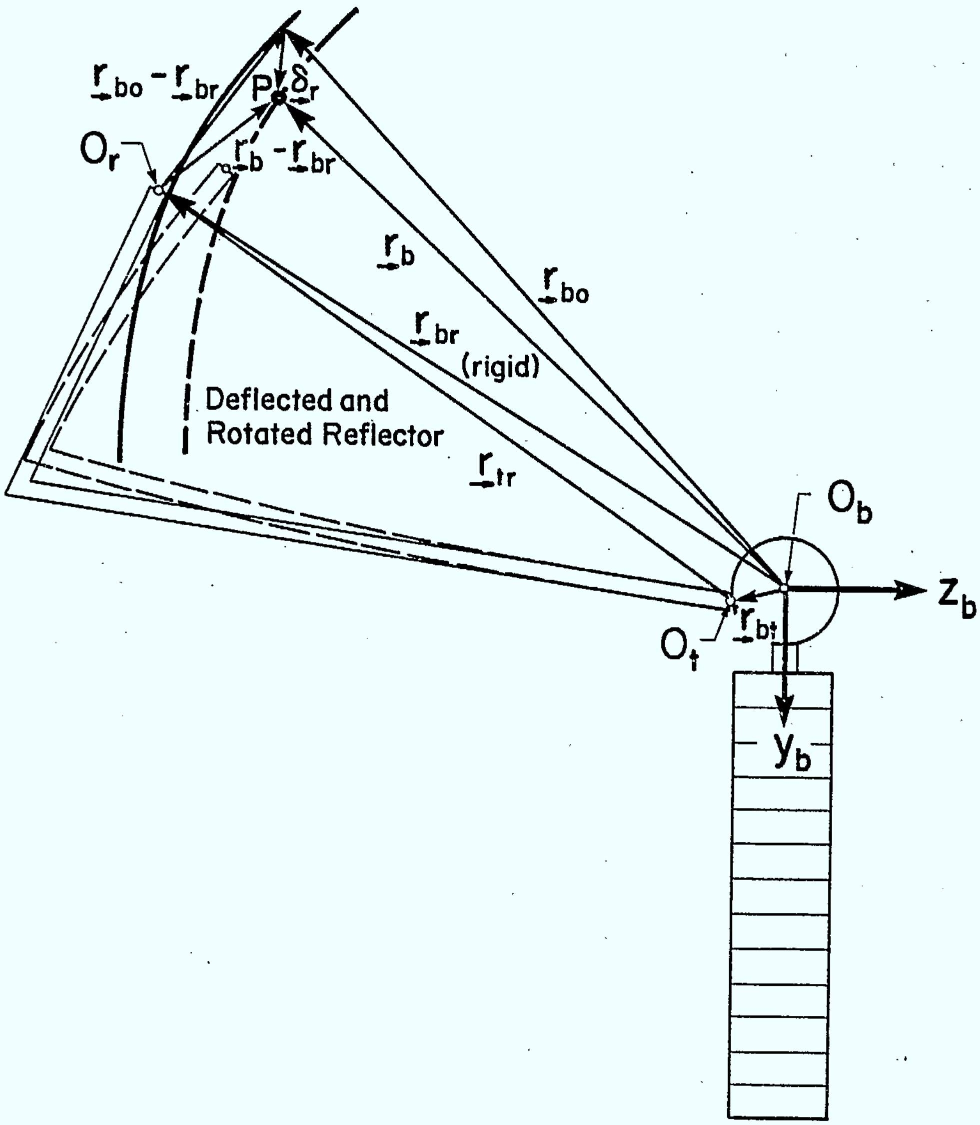

Fig. B2 Position after Structural Deformation of the Tower and after Rotation of the Reflector at the Hub Gimbals

$$\underline{r}_{br} = [0, -\ell_y, -\ell_z] \tag{B.4}$$

where it is assumed that $\ell_z \simeq f$ (see Fig. B3). Then, given

$$\underline{C}_{bt} = \begin{bmatrix} 1 & 0 & 0 \\ 0 & -\cos\gamma_1 & -\sin\gamma_1 \\ 0 & \sin\gamma_1 & -\cos\gamma_1 \end{bmatrix}; \quad \underline{C}_{br} = \begin{bmatrix} 0 & 1 & 0 \\ -\cos\gamma_3 & 0 & \sin\gamma_3 \\ \sin\gamma_3 & 0 & \cos\gamma_3 \end{bmatrix} \tag{B.5}$$

where $\gamma_1 = 2.8^o$ and $\gamma_3 = 14.2^o$, so that it is reasonable to assume small angles, and approximating $(\underline{r}_{bo} - \underline{r}_{br})$ by $(\underline{r}_b - \underline{r}_{br})$, (B.2) becomes

$$\underline{r}_{bo} = \begin{bmatrix} x_b \\ y_b \\ z_b \end{bmatrix} - \begin{bmatrix} \delta_1 \\ -\delta_2 \\ -\delta_3 \end{bmatrix} - \begin{bmatrix} 0 & \alpha_3 & -(\beta_1 + \alpha_2) \\ \alpha_3 & 0 & -(\beta_2 + \alpha_1) \\ (\beta_1 + \alpha_2) & (\beta_2 + \alpha_1) & 0 \end{bmatrix} \begin{bmatrix} x_b \\ y_b + \ell_y \\ z_b + f \end{bmatrix} \tag{B.6}$$

Equation (B.6) is analogous to (22) of Appendix D. Furthermore, the remainder of the equations in the Reflector Deformations section still apply provided the following variable transformations are performed:

$$\begin{bmatrix} \delta_x \\ \delta_y \\ \delta_z \\ \alpha_x \\ \alpha_y \\ \alpha_z \\ \ell_c \end{bmatrix} \rightarrow \begin{bmatrix} \delta_1 \\ -\delta_2 \\ -\delta_3 \\ (\alpha_1 + \beta_2) \\ -(\alpha_2 + \beta_1) \\ -\alpha_3 \\ \ell_y \end{bmatrix} \tag{B.7}$$

Beam Pointing Error

The total beam pointing error ($\underline{\theta}_p = \underline{0}$, ideally) now consists of two components, one ($\underline{\theta}_r$) associated with the structural deformations in the tower and the other ($\underline{\beta}_r$) associated with the gimbal angles at the reflector hub:

$$\underline{\theta}_p = \underline{\theta}_r + \underline{\beta}_r \tag{B.8}$$

As only the small rotations of the groundward beam about the x_b & y_b bus axes are of interest (to first-order the pointing error is independent of rotations about z_b), it follows from Appendix D of MSAT-1 that

$$\begin{aligned} \theta_{px} &= -\delta n_{r2} = -\delta n_2 + n_{i2}\delta n_3/(1 + n_{i3}) \\ \theta_{py} &= \delta n_{r1} = \delta n_1 - n_{i1}\delta n_3/(1 + n_{i3}) \end{aligned} \tag{B.9}$$

where the right-hand sides of (B.9) can be expanded using the equations obtained by applying (B.7) in the previous section. Performing this expansion yields

$$\begin{bmatrix} \theta_{px} \\ \theta_{py} \end{bmatrix} = \begin{bmatrix} \theta_{rx} \\ \theta_{ry} \end{bmatrix} + \begin{bmatrix} \beta_{rx} \\ \beta_{ry} \end{bmatrix} \tag{B.10}$$

where

$$\begin{bmatrix} \theta_{rx} \\ \theta_{ry} \end{bmatrix} = \underline{P}_{r\delta} f^{-1} \underline{\delta} + \underline{P}_{r\alpha} \underline{\alpha} \tag{B.11}$$

$$\begin{bmatrix} \beta_{rx} \\ \beta_{ry} \end{bmatrix} = \underline{P}_{r\beta} \underline{\beta} \tag{B.12}$$

$$\underline{\delta} = [\delta_1, \delta_2, \delta_3]^T \; ; \; \underline{\alpha} = [\alpha_1, \alpha_2, \alpha_3]^T \; ; \; \underline{\beta} = [\beta_1, \beta_2]^T \tag{B.13}$$

$$\begin{aligned}
P_{r\delta 11} &= \tfrac{1}{2} n_{1i} n_{i2} & P_{r\alpha 11} &= \tfrac{1}{2}(3 + n_{i3} - n_{i2}^2) + \tfrac{1}{2} n_{i2}(1 + n_{i3})(\ell_y/f) \\
P_{r\delta 12} &= \tfrac{1}{2}(1 + n_{i3} - n_{i2}^2) & P_{r\alpha 21} &= \tfrac{1}{2} n_{i1} n_{i2} - \tfrac{1}{2} n_{i1}(1 + n_{i3})(\ell_y/f) \\
P_{r\delta 21} &= \tfrac{1}{2}(1 + n_{i3} - n_{i1}^2) & P_{r\alpha 12} &= -\tfrac{1}{2} n_{i1} n_{i2} \\
P_{r\delta 22} &= P_{r\delta 11} & P_{r\alpha 22} &= -\tfrac{1}{2}(3 + n_{i3} - n_{i1}^2) \\
P_{r\delta 13} &= -\tfrac{1}{2} n_{i2}(1 + n_{i3}) & P_{r\alpha 13} &= \tfrac{1}{2} n_{i1} n_{i2}(\ell_y/f) \\
P_{r\delta 23} &= \tfrac{1}{2} n_{i1}(1 + n_{i3}) & P_{r\alpha 23} &= \tfrac{1}{2}(1 + n_{i3} - n_{i1}^2)(\ell_y/f)
\end{aligned} \tag{B.14}$$

$$\underline{P}_{r\beta} = \underline{P}_{r\alpha} \begin{bmatrix} 0 & 1 \\ 1 & 0 \\ 0 & 0 \end{bmatrix} \tag{B.15}$$

Interpretation in Terms of f/D_p Ratio

As stated in Appendix D of MSAT-1, instead of tracking the incident ray $\underline{n}_i$ for each ray emanating from the reflector (see Fig. B1), only a typical ray is considered. The chosen ray is taken to be the one arriving at O_r, the center of the undeflected, unrotated reflector. From Fig. B3, the direction cosines of this ray are, to a good approximation,

$$n_{i1} = 0 \; ; \quad n_{i2} = \sin\chi \; ; \quad n_{i3} = \cos\chi \tag{B.16}$$

where, from the same figure,

$$\tan \chi = \ell_y/\ell_z \tag{B.17}$$

Also, given that the equation for the 'parent' parabolic reflector, a portion of which forms the MSAT reflector, is

$$x_b^2 + y_b^2 - 4f(z_b + f) = 0 \tag{B.18}$$

and given that the coordinates of O_r are $[x_b,y_b,z_b] = [0,-\ell_y,-\ell_z]$, it follows that

$$\tan \chi = 4 \left(\frac{f}{\ell_y}\right) \div \left[4\left(\frac{f}{\ell_y}\right)^2 - 1 \right] \tag{B.19}$$

Furthermore, since γ_1 and γ_2 (see Fig. B3) are small angles,

$$\ell_y \simeq \frac{1}{4} D_p \; ; \quad \ell_z \simeq f \tag{B.20}$$

where f and D_p are the focal length and aperture of the 'parent' reflector. Therefore, combining (B.17) - (B.20) one obtains

$$\tan \chi \simeq 16f^*/(64f^{*2}-1) \simeq \ell_y/f \tag{B.21}$$

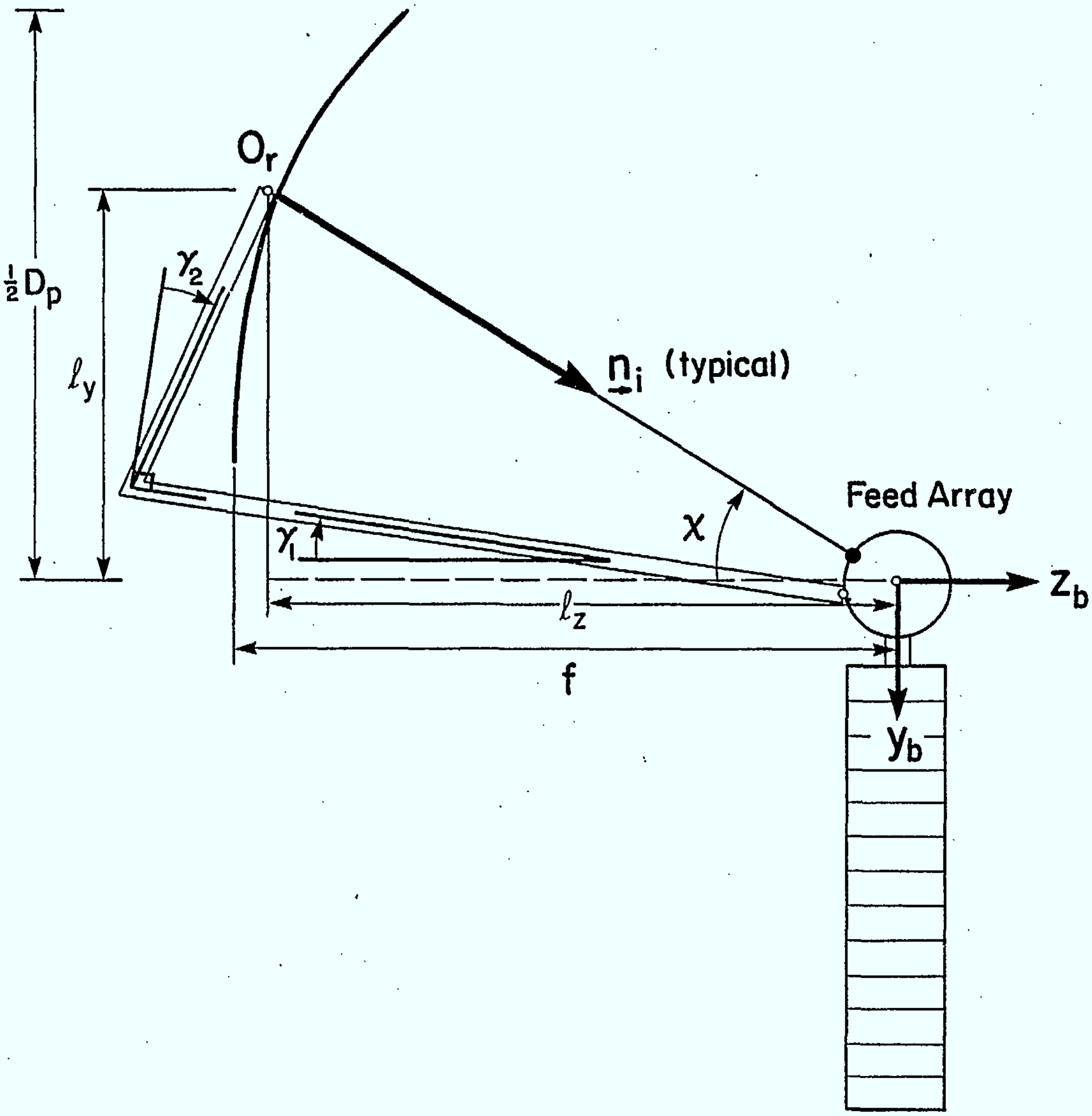

Fig. B3 Determination of the Angle χ

where

$$f^* = f/D_p \tag{B.22}$$

However, for $f^* >> 1/8$, $16f^*/(64f^{*2}-1) \simeq 1/(4f^*)$ and, therefore,

$$\ell_y/f \simeq 1/(4f^*) \tag{B.23}$$

Substitution of (B.16) and (B.23) into (B.14) of the previous section yields

$$\underline{P}_{r\delta} = \tfrac{1}{2}(1 + \cos\chi)\begin{bmatrix} 0 & \cos\chi & -\sin\chi \\ 1 & 0 & 0 \end{bmatrix} \tag{B.24}$$

$$\underline{P}_{r\alpha} = \begin{bmatrix} P_{11} & 0 & 0 \\ 0 & P_{22} & P_{23} \end{bmatrix} \tag{B.25}$$

where

$$\begin{aligned} P_{11} &= \tfrac{1}{2}(2 + \cos\chi + \cos^2\chi) + \tfrac{1}{2}(4f^*)^{-1}\sin\chi(1 + \cos\chi) \\ P_{22} &= -\tfrac{1}{2}(3 + \cos\chi) \\ P_{23} &= \tfrac{1}{2}(4f^*)^{-1}(1 + \cos\chi) \end{aligned} \tag{B.26}$$

For the MSAT spacecraft, $f^* = 0.514$, based on the assumed values $(f, D_p) = (43.7\text{m}, 85\text{m})$.

The Penalty Function

The modifications necessary to the penalty function as a consequence of including small gimbal angles at the reflector hub are detailed in Section 2.5.2 of this report.

Concluding Remarks

Finally, the concluding remarks cited in Appendix D are equally applicable here; however, the following changes in equation numbers are necessary:

$$\begin{bmatrix} (40) \\ (43) \\ (44) \\ (45) \\ (46) \\ (48) \\ (49) \\ (50) \end{bmatrix} \rightarrow \begin{bmatrix} (B.21) \\ (B.24) \\ (B.25) \\ (2.53) \\ (2.55) \\ (2.62) \\ (2.59) \\ (2.60) \end{bmatrix}$$

It is noteworthy that the introduction of gimbal angles at the reflector hub introduces additional terms which do not require knowledge of any extra spacecraft parameters. All one must know to evaluate the new scalar weighted penalty functions is still the four weights (w_1; w_2; w_3; w_4) and the f/D_p ratio.

Appendix C

DESIGN MODEL

for the

MSAT Spacecraft

*** RETAINED MODAL CONTROL DISTRIBUTION MATRIX ***

ROW \ COL	1	2	3	4	5	6
1	0.000D-01	0.000D-01	0.000D-01	0.000D-01	0.000D-01	8.410D-03
2	0.000D-01	0.000D-01	0.000D-01	0.000D-01	0.000D-01	-1.457D-02
3	0.000D-01	0.000D-01	0.000D-01	0.000D-01	0.000D-01	0.000D-01
4	9.094D-04	0.000D-01	0.000D-01	0.000D-01	0.000D-01	5.729D-03
5	-3.859D-07	1.047D-03	0.000D-01	0.000D-01	0.000D-01	3.806D-03
6	-9.257D-07	7.331D-04	2.003D-03	0.000D-01	0.000D-01	1.022D-02
7	-9.174D-08	1.210D-04	1.441D-04	6.944D-03	0.000D-01	1.289D-03
8	-4.708D-05	1.119D-07	2.213D-07	6.791D-08	6.921D-03	-8.075D-04
9	-8.282D-07	-5.856D-04	1.157D-03	-5.553D-04	-2.199D-06	6.530D-03
10	-9.888D-04	2.133D-07	5.812D-06	-1.500D-06	-2.577D-03	-3.368D-03
11	8.859D-07	-3.964D-04	-5.932D-03	8.518D-04	1.731D-06	-2.485D-02
12	-4.329D-06	-5.918D-03	2.746D-04	4.838D-03	-2.422D-06	-6.475D-04

ROW \ COL	7	8	9	10	11	12
1	8.410D-03	-8.410D-03	-8.410D-03	8.410D-03	8.410D-03	-8.410D-03
2	1.457D-02	1.457D-02	-1.457D-02	-1.457D-02	1.457D-02	1.457D-02
3	0.000D-01	0.000D-01	0.000D-01	0.000D-01	0.000D-01	0.000D-01
4	-5.729D-03	-5.729D-03	5.729D-03	-2.869D-02	2.869D-02	2.869D-02
5	3.811D-03	-3.806D-03	-3.811D-03	-1.906D-02	-1.908D-02	1.906D-02
6	-7.078D-03	7.133D-03	-1.027D-02	9.299D-03	9.284D-03	-9.299D-03
7	4.539D-05	-4.112D-05	-1.293D-03	-2.675D-04	-2.702D-04	2.675D-04
8	8.081D-04	8.094D-04	-8.100D-04	9.735D-04	-9.725D-04	-9.735D-04
9	-3.478D-03	3.488D-03	-6.539D-03	-4.826D-02	-4.783D-02	4.826D-02
10	3.370D-03	3.419D-03	-3.421D-03	-1.087D-01	1.085D-01	1.087D-01
11	2.639D-02	-2.653D-02	2.499D-02	5.095D-02	5.079D-02	-5.095D-02
12	-3.014D-03	3.025D-03	6.358D-04	-2.418D-01	-2.413D-01	2.418D-01

ROW \ COL	13
1	-8.410D-03
2	-1.457D-02
3	0.000D-01
4	-2.869D-02
5	1.908D-02
6	-9.284D-03
7	2.702D-04
8	9.725D-04
9	4.783D-02
10	-1.085D-01
11	-5.079D-02
12	2.413D-01

*** RETAINED MODAL OUTPUT MATRIX ***

ROW \ COL	1	2	3	4	5	6
1	0.000D-01	0.000D-01	0.000D-01	9.094D-04	-3.859D-07	-9.257D-07
2	0.000D-01	0.000D-01	0.000D-01	0.000D-01	1.047D-03	7.331D-04
3	0.000D-01	0.000D-01	0.000D-01	0.000D-01	0.000D-01	2.003D-03
4	0.000D-01	0.000D-01	0.000D-01	0.000D-01	0.000D-01	0.000D-01
5	0.000D-01	0.000D-01	0.000D-01	0.000D-01	0.000D-01	0.000D-01
6	0.000D-01	0.000D-01	0.000D-01	0.000D-01	0.000D-01	0.000D-01
7	0.000D-01	0.000D-01	0.000D-01	0.000D-01	0.000D-01	0.000D-01
8	0.000D-01	0.000D-01	0.000D-01	0.000D-01	0.000D-01	0.000D-01
9	0.000D-01	0.000D-01	0.000D-01	0.000D-01	0.000D-01	0.000D-01
10	0.000D-01	0.000D-01	0.000D-01	0.000D-01	0.000D-01	0.000D-01
11	0.000D-01	0.000D-01	0.000D-01	0.000D-01	0.000D-01	0.000D-01

ROW \ COL	7	8	9	10	11	12
1	-9.174D-08	-4.708D-05	-8.282D-07	-9.888D-04	8.859D-07	-4.329D-06
2	1.210D-04	1.119D-07	-5.856D-04	2.133D-07	-3.964D-04	-5.918D-03
3	1.441D-04	2.213D-07	1.157D-03	5.812D-06	-5.932D-03	2.746D-04
4	0.000D-01	0.000D-01	-1.756D-03	-3.172D-06	2.786D-03	-6.200D-03
5	0.000D-01	0.000D-01	-2.418D-06	-5.019D-04	-1.230D-06	-4.426D-06
6	0.000D-01	0.000D-01	2.208D-06	1.617D-03	-9.652D-07	3.638D-06
7	0.000D-01	0.000D-01	4.200D-06	3.425D-03	-2.497D-06	6.796D-06
8	0.000D-01	0.000D-01	5.736D-05	1.776D-06	-1.050D-03	-1.114D-02
9	0.000D-01	0.000D-01	3.335D-03	8.002D-06	-6.323D-03	-6.592D-04
10	6.944D-03	6.791D-08	-5.553D-04	-1.500D-06	8.518D-04	4.838D-03
11	0.000D-01	6.921D-03	-2.199D-06	-2.577D-03	1.731D-06	-2.422D-06

*** RETAINED MODAL OUTPUT WEIGHTING MATRIX ***

ROW \ COL	1	2	3	4	5	6
1	0.000D-01	0.000D-01	0.000D-01	0.000D-01	0.000D-01	0.000D-01
2	0.000D-01	0.000D-01	0.000D-01	0.000D-01	0.000D-01	0.000D-01
3	0.000D-01	0.000D-01	0.000D-01	0.000D-01	0.000D-01	0.000D-01
4	0.000D-01	0.000D-01	0.000D-01	1.654D-06	-7.019D-10	-1.684D-09
5	0.000D-01	0.000D-01	0.000D-01	-7.019D-10	2.193D-06	1.535D-06
6	0.000D-01	0.000D-01	0.000D-01	-1.684D-09	1.535D-06	5.891D-06
7	0.000D-01	0.000D-01	0.000D-01	-1.669D-10	-1.388D-05	-9.374D-06
8	0.000D-01	0.000D-01	0.000D-01	1.281D-05	-5.342D-09	-1.244D-08
9	0.000D-01	0.000D-01	0.000D-01	-4.923D-10	-3.452D-07	2.539D-06
10	0.000D-01	0.000D-01	0.000D-01	-1.237D-06	1.122D-09	1.565D-08
11	0.000D-01	0.000D-01	0.000D-01	-3.737D-10	-7.123D-07	-1.476D-05
12	0.000D-01	0.000D-01	0.000D-01	-4.531D-09	-6.014D-06	-3.550D-06

ROW \ COL	7	8	9	10	11	12
1	0.000D-01	0.000D-01	0.000D-01	0.000D-01	0.000D-01	0.000D-01
2	0.000D-01	0.000D-01	0.000D-01	0.000D-01	0.000D-01	0.000D-01
3	0.000D-01	0.000D-01	0.000D-01	0.000D-01	0.000D-01	0.000D-01
4	-1.669D-10	1.281D-05	-4.923D-10	-1.237D-06	-3.737D-10	-4.531D-09
5	-1.388D-05	-5.342D-09	-3.452D-07	1.122D-09	-7.123D-07	-6.014D-06
6	-9.374D-06	-1.244D-08	2.539D-06	1.565D-08	-1.476D-05	-3.550D-06
7	1.791D-04	-9.717D-10	-3.295D-06	-3.628D-09	2.724D-06	-3.001D-06
8	-9.717D-10	1.999D-04	4.331D-09	-5.198D-06	-1.999D-08	-9.630D-09
9	-3.295D-06	4.331D-09	2.014D-06	8.746D-09	-8.075D-06	3.891D-06
10	-3.628D-09	-5.198D-06	8.746D-09	1.115D-06	-4.195D-08	5.237D-09
11	2.724D-06	-1.999D-08	-8.075D-06	-4.195D-08	4.247D-05	3.417D-07
12	-3.001D-06	-9.630D-09	3.891D-06	5.237D-09	3.417D-07	3.514D-05

*** RETAINED MODAL DAMPING MATRIX ***

ROW \ COL.	1	2	3	4
1	1.846D-03	2.519D-06	-1.700D-03	3.255D-03
2	2.519D-06	3.409D-03	-6.900D-06	1.146D-05
3	-1.700D-03	-6.900D-06	1.711D-02	-4.585D-03
4	3.255D-03	1.146D-05	-4.585D-03	4.215D-02

*** RETAINED MODAL ANGULAR MOMENTUM MATRIX FOR 1-AXIS ***

ROW \ COL	1	2	3	4	5	6
1	0.000D-01	0.000D-01	0.000D-01	0.000D-01	0.000D-01	0.000D-01
2	0.000D-01	0.000D-01	0.000D-01	0.000D-01	0.000D-01	0.000D-01
3	0.000D-01	0.000D-01	0.000D-01	0.000D-01	0.000D-01	0.000D-01
4	0.000D-01	0.000D-01	0.000D-01	0.000D-01	0.000D-01	0.000D-01
5	0.000D-01	0.000D-01	0.000D-01	0.000D-01	0.000D-01	2.098D-06
6	0.000D-01	0.000D-01	0.000D-01	0.000D-01	-2.098D-06	0.000D-01
7	0.000D-01	0.000D-01	0.000D-01	0.000D-01	-1.509D-07	1.368D-07
8	0.000D-01	0.000D-01	0.000D-01	0.000D-01	-2.317D-10	6.195D-11
9	0.000D-01	0.000D-01	0.000D-01	0.000D-01	-1.211D-06	-2.021D-06
10	0.000D-01	0.000D-01	0.000D-01	0.000D-01	-6.086D-09	-3.833D-09
11	0.000D-01	0.000D-01	0.000D-01	0.000D-01	6.212D-06	3.555D-06
12	0.000D-01	0.000D-01	0.000D-01	0.000D-01	-2.875D-07	-1.206D-05

ROW \ COL	7	8	9	10	11	12
1	0.000D-01	0.000D-01	0.000D-01	0.000D-01	0.000D-01	0.000D-01
2	0.000D-01	0.000D-01	0.000D-01	0.000D-01	0.000D-01	0.000D-01
3	0.000D-01	0.000D-01	0.000D-01	0.000D-01	0.000D-01	0.000D-01
4	0.000D-01	0.000D-01	0.000D-01	0.000D-01	0.000D-01	0.000D-01
5	1.509D-07	2.317D-10	1.211D-06	6.086D-09	-6.212D-06	2.875D-07
6	-1.368D-07	-6.195D-11	2.021D-06	3.833D-09	-3.555D-06	1.206D-05
7	0.000D-01	1.065D-11	2.243D-07	6.724D-10	-6.607D-07	8.860D-07
8	-1.065D-11	0.000D-01	2.591D-10	6.032D-13	-5.762D-10	1.340D-09
9	-2.243D-07	-2.591D-10	0.000D-01	-3.650D-09	3.932D-06	6.684D-06
10	-6.724D-10	-6.032D-13	3.650D-09	0.000D-01	1.038D-09	3.445D-08
11	6.607D-07	5.762D-10	-3.932D-06	-1.038D-09	0.000D-01	-3.521D-05
12	-8.860D-07	-1.340D-09	-6.684D-06	-3.445D-08	3.521D-05	0.000D-01

*** RETAINED MODAL ANGULAR MOMENTUM MATRIX FOR 2-AXIS ***

ROW \ COL	1	2	3	4	5	6
1	0.000D-01	0.000D-01	0.000D-01	0.000D-01	0.000D-01	0.000D-01
2	0.000D-01	0.000D-01	0.000D-01	0.000D-01	0.000D-01	0.000D-01
3	0.000D-01	0.000D-01	0.000D-01	0.000D-01	0.000D-01	0.000D-01
4	0.000D-01	0.000D-01	0.000D-01	0.000D-01	0.000D-01	-1.822D-06
5	0.000D-01	0.000D-01	0.000D-01	0.000D-01	0.000D-01	7.731D-10
6	0.000D-01	0.000D-01	0.000D-01	1.822D-06	-7.731D-10	0.000D-01
7	0.000D-01	0.000D-01	0.000D-01	1.310D-07	-5.561D-11	5.040D-11
8	0.000D-01	0.000D-01	0.000D-01	2.013D-10	-8.541D-14	9.432D-08
9	0.000D-01	0.000D-01	0.000D-01	1.052D-06	-4.464D-10	5.886D-10
10	0.000D-01	0.000D-01	0.000D-01	5.285D-09	-2.243D-12	1.981D-06
11	0.000D-01	0.000D-01	0.000D-01	-5.395D-06	2.289D-09	3.716D-09
12	0.000D-01	0.000D-01	0.000D-01	2.497D-07	-1.060D-10	8.418D-09

ROW \ COL	7	8	9	10	11	12
1	0.000D-01	0.000D-01	0.000D-01	0.000D-01	0.000D-01	0.000D-01
2	0.000D-01	0.000D-01	0.000D-01	0.000D-01	0.000D-01	0.000D-01
3	0.000D-01	0.000D-01	0.000D-01	0.000D-01	0.000D-01	0.000D-01
4	-1.310D-07	-2.013D-10	-1.052D-06	-5.285D-09	5.395D-06	-2.497D-07
5	5.561D-11	8.541D-14	4.464D-10	2.243D-12	-2.289D-09	1.060D-10
6	-5.040D-11	-9.432D-08	-5.886D-10	-1.981D-06	-3.716D-09	-8.418D-09
7	0.000D-01	-6.784D-09	-1.323D-11	-1.425D-07	-4.166D-10	-5.986D-10
8	6.784D-09	0.000D-01	5.446D-08	5.477D-11	-2.793D-07	1.293D-08
9	1.323D-11	-5.446D-08	0.000D-01	-1.144D-06	-3.889D-09	-4.780D-09
10	1.425D-07	-5.477D-11	1.144D-06	0.000D-01	-5.866D-06	2.715D-07
11	4.166D-10	2.793D-07	3.889D-09	5.866D-06	0.000D-01	2.544D-08
12	5.986D-10	-1.293D-08	4.780D-09	-2.715D-07	-2.544D-08	0.000D-01

*** RETAINED MODAL ANGULAR MOMENTUM MATRIX FOR 3-AXIS ***

ROW \ COL	1	2	3	4	5	6
1	0.000D-01	0.000D-01	0.000D-01	0.000D-01	0.000D-01	0.000D-01
2	0.000D-01	0.000D-01	0.000D-01	0.000D-01	0.000D-01	0.000D-01
3	0.000D-01	0.000D-01	0.000D-01	0.000D-01	0.000D-01	0.000D-01
4	0.000D-01	0.000D-01	0.000D-01	0.000D-01	9.522D-07	6.667D-07
5	0.000D-01	0.000D-01	0.000D-01	-9.522D-07	0.000D-01	6.863D-10
6	0.000D-01	0.000D-01	0.000D-01	-6.667D-07	-6.863D-10	0.000D-01
7	0.000D-01	0.000D-01	0.000D-01	-1.100D-07	-4.937D-11	4.474D-11
8	0.000D-01	0.000D-01	0.000D-01	-1.018D-10	-4.930D-08	-3.451D-08
9	0.000D-01	0.000D-01	0.000D-01	5.325D-07	-1.093D-09	-1.149D-09
10	0.000D-01	0.000D-01	0.000D-01	-1.940D-10	-1.035D-06	-7.249D-07
11	0.000D-01	0.000D-01	0.000D-01	3.605D-07	7.747D-10	2.825D-10
12	0.000D-01	0.000D-01	0.000D-01	5.381D-06	-6.816D-09	-8.651D-09

ROW \ COL	7	8	9	10	11	12
1	0.000D-01	0.000D-01	0.000D-01	0.000D-01	0.000D-01	0.000D-01
2	0.000D-01	0.000D-01	0.000D-01	0.000D-01	0.000D-01	0.000D-01
3	0.000D-01	0.000D-01	0.000D-01	0.000D-01	0.000D-01	0.000D-01
4	1.100D-07	1.018D-10	-5.325D-07	1.940D-10	-3.605D-07	-5.381D-06
5	4.937D-11	4.930D-08	1.093D-09	1.035D-06	-7.747D-10	6.816D-09
6	-4.474D-11	3.451D-08	1.149D-09	7.249D-07	-2.825D-10	8.651D-09
7	0.000D-01	5.696D-09	1.539D-10	1.196D-07	-7.083D-11	1.067D-09
8	-5.696D-09	0.000D-01	2.757D-08	1.006D-10	1.866D-08	2.786D-07
9	-1.539D-10	-2.757D-08	0.000D-01	-5.790D-07	8.471D-10	2.366D-09
10	-1.196D-07	-1.006D-10	5.790D-07	0.000D-01	3.920D-07	5.851D-06
11	7.083D-11	-1.866D-08	-8.471D-10	-3.920D-07	0.000D-01	-6.958D-09
12	-1.067D-09	-2.786D-07	-2.366D-09	-5.851D-06	6.958D-09	0.000D-01

*** RETAINED FREQUENCIES ***

SELECTED MODES	FREQUENCY (RAD/SEC)	(HZ)
1	0.0000000000000000D-01	0.0000000000000000D-01
2	0.0000000000000000D-01	0.0000000000000000D-01
3	0.0000000000000000D-01	0.0000000000000000D-01
4	0.0000000000000000D-01	0.0000000000000000D-01
5	0.0000000000000000D-01	0.0000000000000000D-01
6	0.0000000000000000D-01	0.0000000000000000D-01
7	0.0000000000000000D-01	0.0000000000000000D-01
8	0.0000000000000000D-01	0.0000000000000000D-01
9	1.2434952868889490D-01	1.9790842161985070D-02
10	2.3952489001995300D-01	3.8121570240218110D-02
11	5.5629553169353050D-01	8.8537183688959500D-02
12	7.7963639163821000D-01	1.2408298554354990D-01

Table C-1

Relationship of Design Model Frequencies to Original Spacecraft Model Frequencies (Table 8)

Design Model Mode Number	Original Model Mode Number: Combined	Rigid	Flexible	Importance According To Modal Cost Analysis
1	1	1		Retain Rigid Mode
2	2	2		
3	3	3		
4	4	4		
5	5	5		
6	6	6		
7	7	7		
8	8	8		
9	9		1	1
10	11		3	3
11	13		5	4
12	16		8	2

*** RETAINED EIGENVECTORS ***

ROW \ COL	1	2	3	4	5	6
1	1.682D-02	0.000D-01	0.000D-01	0.000D-01	7.617D-03	3.139D-03
2	0.000D-01	1.682D-02	0.000D-01	-6.615D-03	2.807D-06	3.172D-05
3	0.000D-01	0.000D-01	1.682D-02	9.961D-04	-1.348D-05	-1.016D-05
4	0.000D-01	0.000D-01	0.000D-01	9.094D-04	-3.859D-07	-9.257D-07
5	0.000D-01	0.000D-01	0.000D-01	0.000D-01	1.047D-03	7.331D-04
6	0.000D-01	0.000D-01	0.000D-01	0.000D-01	0.000D-01	2.003D-03
7	0.000D-01	0.000D-01	0.000D-01	0.000D-01	0.000D-01	0.000D-01
8	0.000D-01	0.000D-01	0.000D-01	0.000D-01	0.000D-01	0.000D-01
9	0.000D-01	0.000D-01	0.000D-01	0.000D-01	0.000D-01	0.000D-01
10	0.000D-01	0.000D-01	0.000D-01	0.000D-01	0.000D-01	0.000D-01
11	0.000D-01	0.000D-01	0.000D-01	0.000D-01	0.000D-01	0.000D-01
12	0.000D-01	0.000D-01	0.000D-01	0.000D-01	0.000D-01	0.000D-01
13	0.000D-01	0.000D-01	0.000D-01	0.000D-01	0.000D-01	0.000D-01
14	0.000D-01	0.000D-01	0.000D-01	0.000D-01	0.000D-01	0.000D-01

ROW \ COL	7	8	9	10	11	12
1	1.334D-03	5.777D-07	3.051D-03	1.986D-06	1.541D-03	-3.661D-03
2	2.464D-06	9.338D-04	5.393D-06	3.920D-03	-8.289D-05	6.760D-06
3	-1.609D-06	-2.016D-04	3.738D-05	4.209D-03	-5.252D-06	6.496D-05
4	-9.174D-08	-4.708D-05	-8.282D-07	-9.888D-04	8.859D-07	-4.329D-06
5	1.210D-04	1.119D-07	-5.856D-04	2.133D-07	-3.964D-04	-5.918D-03
6	1.441D-04	2.213D-07	1.157D-03	5.812D-06	-5.932D-03	2.746D-04
7	6.944D-03	6.791D-08	-5.553D-04	-1.500D-06	8.518D-04	4.838D-03
8	0.000D-01	6.921D-03	-2.199D-06	-2.577D-03	1.731D-06	-2.422D-06
9	0.000D-01	0.000D-01	-7.672D-02	-1.386D-04	1.218D-01	-2.709D-01
10	0.000D-01	0.000D-01	-1.057D-04	-2.193D-02	-5.374D-05	-1.934D-04
11	0.000D-01	0.000D-01	9.647D-05	7.066D-02	-4.218D-05	1.590D-04
12	0.000D-01	0.000D-01	4.200D-06	3.425D-03	-2.497D-06	6.796D-06
13	0.000D-01	0.000D-01	5.736D-05	1.776D-06	-1.050D-03	-1.114D-02
14	0.000D-01	0.000D-01	3.335D-03	8.002D-06	-6.323D-03	-6.592D-04

Appendix D

EVALUATION MODEL

for the

MSAT Spacecraft

*** RETAINED MODAL CONTROL DISTRIBUTION MATRIX ***

ROW \ COL	1	2	3	4	5	6
1	0.000D-01	0.000D-01	0.000D-01	0.000D-01	0.000D-01	8.410D-03
2	0.000D-01	0.000D-01	0.000D-01	0.000D-01	0.000D-01	-1.457D-02
3	0.000D-01	0.000D-01	0.000D-01	0.000D-01	0.000D-01	0.000D-01
4	9.094D-04	0.000D-01	0.000D-01	0.000D-01	0.000D-01	5.729D-03
5	-3.859D-07	1.047D-03	0.000D-01	0.000D-01	0.000D-01	3.806D-03
6	-9.257D-07	7.331D-04	2.003D-03	0.000D-01	0.000D-01	1.022D-02
7	-9.174D-08	1.210D-04	1.441D-04	6.944D-03	0.000D-01	1.289D-03
8	-4.708D-05	1.119D-07	2.213D-07	6.791D-08	6.921D-03	-8.075D-04
9	-8.282D-07	-5.856D-04	1.157D-03	-5.553D-04	-2.199D-06	6.530D-03
10	-3.625D-04	3.905D-06	-1.515D-05	5.403D-06	-6.851D-04	1.044D-03
11	-9.888D-04	2.133D-07	5.812D-06	-1.500D-06	-2.577D-03	-3.368D-03
12	8.859D-07	-3.964D-04	-5.932D-03	8.518D-04	1.731D-06	-2.485D-02
13	-1.407D-06	-3.743D-04	3.110D-03	1.688D-05	-8.184D-07	1.358D-02
14	-4.329D-06	-5.918D-03	2.746D-04	4.838D-03	-2.422D-06	-6.475D-04
15	9.650D-03	-1.270D-04	-4.746D-05	8.906D-05	-2.665D-03	4.183D-03
16	3.582D-06	-2.459D-03	-2.900D-04	-1.641D-02	-3.707D-06	-1.505D-03
17	-6.085D-03	2.712D-06	2.644D-05	9.890D-06	-5.304D-03	-1.833D-03
18	1.817D-06	-5.308D-04	-1.342D-04	1.197D-01	-9.102D-07	-5.342D-04
19	-1.854D-06	3.178D-04	8.974D-05	1.803D-01	2.451D-04	3.438D-04

ROW \ COL	7	8	9	10	11	12
1	8.410D-03	-8.410D-03	-8.410D-03	8.410D-03	8.410D-03	-8.410D-03
2	1.457D-02	1.457D-02	-1.457D-02	-1.457D-02	1.457D-02	1.457D-02
3	0.000D-01	0.000D-01	0.000D-01	0.000D-01	0.000D-01	0.000D-01
4	-5.729D-03	-5.729D-03	5.729D-03	-2.869D-02	2.869D-02	2.869D-02
5	3.811D-03	-3.806D-03	-3.811D-03	-1.906D-02	-1.908D-02	1.906D-02
6	-7.078D-03	7.133D-03	-1.027D-02	9.299D-03	9.284D-03	-9.299D-03
7	4.539D-05	-4.112D-05	-1.293D-03	-2.675D-04	-2.702D-04	2.675D-04
8	8.081D-04	8.094D-04	-8.100D-04	9.735D-04	-9.725D-04	-9.735D-04
9	-3.478D-03	3.488D-03	-6.539D-03	-4.826D-02	-4.783D-02	4.826D-02
10	-1.055D-03	-1.175D-03	1.186D-03	-5.105D-02	5.178D-02	5.105D-02
11	3.370D-03	3.419D-03	-3.421D-03	-1.087D-01	1.085D-01	1.087D-01
12	2.639D-02	-2.653D-02	2.499D-02	5.095D-02	5.079D-02	-5.095D-02
13	-1.328D-02	1.336D-02	-1.365D-02	-4.925D-02	-4.909D-02	4.925D-02
14	-3.014D-03	3.025D-03	6.358D-04	-2.418D-01	-2.413D-01	2.418D-01
15	-4.251D-03	-4.594D-03	4.662D-03	2.639D-01	-2.724D-01	-2.639D-01
16	9.903D-04	-1.007D-03	1.521D-03	3.403D-01	3.403D-01	-3.403D-01
17	1.826D-03	2.062D-03	-2.055D-03	-4.154D-01	4.144D-01	4.154D-01
18	6.243D-04	-6.283D-04	5.383D-04	-2.861D 00	-2.862D 00	2.861D 00
19	-3.829D-04	4.334D-04	-3.943D-04	-4.259D 00	-4.278D 00	4.259D 00

(Cont'd)

ROW \ COL 13

1	-8.410D-03
2	-1.457D-02
3	0.000D-01
4	-2.869D-02
5	1.908D-02
6	-9.284D-03
7	2.702D-04
8	9.725D-04
9	4.783D-02
10	-5.178D-02
11	-1.085D-01
12	-5.079D-02
13	4.909D-02
14	2.413D-01
15	2.724D-01
16	-3.403D-01
17	-4.144D-01
18	2.862D 00
19	4.278D 00

*** RETAINED MODAL OUTPUT MATRIX ***

ROW \ COL	1	2	3	4	5	6
1	0.000D-01	0.000D-01	0.000D-01	9.094D-04	-3.859D-07	-9.257D-07
2	0.000D-01	0.000D-01	0.000D-01	0.000D-01	1.047D-03	7.331D-04
3	0.000D-01	0.000D-01	0.000D-01	0.000D-01	0.000D-01	2.003D-03
4	0.000D-01	0.000D-01	0.000D-01	0.000D-01	0.000D-01	0.000D-01
5	0.000D-01	0.000D-01	0.000D-01	0.000D-01	0.000D-01	0.000D-01
6	0.000D-01	0.000D-01	0.000D-01	0.000D-01	0.000D-01	0.000D-01
7	0.000D-01	0.000D-01	0.000D-01	0.000D-01	0.000D-01	0.000D-01
8	0.000D-01	0.000D-01	0.000D-01	0.000D-01	0.000D-01	0.000D-01
9	0.000D-01	0.000D-01	0.000D-01	0.000D-01	0.000D-01	0.000D-01
10	0.000D-01	0.000D-01	0.000D-01	0.000D-01	0.000D-01	0.000D-01
11	0.000D-01	0.000D-01	0.000D-01	0.000D-01	0.000D-01	0.000D-01

ROW \ COL	7	8	9	10	11	12
1	-9.174D-08	-4.708D-05	-8.282D-07	-3.625D-04	-9.888D-04	8.859D-07
2	1.210D-04	1.119D-07	-5.856D-04	3.905D-06	2.133D-07	-3.964D-04
3	1.441D-04	2.213D-07	1.157D-03	-1.515D-05	5.812D-06	-5.932D-03
4	0.000D-01	0.000D-01	-1.756D-03	1.504D-05	-3.172D-06	2.786D-03
5	0.000D-01	0.000D-01	-2.418D-06	-5.987D-04	-5.019D-04	-1.230D-06
6	0.000D-01	0.000D-01	2.208D-06	6.242D-04	1.617D-03	-9.652D-07
7	0.000D-01	0.000D-01	4.200D-06	1.211D-03	3.425D-03	-2.497D-06
8	0.000D-01	0.000D-01	5.736D-05	-2.287D-06	1.776D-06	-1.050D-03
9	0.000D-01	0.000D-01	3.335D-03	-3.071D-05	8.002D-06	-6.323D-03
10	6.944D-03	6.791D-08	-5.553D-04	5.403D-06	-1.500D-06	8.518D-04
11	0.000D-01	6.921D-03	-2.199D-06	-6.851D-04	-2.577D-03	1.731D-06

ROW \ COL	13	14	15	16	17	18
1	-1.407D-06	-4.329D-06	9.650D-03	3.582D-06	-6.085D-03	1.817D-06
2	-3.743D-04	-5.918D-03	-1.270D-04	-2.459D-03	2.712D-06	-5.308D-04
3	3.110D-03	2.746D-04	-4.746D-05	-2.900D-04	2.644D-05	-1.342D-04
4	-2.075D-03	-6.200D-03	-9.882D-05	-2.307D-03	-1.146D-05	-4.845D-04
5	-4.650D-07	-4.426D-06	9.933D-03	3.553D-06	-6.069D-03	1.808D-06
6	1.052D-06	3.638D-06	-4.682D-03	-1.563D-06	3.058D-03	-8.696D-07
7	2.209D-06	6.796D-06	-7.090D-03	9.175D-08	1.134D-02	-8.927D-07
8	-5.249D-04	-1.114D-02	-2.104D-04	1.367D-02	-8.302D-06	-1.178D-01
9	3.207D-03	-6.592D-04	-3.270D-05	-3.466D-03	2.847D-05	2.352D-02
10	1.688D-05	4.838D-03	8.906D-05	-1.641D-02	9.890D-06	1.197D-01
11	-8.184D-07	-2.422D-06	-2.665D-03	-3.707D-06	-5.304D-03	-9.102D-07

ROW \ COL	19
1	-1.854D-06
2	3.178D-04
3	8.974D-05
4	3.364D-04
5	-2.456D-07
6	1.519D-06
7	-2.431D-04
8	-1.769D-01
9	3.307D-02
10	1.803D-01
11	2.451D-04

*** RETAINED MODAL OUTPUT WEIGHTING MATRIX ***

ROW \ COL	1	2	3	4	5	6
1	0.000D-01	0.000D-01	0.000D-01	0.000D-01	0.000D-01	0.000D-01
2	0.000D-01	0.000D-01	0.000D-01	0.000D-01	0.000D-01	0.000D-01
3	0.000D-01	0.000D-01	0.000D-01	0.000D-01	0.000D-01	0.000D-01
4	0.000D-01	0.000D-01	0.000D-01	1.654D-06	-7.019D-10	-1.684D-09
5	0.000D-01	0.000D-01	0.000D-01	-7.019D-10	2.193D-06	1.535D-06
6	0.000D-01	0.000D-01	0.000D-01	-1.684D-09	1.535D-06	5.891D-06
7	0.000D-01	0.000D-01	0.000D-01	-1.669D-10	-1.388D-05	-9.374D-06
8	0.000D-01	0.000D-01	0.000D-01	1.281D-05	-5.342D-09	-1.244D-08
9	0.000D-01	0.000D-01	0.000D-01	-4.923D-10	-3.452D-07	2.539D-06
10	0.000D-01	0.000D-01	0.000D-01	-3.820D-07	2.107D-09	-3.467D-08
11	0.000D-01	0.000D-01	0.000D-01	-1.237D-06	1.122D-09	1.565D-08
12	0.000D-01	0.000D-01	0.000D-01	-3.737D-10	-7.123D-07	-1.476D-05
13	0.000D-01	0.000D-01	0.000D-01	-7.363D-10	-2.598D-07	7.295D-06
14	0.000D-01	0.000D-01	0.000D-01	-4.531D-09	-6.014D-06	-3.550D-06
15	0.000D-01	0.000D-01	0.000D-01	8.791D-06	-1.360D-07	-2.157D-07
16	0.000D-01	0.000D-01	0.000D-01	3.103D-09	-3.532D-06	-3.170D-06
17	0.000D-01	0.000D-01	0.000D-01	-5.642D-06	7.196D-09	7.267D-08
18	0.000D-01	0.000D-01	0.000D-01	1.666D-09	5.983D-06	3.866D-06
19	0.000D-01	0.000D-01	0.000D-01	-6.046D-10	1.010D-05	7.286D-06

ROW \ COL	7	8	9	10	11	12
1	0.000D-01	0.000D-01	0.000D-01	0.000D-01	0.000D-01	0.000D-01
2	0.000D-01	0.000D-01	0.000D-01	0.000D-01	0.000D-01	0.000D-01
3	0.000D-01	0.000D-01	0.000D-01	0.000D-01	0.000D-01	0.000D-01
4	-1.669D-10	1.281D-05	-4.923D-10	-3.820D-07	-1.237D-06	-3.737D-10
5	-1.388D-05	-5.342D-09	-3.452D-07	2.107D-09	1.122D-09	-7.123D-07
6	-9.374D-06	-1.244D-08	2.539D-06	-3.467D-08	1.565D-08	-1.476D-05
7	1.791D-04	-9.717D-10	-3.295D-06	2.529D-08	-3.628D-09	2.724D-06
8	-9.717D-10	1.999D-04	4.331D-09	-7.973D-07	-5.198D-06	-1.999D-08
9	-3.295D-06	4.331D-09	2.014D-06	-2.356D-08	8.746D-09	-8.075D-06
10	2.529D-08	-7.973D-07	-2.356D-08	1.350D-07	3.797D-07	1.066D-07
11	-3.628D-09	-5.198D-06	8.746D-09	3.797D-07	1.115D-06	-4.195D-08
12	2.724D-06	-1.999D-08	-8.075D-06	1.066D-07	-4.195D-08	4.247D-05
13	-1.197D-06	9.290D-09	4.569D-06	-5.779D-08	2.283D-08	-2.203D-05
14	-3.001D-06	-9.630D-09	3.891D-06	-2.685D-08	5.237D-09	3.417D-07
15	-3.335D-08	-2.116D-07	6.772D-10	-3.498D-06	-9.548D-06	3.966D-07
16	1.188D-05	-2.909D-09	8.033D-07	-3.746D-09	-6.353D-09	3.299D-06
17	-1.961D-08	-1.402D-06	4.060D-08	2.212D-06	-6.061D-06	-1.951D-07
18	-8.364D-05	-9.229D-11	1.723D-06	-1.308D-08	-6.187D-10	-6.067D-07
19	-1.247D-04	1.677D-08	2.325D-06	-1.888D-08	5.420D-09	-3.412D-06

(Cont'd)

ROW \ COL	13	14	15	16	17	18
1	0.000D-01	0.000D-01	0.000D-01	0.000D-01	0.000D-01	0.000D-01
2	0.000D-01	0.000D-01	0.000D-01	0.000D-01	0.000D-01	0.000D-01
3	0.000D-01	0.000D-01	0.000D-01	0.000D-01	0.000D-01	0.000D-01
4	-7.363D-10	-4.531D-09	8.791D-06	3.103D-09	-5.642D-06	1.666D-09
5	-2.598D-07	-6.014D-06	-1.360D-07	-3.532D-06	7.196D-09	5.983D-06
6	7.295D-06	-3.550D-06	-2.157D-07	-3.170D-06	7.267D-08	3.866D-06
7	-1.197D-06	-3.001D-06	-3.335D-08	1.188D-05	-1.961D-08	-8.364D-05
8	9.290D-09	-9.630D-09	-2.116D-07	-2.909D-09	-1.402D-06	-9.229D-11
9	4.569D-06	3.891D-06	6.772D-10	8.033D-07	4.060D-08	1.723D-06
10	-5.779D-08	-2.685D-08	-3.498D-06	-3.746D-09	2.212D-06	-1.308D-08
11	2.283D-08	5.237D-09	-9.548D-06	-6.353D-09	6.061D-06	-6.187D-10
12	-2.203D-05	3.417D-07	3.966D-07	3.299D-06	-1.951D-07	-6.067D-07
13	1.176D-05	3.262D-06	-1.431D-07	-2.774D-07	1.064D-07	4.860D-07
14	3.262D-06	3.514D-05	6.943D-07	1.429D-05	1.941D-08	4.186D-06
15	-1.431D-07	6.943D-07	9.314D-05	3.628D-07	-5.872D-05	9.675D-08
16	-2.774D-07	1.429D-05	3.628D-07	6.982D-06	-3.936D-08	-4.356D-06
17	1.064D-07	1.941D-08	-5.872D-05	-3.936D-08	3.704D-05	-5.049D-09
18	4.860D-07	4.186D-06	9.675D-08	-4.356D-06	-5.049D-09	3.930D-05
19	1.393D-06	-2.256D-07	-5.715D-08	-9.337D-06	3.233D-08	5.806D-05

ROW \ COL	19
1	0.000D-01
2	0.000D-01
3	0.000D-01
4	-6.046D-10
5	1.010D-05
6	7.286D-06
7	-1.247D-04
8	1.677D-08
9	2.325D-06
10	-1.888D-08
11	5.420D-09
12	-3.412D-06
13	1.393D-06
14	-2.256D-07
15	-5.715D-08
16	-9.337D-06
17	3.233D-08
18	5.806D-05
19	8.709D-05

*** RETAINED MODAL DAMPING MATRIX ***

ROW \ COL	1	2	3	4	5	6
1	1.846D-03	-5.509D-06	2.519D-06	-1.700D-03	1.237D-03	3.255D-03
2	-5.509D-06	1.706D-03	3.644D-04	2.246D-05	-1.446D-05	-2.771D-05
3	2.519D-06	3.644D-04	3.409D-03	-6.900D-06	5.243D-06	1.146D-05
4	-1.700D-03	2.246D-05	-6.900D-06	1.711D-02	-6.647D-03	-4.585D-03
5	1.237D-03	-1.446D-05	5.243D-06	-6.647D-03	1.109D-02	5.880D-03
6	3.255D-03	-2.771D-05	1.146D-05	-4.585D-03	5.880D-03	4.215D-02
7	4.718D-05	-3.210D-03	-8.921D-03	-2.764D-05	7.188D-05	6.426D-04
8	1.500D-03	-1.495D-05	7.907D-08	-1.707D-03	2.124D-03	1.163D-02
9	1.057D-05	2.151D-03	6.351D-03	-2.617D-05	2.508D-05	7.470D-05
10	-1.173D-03	1.330D-05	-7.460D-06	4.837D-03	-2.683D-04	2.760D-02
11	-2.607D-03	2.564D-05	-3.086D-05	8.077D-03	-1.308D-03	3.694D-02

ROW \ COL	7	8	9	10	11
1	4.718D-05	1.500D-03	1.057D-05	-1.173D-03	-2.607D-03
2	-3.210D-03	-1.495D-05	2.151D-03	1.330D-05	2.564D-05
3	-8.921D-03	7.907D-08	6.351D-03	-7.460D-06	-3.086D-05
4	-2.764D-05	-1.707D-03	-2.617D-05	4.837D-03	8.077D-03
5	7.188D-05	2.124D-03	2.508D-05	-2.683D-04	-1.308D-03
6	6.426D-04	1.163D-02	7.470D-05	2.760D-02	3.694D-02
7	1.501D-01	3.174D-04	-8.721D-02	5.814D-04	6.131D-04
8	3.174D-04	5.610D-02	-2.360D-05	-1.229D-01	-1.896D-01
9	-8.721D-02	-2.360D-05	1.056D-01	6.325D-05	-1.322D-04
10	5.814D-04	-1.229D-01	6.325D-05	1.055D 00	1.446D 00
11	6.131D-04	-1.896D-01	-1.322D-04	1.446D 00	2.342D 00

*** RETAINED MODAL ANGULAR MOMENTUM MATRIX FOR 1-AXIS ***

ROW \ COL	1	2	3	4	5	6
1	0.000D-01	0.000D-01	0.000D-01	0.000D-01	0.000D-01	0.000D-01
2	0.000D-01	0.000D-01	0.000D-01	0.000D-01	0.000D-01	0.000D-01
3	0.000D-01	0.000D-01	0.000D-01	0.000D-01	0.000D-01	0.000D-01
4	0.000D-01	0.000D-01	0.000D-01	0.000D-01	0.000D-01	0.000D-01
5	0.000D-01	0.000D-01	0.000D-01	0.000D-01	0.000D-01	2.098D-06
6	0.000D-01	0.000D-01	0.000D-01	0.000D-01	-2.098D-06	0.000D-01
7	0.000D-01	0.000D-01	0.000D-01	0.000D-01	-1.509D-07	1.368D-07
8	0.000D-01	0.000D-01	0.000D-01	0.000D-01	-2.317D-10	6.195D-11
9	0.000D-01	0.000D-01	0.000D-01	0.000D-01	-1.211D-06	-2.021D-06
10	0.000D-01	0.000D-01	0.000D-01	0.000D-01	1.586D-08	1.893D-08
11	0.000D-01	0.000D-01	0.000D-01	0.000D-01	-6.086D-09	-3.833D-09
12	0.000D-01	0.000D-01	0.000D-01	0.000D-01	6.212D-06	3.555D-06
13	0.000D-01	0.000D-01	0.000D-01	0.000D-01	-3.257D-06	-3.030D-06
14	0.000D-01	0.000D-01	0.000D-01	0.000D-01	-2.875D-07	-1.206D-05
15	0.000D-01	0.000D-01	0.000D-01	0.000D-01	4.970D-08	-2.197D-07
16	0.000D-01	0.000D-01	0.000D-01	0.000D-01	3.037D-07	-4.713D-06
17	0.000D-01	0.000D-01	0.000D-01	0.000D-01	-2.768D-08	-1.395D-08
18	0.000D-01	0.000D-01	0.000D-01	0.000D-01	1.406D-07	-9.651D-07
19	0.000D-01	0.000D-01	0.000D-01	0.000D-01	-9.397D-08	5.710D-07

ROW \ COL	7	8	9	10	11	12
1	0.000D-01	0.000D-01	0.000D-01	0.000D-01	0.000D-01	0.000D-01
2	0.000D-01	0.000D-01	0.000D-01	0.000D-01	0.000D-01	0.000D-01
3	0.000D-01	0.000D-01	0.000D-01	0.000D-01	0.000D-01	0.000D-01
4	0.000D-01	0.000D-01	0.000D-01	0.000D-01	0.000D-01	0.000D-01
5	1.509D-07	2.317D-10	1.211D-06	-1.586D-08	6.086D-09	-6.212D-06
6	-1.368D-07	-6.195D-11	2.021D-06	-1.893D-08	3.833D-09	-3.555D-06
7	0.000D-01	1.065D-11	2.243D-07	-2.396D-09	6.724D-10	-6.607D-07
8	-1.065D-11	0.000D-01	2.591D-10	-2.560D-12	6.032D-13	-5.762D-10
9	-2.243D-07	-2.591D-10	0.000D-01	4.355D-09	-3.650D-09	3.932D-06
10	2.396D-09	2.560D-12	-4.355D-09	0.000D-01	2.593D-11	-2.917D-08
11	-6.724D-10	-6.032D-13	3.650D-09	-2.593D-11	0.000D-01	1.038D-09
12	6.607D-07	5.762D-10	-3.932D-06	2.917D-08	-1.038D-09	0.000D-01
13	-4.303D-07	-4.309D-10	1.388D-06	-6.474D-09	-2.839D-09	3.454D-06
14	-8.860D-07	-1.340D-09	-6.684D-06	8.858D-08	-3.445D-08	3.521D-05
15	-1.256D-08	-2.280D-11	-1.747D-07	2.110D-09	-7.280D-10	7.347D-07
16	-3.192D-07	-5.117D-10	-3.014D-06	3.838D-08	-1.423D-08	1.447D-05
17	-2.808D-09	-2.359D-12	1.862D-08	-1.443D-10	1.012D-11	-5.607D-09
18	-6.025D-08	-1.025D-10	-6.926D-07	8.566D-09	-3.056D-09	3.096D-06
19	3.494D-08	6.030D-11	4.202D-07	-5.165D-09	1.828D-09	-1.850D-06

(Cont'd)

ROW \ COL	13	14	15	16	17	18
1	0.000D-01	0.000D-01	0.000D-01	0.000D-01	0.000D-01	0.000D-01
2	0.000D-01	0.000D-01	0.000D-01	0.000D-01	0.000D-01	0.000D-01
3	0.000D-01	0.000D-01	0.000D-01	0.000D-01	0.000D-01	0.000D-01
4	0.000D-01	0.000D-01	0.000D-01	0.000D-01	0.000D-01	0.000D-01
5	3.257D-06	2.875D-07	-4.970D-08	-3.037D-07	2.768D-08	-1.406D-07
6	3.030D-06	1.206D-05	2.197D-07	4.713D-06	1.395D-08	9.651D-07
7	4.303D-07	8.860D-07	1.256D-08	3.192D-07	2.808D-09	6.025D-08
8	4.309D-10	1.340D-09	2.280D-11	5.117D-10	2.359D-12	1.025D-10
9	-1.388D-06	6.684D-06	1.747D-07	3.014D-06	-1.862D-08	6.926D-07
10	6.474D-09	-8.858D-08	-2.110D-09	-3.838D-08	1.443D-10	-8.566D-09
11	2.839D-09	3.445D-08	7.280D-10	1.423D-08	-1.012D-11	3.056D-09
12	-3.454D-06	-3.521D-05	-7.347D-07	-1.447D-05	5.607D-09	-3.096D-06
13	0.000D-01	1.830D-05	4.128D-07	7.756D-06	-1.833D-08	1.701D-06
14	-1.830D-05	0.000D-01	3.157D-07	2.391D-06	-1.572D-07	9.401D-07
15	-4.128D-07	-3.157D-07	0.000D-01	-7.986D-08	-3.229D-09	-8.146D-09
16	-7.756D-06	-2.391D-06	7.986D-08	0.000D-01	-6.422D-08	1.761D-07
17	1.833D-08	1.572D-07	3.229D-09	6.422D-08	0.000D-01	1.367D-08
18	-1.701D-06	-9.401D-07	8.146D-09	-1.761D-07	-1.367D-08	0.000D-01
19	1.022D-06	6.183D-07	-3.687D-09	1.285D-07	8.160D-09	4.974D-09

ROW \ COL	19
1	0.000D-01
2	0.000D-01
3	0.000D-01
4	0.000D-01
5	9.397D-08
6	-5.710D-07
7	-3.494D-08
8	-6.030D-11
9	-4.202D-07
10	5.165D-09
11	-1.828D-09
12	1.850D-06
13	-1.022D-06
14	-6.183D-07
15	3.687D-09
16	-1.285D-07
17	-8.160D-09
18	-4.974D-09
19	0.000D-01

*** RETAINED MODAL ANGULAR MOMENTUM MATRIX FOR 2-AXIS ***

ROW \ COL	1	2	3	4	5	6
1	0.000D-01	0.000D-01	0.000D-01	0.000D-01	0.000D-01	0.000D-01
2	0.000D-01	0.000D-01	0.000D-01	0.000D-01	0.000D-01	0.000D-01
3	0.000D-01	0.000D-01	0.000D-01	0.000D-01	0.000D-01	0.000D-01
4	0.000D-01	0.000D-01	0.000D-01	0.000D-01	0.000D-01	-1.822D-06
5	0.000D-01	0.000D-01	0.000D-01	0.000D-01	0.000D-01	7.731D-10
6	0.000D-01	0.000D-01	0.000D-01	1.822D-06	-7.731D-10	0.000D-01
7	0.000D-01	0.000D-01	0.000D-01	1.310D-07	-5.561D-11	5.040D-11
8	0.000D-01	0.000D-01	0.000D-01	2.013D-10	-8.541D-14	9.432D-08
9	0.000D-01	0.000D-01	0.000D-01	1.052D-06	-4.464D-10	5.886D-10
10	0.000D-01	0.000D-01	0.000D-01	-1.378D-08	5.846D-12	7.262D-07
11	0.000D-01	0.000D-01	0.000D-01	5.285D-09	-2.243D-12	1.981D-06
12	0.000D-01	0.000D-01	0.000D-01	-5.395D-06	2.289D-09	3.716D-09
13	0.000D-01	0.000D-01	0.000D-01	2.828D-06	-1.200D-09	-6.068D-11
14	0.000D-01	0.000D-01	0.000D-01	2.497D-07	-1.060D-10	8.418D-09
15	0.000D-01	0.000D-01	0.000D-01	-4.316D-08	1.832D-11	-1.933D-05
16	0.000D-01	0.000D-01	0.000D-01	-2.637D-07	1.119D-10	-6.908D-09
17	0.000D-01	0.000D-01	0.000D-01	2.404D-08	-1.020D-11	1.219D-05
18	0.000D-01	0.000D-01	0.000D-01	-1.221D-07	5.180D-11	-3.515D-09
19	0.000D-01	0.000D-01	0.000D-01	8.161D-08	-3.463D-11	3.631D-09

ROW \ COL	7	8	9	10	11	12
1	0.000D-01	0.000D-01	0.000D-01	0.000D-01	0.000D-01	0.000D-01
2	0.000D-01	0.000D-01	0.000D-01	0.000D-01	0.000D-01	0.000D-01
3	0.000D-01	0.000D-01	0.000D-01	0.000D-01	0.000D-01	0.000D-01
4	-1.310D-07	-2.013D-10	-1.052D-06	1.378D-08	-5.285D-09	5.395D-06
5	5.561D-11	8.541D-14	4.464D-10	-5.846D-12	2.243D-12	-2.289D-09
6	-5.040D-11	-9.432D-08	-5.886D-10	-7.262D-07	-1.981D-06	-3.716D-09
7	0.000D-01	-6.784D-09	-1.323D-11	-5.223D-08	-1.425D-07	-4.166D-10
8	6.784D-09	0.000D-01	5.446D-08	-7.935D-10	5.477D-11	-2.793D-07
9	1.323D-11	-5.446D-08	0.000D-01	-4.193D-07	-1.144D-06	-3.889D-09
10	5.223D-08	7.935D-10	4.193D-07	0.000D-01	1.709D-08	-2.150D-06
11	1.425D-07	-5.477D-11	1.144D-06	-1.709D-08	0.000D-01	-5.866D-06
12	4.166D-10	2.793D-07	3.889D-09	2.150D-06	5.866D-06	0.000D-01
13	-8.261D-11	-1.464D-07	-9.487D-10	-1.127D-06	-3.075D-06	-5.590D-09
14	5.986D-10	-1.293D-08	4.780D-09	-9.958D-08	-2.715D-07	-2.544D-08
15	-1.391D-06	9.879D-11	-1.116D-05	1.634D-07	-9.151D-09	5.725D-05
16	-4.896D-10	1.365D-08	-3.903D-09	1.052D-07	2.868D-07	2.099D-08
17	8.768D-07	1.020D-10	7.038D-06	-1.018D-07	9.221D-09	-3.610D-05
18	-2.495D-10	6.319D-09	-1.990D-09	4.868D-08	1.327D-07	1.066D-08
19	2.589D-10	-4.225D-09	2.070D-09	-3.256D-08	-8.873D-08	-1.092D-08

(Cont'd)

ROW \ COL	13	14	15	16	17	18
1	0.000D-01	0.000D-01	0.000D-01	0.000D-01	0.000D-01	0.000D-01
2	0.000D-01	0.000D-01	0.000D-01	0.000D-01	0.000D-01	0.000D-01
3	0.000D-01	0.000D-01	0.000D-01	0.000D-01	0.000D-01	0.000D-01
4	-2.828D-06	-2.497D-07	4.316D-08	2.637D-07	-2.404D-08	1.221D-07
5	1.200D-09	1.060D-10	-1.832D-11	-1.119D-10	1.020D-11	-5.180D-11
6	6.068D-11	-8.418D-09	1.933D-05	6.908D-09	-1.219D-05	3.515D-09
7	8.261D-11	-5.986D-10	1.391D-06	4.896D-10	-8.768D-07	2.495D-10
8	1.464D-07	1.293D-08	-9.879D-11	-1.365D-08	-1.020D-10	-6.319D-09
9	9.487D-10	-4.780D-09	1.116D-05	3.903D-09	-7.038D-06	1.990D-09
10	1.127D-06	9.958D-08	-1.634D-07	-1.052D-07	1.018D-07	-4.868D-08
11	3.075D-06	2.715D-07	9.151D-09	-2.868D-07	-9.221D-09	-1.327D-07
12	5.590D-09	2.544D-08	-5.725D-05	-2.099D-08	3.610D-05	-1.066D-08
13	0.000D-01	-1.308D-08	3.001D-05	1.073D-08	-1.892D-05	5.461D-09
14	1.308D-08	0.000D-01	2.649D-06	-2.719D-10	-1.671D-06	-8.227D-11
15	-3.001D-05	-2.649D-06	0.000D-01	2.799D-06	3.367D-08	1.295D-06
16	-1.073D-08	2.719D-10	-2.799D-06	0.000D-01	1.765D-06	-4.604D-11
17	1.892D-05	1.671D-06	-3.367D-08	-1.765D-06	0.000D-01	-8.167D-07
18	-5.461D-09	8.227D-11	-1.295D-06	4.604D-11	8.167D-07	0.000D-01
19	5.639D-09	1.205D-10	8.659D-07	-2.162D-10	-5.460D-07	-8.580D-11

ROW \ COL	19
1	0.000D-01
2	0.000D-01
3	0.000D-01
4	-8.161D-08
5	3.463D-11
6	-3.631D-09
7	-2.589D-10
8	4.225D-09
9	-2.070D-09
10	3.256D-08
11	8.873D-08
12	1.092D-08
13	-5.639D-09
14	-1.205D-10
15	-8.659D-07
16	2.162D-10
17	5.460D-07
18	8.580D-11
19	0.000D-01

*** RETAINED MODAL ANGULAR MOMENTUM MATRIX FOR 3-AXIS ***

ROW \ COL	1	2	3	4	5	6
1	0.000D-01	0.000D-01	0.000D-01	0.000D-01	0.000D-01	0.000D-01
2	0.000D-01	0.000D-01	0.000D-01	0.000D-01	0.000D-01	0.000D-01
3	0.000D-01	0.000D-01	0.000D-01	0.000D-01	0.000D-01	0.000D-01
4	0.000D-01	0.000D-01	0.000D-01	0.000D-01	9.522D-07	6.667D-07
5	0.000D-01	0.000D-01	0.000D-01	-9.522D-07	0.000D-01	6.863D-10
6	0.000D-01	0.000D-01	0.000D-01	-6.667D-07	-6.863D-10	0.000D-01
7	0.000D-01	0.000D-01	0.000D-01	-1.100D-07	-4.937D-11	4.474D-11
8	0.000D-01	0.000D-01	0.000D-01	-1.018D-10	-4.930D-08	-3.451D-08
9	0.000D-01	0.000D-01	0.000D-01	5.325D-07	-1.093D-09	-1.149D-09
10	0.000D-01	0.000D-01	0.000D-01	-3.551D-09	-3.795D-07	-2.657D-07
11	0.000D-01	0.000D-01	0.000D-01	-1.940D-10	-1.035D-06	-7.249D-07
12	0.000D-01	0.000D-01	0.000D-01	3.605D-07	7.747D-10	2.825D-10
13	0.000D-01	0.000D-01	0.000D-01	3.404D-07	-1.617D-09	-1.378D-09
14	0.000D-01	0.000D-01	0.000D-01	5.381D-06	-6.816D-09	-8.651D-09
15	0.000D-01	0.000D-01	0.000D-01	1.155D-07	1.010D-05	7.074D-06
16	0.000D-01	0.000D-01	0.000D-01	2.236D-06	2.802D-09	3.500D-10
17	0.000D-01	0.000D-01	0.000D-01	-2.466D-09	-6.371D-06	-4.461D-06
18	0.000D-01	0.000D-01	0.000D-01	4.827D-07	1.697D-09	8.404D-10
19	0.000D-01	0.000D-01	0.000D-01	-2.890D-07	-1.818D-09	-1.065D-09

ROW \ COL	7	8	9	10	11	12
1	0.000D-01	0.000D-01	0.000D-01	0.000D-01	0.000D-01	0.000D-01
2	0.000D-01	0.000D-01	0.000D-01	0.000D-01	0.000D-01	0.000D-01
3	0.000D-01	0.000D-01	0.000D-01	0.000D-01	0.000D-01	0.000D-01
4	1.100D-07	1.018D-10	-5.325D-07	3.551D-09	1.940D-10	-3.605D-07
5	4.937D-11	4.930D-08	1.093D-09	3.795D-07	1.035D-06	-7.747D-10
6	-4.474D-11	3.451D-08	1.149D-09	2.657D-07	7.249D-07	-2.825D-10
7	0.000D-01	5.696D-09	1.539D-10	4.385D-08	1.196D-07	-7.083D-11
8	-5.696D-09	0.000D-01	2.757D-08	-1.433D-10	1.006D-10	1.866D-08
9	-1.539D-10	-2.757D-08	0.000D-01	-2.123D-07	-5.790D-07	8.471D-10
10	-4.385D-08	1.433D-10	2.123D-07	0.000D-01	3.784D-09	1.437D-07
11	-1.196D-07	-1.006D-10	5.790D-07	-3.784D-09	0.000D-01	3.920D-07
12	7.083D-11	-1.866D-08	-8.471D-10	-1.437D-07	-3.920D-07	0.000D-01
13	-2.045D-10	-1.762D-08	5.137D-10	-1.357D-07	-3.702D-07	8.893D-10
14	-1.067D-09	-2.786D-07	-2.366D-09	-2.145D-06	-5.851D-06	6.958D-09
15	1.168D-06	-4.900D-09	-5.651D-06	-8.354D-09	-1.235D-07	-3.825D-06
16	2.078D-10	-1.158D-07	-4.134D-09	-8.912D-07	-2.431D-06	7.583D-10
17	-7.362D-07	-5.533D-10	3.563D-06	-2.278D-08	1.384D-09	2.412D-06
18	1.711D-10	-2.499D-08	-1.503D-09	-1.924D-07	-5.249D-07	-2.498D-10
19	-1.951D-10	1.496D-08	1.349D-09	1.152D-07	3.143D-07	4.532D-10

(Cont'd)

ROW \ COL	13	14	15	16	17	18
1	0.000D-01	0.000D-01	0.000D-01	0.000D-01	0.000D-01	0.000D-01
2	0.000D-01	0.000D-01	0.000D-01	0.000D-01	0.000D-01	0.000D-01
3	0.000D-01	0.000D-01	0.000D-01	0.000D-01	0.000D-01	0.000D-01
4	-3.404D-07	-5.381D-06	-1.155D-07	-2.236D-06	2.466D-09	-4.827D-07
5	1.617D-09	6.816D-09	-1.010D-05	-2.802D-09	6.371D-06	-1.697D-09
6	1.378D-09	8.651D-09	-7.074D-06	-3.500D-10	4.461D-06	-8.404D-10
7	2.045D-10	1.067D-09	-1.168D-06	-2.078D-10	7.362D-07	-1.711D-10
8	1.762D-08	2.786D-07	4.900D-09	1.158D-07	5.533D-10	2.499D-08
9	-5.137D-10	2.366D-09	5.651D-06	4.134D-09	-3.563D-06	1.503D-09
10	1.357D-07	2.145D-06	8.354D-09	8.912D-07	2.278D-08	1.924D-07
11	3.702D-07	5.851D-06	1.235D-07	2.431D-06	-1.384D-09	5.249D-07
12	-8.893D-10	-6.958D-09	3.825D-06	-7.583D-10	-2.412D-06	2.498D-10
13	0.000D-01	6.704D-09	3.612D-06	4.800D-09	-2.278D-06	1.427D-09
14	-6.704D-09	0.000D-01	5.710D-05	3.184D-08	-3.601D-05	1.305D-08
15	-3.612D-06	-5.710D-05	0.000D-01	-2.373D-05	-7.467D-07	-5.122D-06
16	-4.800D-09	-3.184D-08	2.373D-05	0.000D-01	-1.496D-05	2.565D-09
17	2.278D-06	3.601D-05	7.467D-07	1.496D-05	0.000D-01	3.230D-06
18	-1.427D-09	-1.305D-08	5.122D-06	-2.565D-09	-3.230D-06	0.000D-01
19	1.141D-09	1.234D-08	-3.067D-06	3.419D-09	1.934D-06	4.066D-10

ROW \ COL	19
1	0.000D-01
2	0.000D-01
3	0.000D-01
4	2.890D-07
5	1.818D-09
6	1.065D-09
7	1.951D-10
8	-1.496D-08
9	-1.349D-09
10	-1.152D-07
11	-3.143D-07
12	-4.532D-10
13	-1.141D-09
14	-1.234D-08
15	3.067D-06
16	-3.419D-09
17	-1.934D-06
18	-4.066D-10
19	0.000D-01

*** RETAINED FREQUENCIES ***

SELECTED MODES	FREQUENCY (RAD/SEC)	FREQUENCY (HZ)
1	0.0000000000000000D-01	0.0000000000000000D-01
2	0.0000000000000000D-01	0.0000000000000000D-01
3	0.0000000000000000D-01	0.0000000000000000D-01
4	0.0000000000000000D-01	0.0000000000000000D-01
5	0.0000000000000000D-01	0.0000000000000000D-01
6	0.0000000000000000D-01	0.0000000000000000D-01
7	0.0000000000000000D-01	0.0000000000000000D-01
8	0.0000000000000000D-01	0.0000000000000000D-01
9	1.2434952868889490D-01	1.9790842161985070D-02
10	1.5117997270041770D-01	2.4061039951769270D-02
11	2.3952489001995300D-01	3.8121570240218110D-02
12	5.5629553169353050D-01	8.8537183688959500D-02
13	6.9020123559092970D-01	1.0984893837243020D-01
14	7.7963639163821000D-01	1.2408298554354990D-01
15	1.5532815257821910D 00	2.4721243284155700D-01
16	3.1368829630482690D 00	4.9925042946988320D-01
17	3.9572089569016590D 00	6.2980936633842200D-01
18	9.9489251639172970D 00	1.5834206182887820D 00
19	1.4008315775600510D 01	2.2294927000789990D 00

Table D-1

Relationship of Evaluation Model Frequencies to Original Spacecraft Model Frequencies (Table 8)

Design Model Mode Number	Original Model Mode Number			Importance According to Modal Cost Analysis
	Combined	Rigid	Flexible	
1	1	1		↑ Retain Rigid Modes ↓
2	2	2		
3	3	3		
4	4	4		
5	5	5		
6	6	6		
7	7	7		
8	8	8		
9	9		1	1
10	10		2	6
11	11		3	3
12	13		5	4
13	14		6	7
14	16		8	2
15	21		13	5
16	29		21	11
17	30		22	8
18	37		29	10
19	45		38	9

*** RETAINED EIGENVECTORS ***

ROW \ COL	1	2	3	4	5	6
1	1.682D-02	0.000D-01	0.000D-01	0.000D-01	7.617D-03	3.139D-03
2	0.000D-01	1.682D-02	0.000D-01	-6.615D-03	2.807D-06	3.172D-05
3	0.000D-01	0.000D-01	1.682D-02	9.961D-04	-1.348D-05	-1.016D-05
4	0.000D-01	0.000D-01	0.000D-01	9.094D-04	-3.859D-07	-9.257D-07
5	0.000D-01	0.000D-01	0.000D-01	0.000D-01	1.047D-03	7.331D-04
6	0.000D-01	0.000D-01	0.000D-01	0.000D-01	0.000D-01	2.003D-03
7	0.000D-01	0.000D-01	0.000D-01	0.000D-01	0.000D-01	0.000D-01
8	0.000D-01	0.000D-01	0.000D-01	0.000D-01	0.000D-01	0.000D-01
9	0.000D-01	0.000D-01	0.000D-01	0.000D-01	0.000D-01	0.000D-01
10	0.000D-01	0.000D-01	0.000D-01	0.000D-01	0.000D-01	0.000D-01
11	0.000D-01	0.000D-01	0.000D-01	0.000D-01	0.000D-01	0.000D-01
12	0.000D-01	0.000D-01	0.000D-01	0.000D-01	0.000D-01	0.000D-01
13	0.000D-01	0.000D-01	0.000D-01	0.000D-01	0.000D-01	0.000D-01
14	0.000D-01	0.000D-01	0.000D-01	0.000D-01	0.000D-01	0.000D-01

ROW \ COL	7	8	9	10	11	12
1	1.334D-03	5.777D-07	3.051D-03	-1.135D-05	1.986D-06	1.541D-03
2	2.464D-06	9.338D-04	5.393D-06	-1.287D-03	3.920D-03	-8.289D-05
3	-1.609D-06	-2.016D-04	3.738D-05	5.527D-03	4.209D-03	-5.252D-06
4	-9.174D-08	-4.708D-05	-8.282D-07	-3.625D-04	-9.888D-04	8.859D-07
5	1.210D-04	1.119D-07	-5.856D-04	3.905D-06	2.133D-07	-3.964D-04
6	1.441D-04	2.213D-07	1.157D-03	-1.515D-05	5.812D-06	-5.932D-03
7	6.944D-03	6.791D-08	-5.553D-04	5.403D-06	-1.500D-06	8.518D-04
8	0.000D-01	6.921D-03	-2.199D-06	-6.851D-04	-2.577D-03	1.731D-06
9	0.000D-01	0.000D-01	-7.672D-02	6.574D-04	-1.386D-04	1.218D-01
10	0.000D-01	0.000D-01	-1.057D-04	-2.616D-02	-2.193D-02	-5.374D-05
11	0.000D-01	0.000D-01	9.647D-05	2.728D-02	7.066D-02	-4.218D-05
12	0.000D-01	0.000D-01	4.200D-06	1.211D-03	3.425D-03	-2.497D-06
13	0.000D-01	0.000D-01	5.736D-05	-2.287D-06	1.776D-06	-1.050D-03
14	0.000D-01	0.000D-01	3.335D-03	-3.071D-05	8.002D-06	-6.323D-03

(Cont'd)

ROW \ COL	13	14	15	16	17	18
1	2.933D-04	-3.661D-03	-6.865D-05	-5.147D-04	-7.681D-06	9.009D-05
2	4.152D-05	6.760D-06	-5.107D-03	-9.540D-06	2.245D-03	-2.352D-06
3	1.037D-05	6.496D-05	-6.523D-04	7.605D-06	5.077D-04	1.096D-06
4	-1.407D-06	-4.329D-06	9.650D-03	3.582D-06	-6.085D-03	1.817D-06
5	-3.743D-04	-5.918D-03	-1.270D-04	-2.459D-03	2.712D-06	-5.308D-04
6	3.110D-03	2.746D-04	-4.746D-05	-2.900D-04	2.644D-05	-1.342D-04
7	1.688D-05	4.838D-03	8.906D-05	-1.641D-02	9.890D-06	1.197D-01
8	-8.184D-07	-2.422D-06	-2.665D-03	-3.707D-06	-5.304D-03	-9.102D-07
9	-9.070D-02	-2.709D-01	-4.318D-03	-1.008D-01	-5.008D-04	-2.117D-02
10	-2.032D-05	-1.934D-04	4.341D-01	1.553D-04	-2.652D-01	7.903D-05
11	4.595D-05	1.590D-04	-2.046D-01	-6.828D-05	1.337D-01	-3.800D-05
12	2.209D-06	6.796D-06	-7.090D-03	9.175D-08	1.134D-02	-8.927D-07
13	-5.249D-04	-1.114D-02	-2.104D-04	1.367D-02	-8.302D-06	-1.178D-01
14	3.207D-03	-6.592D-04	-3.270D-05	-3.466D-03	2.847D-05	2.352D-02

ROW \ COL	19
1	-3.916D-05
2	2.916D-05
3	5.202D-06
4	-1.854D-06
5	3.178D-04
6	8.974D-05
7	1.803D-01
8	2.451D-04
9	1.470D-02
10	-1.073D-05
11	6.639D-05
12	-2.431D-04
13	-1.769D-01
14	3.307D-02